Elsevier Editorial System(tm) for Chemical Engineering Journal

Manuscript Draft

Manuscript Number: CEJ-D-15-06962R1

Title: Modelling an aerobic biotrickling filter for biogas desulfurization through a multi-step oxidation mechanism

Article Type: Research Paper

Keywords: Desulfurizing biotrickling filter; biogas; modeling; kinetics; sensitivity analysis; elemental sulfur

Corresponding Author: Dr. David Gabriel, PhD

Corresponding Author's Institution: Universitat Autonoma de Barcelona

First Author: Luis R López, MSc

Order of Authors: Luis R López, MSc ; Antonio D Dorado, PhD; Mabel Mora, PhD; Xavier Gamisans, PhD; Javier Lafuente, PhD; David Gabriel, PhD

Abstract: A dynamic model describing physical-chemical and biological processes for the removal of high loads of H2S from biogas streams in biotrickling filters (BTFs) was developed, calibrated and validated for a wide range of experimental conditions in a lab-scale BTF. The model considers the main processes occurring in the three phases of a BTF (gas, liquid and biofilm) in a co-current flow mode configuration. Furthermore, this model attempts to describe accurately the intermediate (thiosulfate and elemental sulfur) and final products (sulfate) of H2S oxidation.. A sensitivity analysis was performed in order to focus parameters estimation efforts on those parameters that showed the highest influence on the estimation of the H2S removal efficiency, the accumulated mass of sulfur and the sulfate concentration in the liquid phase. Biofilm and liquid layer thicknesses, specific growth rate of biomass over elemental sulfur and the H2S global mass transfer coefficient were the parameters that showed the highest influence on model outputs. Experimental data for model calibration corresponded to the operation of the BTF under stepwise increasing H2S concentrations between 2000 and 10000 ppmv. Once the model was calibrated, validation was performed by simulating a stationary feeding period of 42 days of operation of the BTF at an average concentration of 2000 ppmv and a dynamic operation period were the BTF was operated under variable inlet H2S concentration between 1000 and 5000 ppmv to simulate load fluctuations occurring in industrial facilities. The model described the reactor performance in terms of H2S removal and predicted satisfactorily the main intermediate and final products produced during the biological oxidation process.

Response to Reviewers: ANSWERS to Reviewer's comments to the Author:

We deeply thank the reviewer comments and observations since most of them helped to improve the quality and readability of the manuscript. We have addressed all comments point by point as detailed below. Changes in the manuscript are indicated with a P (page) and L (line) code.

Reviewer #1: Overall, I think this is a good paper. Some comments: Perhaps consider the mass transfer at the interfaces. Meaning, there will be some transfer at the gas to liquid and liquid to biomass interfaces. Also, I think it would be meaningful to consider wetted vs non wetted biofilms and how this would effect your model; having worked with biotrickling filters, there are differences in effluent concentrations when trickling rates are high enough to wet a decent fraction of the packing material.
Answer:
We thank the reviewer by his short but very interesting and useful comments. We agree with the reviewer that mass transfer at the interfaces must be considered in order to have a more realistic approach of the model. Regarding the first comment about gas-liquid mass transfer, a global mass transfer coefficient referred to the liquid phase (KL) was considered in this work (equation 3). Thus, such global coefficient already included the mass transfer both in the gas boundary layer an in the liquid boundary layer (assuming the concept of the double-film theory). In any case, the schematic of the model in the former version (figure 3) was confusing since it was drawn as if no mass transfer resistance occurred in the gas phase.

Derived from the reviewer comment, we thought interesting to include some short sentences about the contribution of both resistances to the overall G-L transport resistance. The individual mass transfer coefficients for both gas species oxygen (O2) and hydrogen sulfide (H2S) were determined using the Billet and Schultes correlations for kg and kl. Result showed that the contribution of the gas phase was only a 0.18% for O2 and a 9.7% for H2S. To clarify, the following modifications and comments were added:

(P3L24) "However, biogas desulfurization requires of much longer gas contact times and, consequently, lower gas velocities that may increase mass transfer resistance in the gas phase."

"Gas-Liquid mass transport is described by a gas-liquid global mass transfer coefficient referred to the liquid phase (KL) that considers both the individual gas and liquid mass transfer resistances". This comment was added both in the description of model assumptions (assumption 6) in section SM2 of the Supplementary Material file and in section 2.2 of the main manuscript (P9L1)

The schematic of the model (now in figure 1) has been modified to show the concentration change in the gas boundary layer when approaching the G-L interface.

(P16L14) "The "K" _("L," "O" _"2")was determined using the Billet and Schultes correlations [34] for the gas and liquid individual mass transfer coefficients kg and kl, respectively, which was in close agreement with "K" _("L," "O" _"2") determined by Dorado et al. [9]. It is worth highlighting that only the liquid-side resistance was significant since based on Billet and Schultes correlations the contribution of individual mass transfer resistances in the gas phase to the overall resistance for both gas species oxygen (O2) and hydrogen sulfide (H2S) were only 0.18% and 9.7% for O2 and H2S, respectively."

Regarding to the second comment about liquid-biofilm mass transfer, we included a diffusion term described by Fick's law in the liquid phase in the former version of the manuscript (equation 4). We agree with the

reviewer about its significance since we really verified running simulations without this term that this term was completely necessary to properly fit our experimental data. We did not deeply show with simulations that importance in the manuscript but to clarify, the following comments were added:

"Mass transfer resistance in the liquid-biofilm interface was described by Fick's law considering that the whole thickness of the liquid phase acted as the liquid boundary layer for mass transport resistance" This comment was added both in the description of model assumptions (assumption 7) in section SM2 of the Supplementary Material file and in section 2.2 in the main manuscript (P9L12)

Regarding the modeling approach about the use of fully wetted or wetted/non-wetted biofilms we agree with the reviewer that this would have a clear impact due to the changing amount of water in the packed bed when the TLV is modified. This is not trivial and no clear consensus exists about the use of one or another modeling approach since lumping of certain parameters may result in similar modeling results. A careful analysis from a modeling perspective must be performed. However, this was not the scope of the manuscript since the TLV was kept constant throughout the study. The following sentence was added:

(P4L3) "Despite no clear consensus has been reached so far and a careful analysis from a modeling perspective must be performed, modeling of biotrickling filters using a wetted/non-wetted biofilm approach seems necessary when the TLV is modified due to the changing amount of water in the packed bed."

Reviewer #2: This contribution presents a model for an aerobic biotrickling filter (BTF) for biogas desulfurization. The model applied to describe the biological processes is the one from Mora et al. [27]. The BTF setup and experimental results regarding the influence of trickling liquid velocity and flow pattern were presented before, by [26]. So the main novelty of this contribution lies in modelling the BTF as such, and in the model calibration and validation based on experimental data. Part of the experimental data used for calibration were published in [26] (Figure 4A and 5A&B from this contribution overlap with Figure 2a from [26]).

Overall, I think the objectives and novelty of the paper should be stated more clearly. The introduction needs to be rewritten in this respect. The results and discussion need to be more to the point. The whole text could be written more compactly without loss of essential information - in fact it could make the message more clear. Figures can be made more clear; the number of figures can be reduced; a graphical representation from the information from Table 2 would allow easier interpretation. The generality of the presented results and the general added value of this contribution needs to be elaborated on, given that the model is calibrated and validated for a specific model set-up.

Note: part of the results in this contribution were previously presented at the EMChIE2015 conference. In my view, they are definitely sufficiently interesting for a journal publication, but that conference paper was written more to-the-point and had a clearer structure than this contribution - so please reconsider it.

The present manuscript contains quite some typos and English language errors.
Answer:
We agree with the reviewer comments, thus, we have tried to focus the revised version on the BTF modeling. We want to stress that, in our opinion, the novelty of the paper was already clearly stated in the first version of the manuscript, however the introduction has been modified following the reviewer comments in order to stress the novelty of this work and the contribution on BTF desulfurization modelling. The numbers of figures has been reduced, considering the specific comments of the reviewer. Table 2 (sensitivity results for key BTF model parameters) was not represented graphically since different figures would be need in order to represent the sensitivity value for each output variable for all the model parameter studied, and therefore a table was considered more appropriate to show in a compact manner the sensitivity analysis results.

SPECIFIC COMMENTS

1-Abstract
line 44: 'respirometric techniques': this is not the focus of this paper but was addressed by Mora et al. [27]
Answer:
(P1 L20) The sentence was removed

2- Abstract: lines 46-51: no need to give a definition of sensitivity analysis in the abstract. Leave out or specify output parameters and process variables.
Answer:
The output process variables studied were included in the sentence as follows:
(P1, L21) "…showed the highest influence on the estimation of the H2S removal efficiency the accumulated mass of sulfur and the sulfate concentration in the liquid phase."

3-Introduction
The introduction should introduce the subject and identify knowledge gaps that will be addressed in this contribution. I expect the introduction of BTF for H2S removal from biogas and the modelling of BTF in general.
Answer:
Knowledge gaps were already stated in the former version of the manuscript (now in P3,L6-24). According to the reviewer suggestions, the introduction was modified including a brief introduction about BTF for H2S removal from biogas. The following paragraph was added in the introduction:
(P2, L15) "Obtaining energy from non-renewable sources is becoming too expensive or too environmentally damaging nowadays. A energy source with high potential for green energy production is biogas. However, in order to have a suitable biogas utilization, impurities such as H2S and reduced sulfur compounds (RSC) produced during the anaerobic fermentation of S-bearing organic molecules must be removed [1]. Removal of H2S is strictly necessary to avoid corrosion of internal combustion engines during co-generation processes as well as for proper performance of further biogas upgrading technologies [2]. Biological technologies such as biotrickling filters (BTF) have demostrated to be a suitable, competitive treatment technology for biogas conditioning when compared to physical-chemical technologies. However, main effort has been focus on experimental works, studying different pollutant loads [3], using different packing materials [4], different oxygen mass transfer devices [5], pH conditions [6] or

gas-liquid flow pattern [7]. Tough process modeling has shown to be a crucial tool to evaluate the technical [1] and economical feasibility [2] of biological processes prior full-scale implementation, few efforts have been made in this direction on biogas desulfurization in BTFs."

4-Introduction

References cited should either be applicable to this topic or be very general; this is not the case for [1]-[4]. Also [5]-[8] seem to be 'thrown in'. Specify what the individual references are about rather than listing references all together.

Answer:

General references or not directly applicable to the topic have been removed. Former paragraph starting from P3L4 until P3L8 has been removed. In general, references have been cited individually and an individual explanation has been provided instead of referencing all together at the end of the sentence. However some references have been kept grouped where the sentence points to a common fact.

5-Introduction

The introduction on biodegradation mechanism and kinetics (p3 line 41 till p4 line 37) is not relevant for the introduction since the biological model was not developed in this contribution. At most, it could be summarized in the model description

Answer:

The introduction on biodegradation mechanism and kinetics has been removed from the introduction section and was summarized in the kinetic model description. Paragraph starting on P4L20 until P5L9 has been removed from the introduction section and summarized on section 2.2.2 (P11L4 to P12L2).

6-Introduction

part. p5 lines29-37 do not belong in the introduction either.

Answer:

This paragraph has been also moved to kinetic model description on P11.

7-Materials and Methods

Before giving details on the reactor dimension and packing, specify the general layout and operating principle (p5, line 48).

Answer:

The operating principle of the reactor is now explained just at the beginning of the section and rewritten as follows:

P5L22: "A laboratory-scale BTF reactor, with an ancillary unit for air supply, was used in this study to remove high loads of H_2S from biogas mimics streams (Fig.1). The biogas mimics consisted in controlled mixtures of H_2S and nitrogen (N_2) fed at the top of the BTF (1). An air flow (2) was firstly fed to an aeration column (3) for air supply to increase the dissolved oxygen (DO) concentration in the liquid phase. Exhaust air (4) from the aeration column was fed at the top of the BTF under a co-current flow pattern and mixed with the biogas inlet stream at an O_2/H_2S supplied ratio of 41.2 (v v-1). After biological degradation on the BTF bed (5), the treated biogas stream (6) leaves the reactor. The liquid phase was continuously recycled from bottom-to-top of the BTF at a trickling liquid velocity (TLV) of 4.4 m h-1 (7). The liquid recirculation line (8) was previously oxygenated in an aeration column. The DO concentration in the recycle and purge lines was monitored in-situ in all the experiments. The reactor pH was also controlled at pHs of around 6.5 and 7 using an ON/OFF control system by automated addition of NaOH 1M or HCl 1 M. An empty bed residence time (EBRT) of 118 s and an average hydraulic retention time (HRT) of 30 ± 4 h were maintained

throughout the study by regulating the purge pump (9) and the mineral medium pump (10). Regarding the packing bed characteristics, the reactor diameter was 7.14 cm with a packed bed volume of 2.80·10-3 m3 (Vbed). Polypropylene Pall rings of 15.9 mm diameter (MACH engineering products, USA) with a specific surface area of 354 m2 m-3 were used."

8-Materials and Methods
Explicitly specify the experimental dataset and the periods 1-2-3. Are these periods consecutive?
Answer:
Experimental conditions presented on data provided on Table 1 (H2S inlet concentration, H2S Loading Rate, O2/H2S volumetric ratio) are commonly enough to describe the operating conditions to facilitate the comparison between different systems with different dimensions. Periods 1-2-3 were not consecutive, all experiments were performed in between a time span of 15 months. The following phrase was added to clarify:
(P7L10) "Periods of table 1 does not correspond to consecutive periods, all experiments were performed in between a time span of 15 months."

9-Materials and Methods
Specify gas flow rate (constant for all experiments?).
Answer:
Gas flow rate is not specified since the key parameter is the gas contact time (EBRT). The gas flow rate can be determined relating the EBRT and the volume of the packed bed. The following phrase was added in order to clarify this.
(P7L4) "…in the lab-scale BTF set up (Fig. 1) operating at constant EBRT and constant biogas flow."

10-Materials and Methods
Is O2 concentration varying - O2/H2S variations only caused by varying H2S?
Answer:
The O2/H2S volumetric ratio varied only due to H2S inlet concentration increase since the air flow rate was kept constant in this work. The following phrase was added in order to clarify this:
(P7L4) "…in the lab-scale BTF set up (Fig. 1) operating at constant EBRT and constant biogas flow."

11-Materials and Methods
Separate description of experimental setup and the model (lines 7, 12 and 42 do not fit here; also reconsider the paragraph starting on p6, line 48).
Answer:
Lines describing model variables on experimental setup description have been removed.

12-Materials and Methods
Figure 1 and Figure 3 could be left out and replaced by (and extended version of) Figure S2, detailing how the different layers in the BTF are described - the description on p7 referring to different indices is difficult to follow without a figure.
Answer:
Figure 1 and 3 and Figure S2 have been merged in order to have a complete description in a single figure (new Figure 1) to help the comprehension of the BTF set up, BTF discretization and biological mechanisms of H2S biological oxidation

13-Materials and Methods
The model description could be written more concisely by describing the meaning of the different balances and by listing the parameters in a 'nomenclature' section.
Answer:
The parameters have been listed in a nomenclature section.

14-Materials and Methods
2.2.2. 'Kinetic model'. Not only kinetic, but also stoichiometry, right? Rather entitle this section 'modelling biological and chemical sulfur conversions'.
Answer:
Right, the name has been changed. To avoid confusion with elemental sulfur, S-compounds has been used instead of sulfur.
(P11L3) "2.2.2 Modeling of biological and chemical S-compounds conversions"

15-Materials and Methods
It would be a strong added value to summarize the biological reactions in Gujer matrix format, to have a clear overview of the state variables and the model stoichiometry and kinetics.
Answer:
The model proposed by Mora et al. 2016 to describe the multi-step sulfide oxidation bioprocess has been summarized in the Gujer Matrix format in Tables 2 and 3 in which the stoichiometry and the kinetic expressions, respectively, are described.

16-Materials and Methods
This whole section needs to be significantly shortened, given that the model was developed by Mora et al. [27].
Answer:
We agree with the reviewer. Since part of the introduction related to general considerations about biodegradation mechanism and kinetics has been moved to this section (see answer to comment #5) the description of the model by Mora et al has been moved to the supplementary material Section SM-4.

17-Materials and Methods
p11, line 28 'no previous works has intended to model such range of intermediate products of biological sulfide oxidation'. If this is a major novelty, it should already be stated in the introduction and. I would also expect a discussion later in the article on whether or not it is important to consider a multi-step oxidation mechanism.
Answer:
This sentence has been moved to the introduction section (P5L16). The discussion about this major novelty has been added as a final discussion on the result section as follows:

(P21 L2) "Especially, accurate model predictions under high H2S-LR and O2 limiting conditions (period 1) could be useful for predicting elemental sulfur accumulation in industrial BTF installations. Therefore, maintenance tasks can be strategically planned"

18-Materials and Methods
2.3 Model implementation.
p13 'set of PDE was discretized'. This information comes late - needed to interpret mass balances.
Answer:

Yes. This paragraph has been moved to (P8L8) in the model development section just before the mass balances.

19. Results and discussion
3.1 Give a definition of the sensitivity function. Did you consider relative or absolute sensitivity? This will of course impact the comparability of the numbers obtained.
Answer:
Sensitivity function definition was included as follows:

(P13L8) "Sensitivity was assessed by increasing and decreasing model parameters by 10% and comparing the relative change of the output variables to a relative change of the model parameter."

Also the word "relative" was added before "sensitivity analysis" throughout the manuscript (mostly in section 3.1, page 13) to indicate that the relative sensitivity was assessed.

20. Results and discussion
Also reconsider the structure of this section, emphasizing the main points. First describe most sensitive parameters, then the least sensitive, afterwards discuss.
Answer:
In the former version of the manuscript the most sensitive output variables were firstly described and, afterwards, the less sensitive. Also, the discussion was already based only on the most sensitive parameters (with higher relative sensitivity function value than 0.1). However, the first sentence in P13L24 was changed to follow the same structure from more to less sensitive variables throughout the discussion.

(P13L24) "The most sensitive output variables were the RE and CL,SO42- that exhibited comparable sensitivities between them at a 10% increase while mS0 was the less sensitive output variable due to its cumulative nature."

21. Results and discussion
p15 'O2 transport rather than H2S transport is the limiting step'. But O2 transport and H2S transport take place in separate reactors, right?
Answer:
The goal of using an external aeration column was to improve the O2 gas-liquid mass transport before air enters the BTF column. The total amount of oxygen supplied to the BTF was the contribution of that supplied to the liquid phase in the aeration column plus the excess air from the aeration column that passed through the packed bed of the reactor. The contribution of the O2 transferred in the aeration column was estimated to be between 10 and 30% of the total (aeration column + reactor) O2 transferred. This discussion has already been made in previous works by Lopez et al. No changes were made to the manuscript.

22. Results and discussion
3.2 The first paragraph (starting on p16 line 49) rather belongs to 'Materials and methods'.
Answer:
The paragraph was moved to the Materials and Methods section (now in P12L10)

23 Results and discussion

p17 '157g of elemental sulfur'. How was this amount determined?
Answer:
Since Kmax is the relation between the maximum amount of elemental sulfur that could be accumulated inside SOB cells before this accumulation completely blocked the biological sulfide consumption such maximum amount of elemental sulfur was determined using the substrate switch constant (Kmax) and the biomass concentration estimated by the model (X) according to K_max=m_(S^0 max)/X. This comment was added to the manuscript as:

(P16L7) "Since Kmax is the relation between the maximum amount of elemental sulfur that could be accumulated inside SOB cells before this accumulation completely blocked the biological sulfide consumption, this maximum amount of elemental sulfur was determined using the substrate switch constant (Kmax) and the biomass concentration estimated by the model (X) according to K_max=m_(S^0 max)/X. Thus, under the calibration conditions, a maximum amount of 157 g of elemental sulfur could be accumulated inside SOB cells, well above the amount of elemental sulfur produced."

24. Results and discussion
p17 Clarify that the results presented in Fig4 and Fig5 are the model calibration results (also in caption Fig 4).
Answer:
Caption in figure 4 was changed. The sentence in the manuscript was changed to:

(P17L4) "In Fig. 3 and Fig. 4 experimental results and model predictions of the effect of stepwise LR increases due to H2S inlet concentration increases corresponding to the model calibration period are presented".

25. Results and discussion
p17 line 59 'Fig 4'. Where to look exactly?
Answer:
Truly, in Figure 4 (now Figure 3) there was no RE plotted but the H2S concentration. The sentence was rewritten as follows:

(P21 L21) "Experimental data in both figures indicate that the system was able to remove almost 100% of H2S inlet concentration at all H2S-LR (Fig. 3A and 3B)."

26. Results and discussion
p20, line 26 'Sulfate concentration increases during steady state'. If the concentration changes, steady state has not yet been reached. What causes the change - do you expect it to keep going on?
Answer:
We agree with the reviewer. We meant "stationary feeding period" instead because the inlet conditions were constant. In fact, a BTF hardly reaches steady-state conditions since there is biomass growth, changes in the preferential paths inside the packed bed etc… Pseudo-steady state conditions were replaced by stationary feeding period throughout the manuscript.

27. Results and discussion
p21 'Overall, the model described processes occurring in the three phases'. Specify which figures correspond to which phase.
Answer:
The sentence was confusing. The sentence now reads as:

(P20L22) “Overall, the model showed to be valid to describe the main processes occurring in the three phases of a BTF, gas phase (Fig. 3A and 3B), liquid phase (Fig. 4A) and solid phase as elemental sulfur (Fig. 4B) in a co-current flow mode configuration”

28. Conclusions
The conclusions are too general. Specify conclusions related to the model set-up, calibration and validation separately.
Answer:
The conclusions have been modified, describing separately each part of the work from the sensitivity analysis until the constant feeding validation period and the dynamic validation period.
Most of this section has been rewritten as follows:

(P21L21) “…… A preliminary assessment through a relative sensitivity analysis allowed determining the most sensitive parameters of the model. Parameters related to O2 mass transport exhibited a larger influence to model output variables considered (RE, CL,SO42- and mS0). The proposed model was calibrated using experimental data, which allowed describing accurately the outlet H2S concentration profile along the BTF bed during H2S-LR increments. Besides describing properly sulfate production, elemental sulfur, the main intermediate product during H2S oxidation, was correctly predicted. Mass transfer parameters (δB, δL, KL,H2S) and kinetic parameters (X, μmax,2) were estimated during BTF model calibration.

Moreover, the BTF model was validated under a stationary feeding period and a dynamic H2S-LR period. Proper gas phase description during both periods was obtained. More importantly, elemental sulfur and sulfate were also in agreement with experimental data. Dynamic validation results demonstrated that the model is able to predict correctly the BTF operation when a variable H2S-LR profile is applied. Hence the BTF model here presented is capable to predict the BTF performance under similar conditions as those found in real plants, making it a suitable tool in order to develop and design control strategies towards process optimization of desulfurizing BTFs.”

29. Conclusions
The last part (p22 lines 19-29) belongs to the discussion rather than the conclusions section.
Answer:
This section was moved to the last part of the discussion on the results section

(P21L2) “Especially, accurate model predictions under high H2S-LR and O2 limiting conditions (period 1) could be useful for predicting elemental sulfur accumulation in industrial BTF installations. Therefore, maintenance tasks can be strategically planned. Moreover, the development of the BTF model can be used for the development and simulation of control strategies towards process optimization. Parameters related to O2 transport are crucial in order to completely oxidaize H2S and avoid the formation of elemental sulfur in the BTF bed, since an excessive accumulation of elemental sulfur can significantly diminish the reactor performance. Therefore, control strategies must be based on the improvement of the oxygen transfer to the liquid phase towards process optimization.”

OTHER REMARKS
Mind using uniform terminology throughout the manuscript:
- steady state (p6) or 'stationary'?
Answer:
See answer to comment #26

- ancillary column - oxygenation column - aeration column
Answer:
Aeration column has been used along the complete manuscript

'biogas mimics stream': just write 'biogas stream' and specify in the M&M section that it is a synthetic stream.
Answer:
Biogas stream has been used along the complete manuscript

p7 line34, sentence incomplete
Answer:
The sentence has been completed as follows

(P7L24) "…interface occurring in the aeration column."

p10 'sump' - you mean a buffer tank? Was not specified in the description of the installation.
Answer:
The sentence has been changed to:
P6L22
"Liquid present in the bottom section of the BTF (7) was recycled to the aeration column"

Figure 4A and Figure 5A&B should be grouped in one figure so it is clear to which LR the results correspond.
Answer:
We tried to group these figures in a single figure but it was too packed that was hardly understable. We kept them split in two as it was presented in the first version of the manuscript. However to clarify Figure 5 (now figure 4), we added the H2S inlet concentration profile to have a clearer reference.

replace 'in coherence with', 'in concordance with' by 'in agreement with' or 'correspond with'.
Answer:
They have been changed along the manuscript

References
- all authors should be listed for each publication, do not use 'et al.'
Answer:
All authors are now listed in the references

- give full and accurate reference, including volume and page numbers, e.g. for [26] and [27]
Answer:
Reference [26] now reference [7] does not have a volume and page numbers yet.
Reference [27] now reference [21] has been modified and the volume and page numbers have been added.

- avoid typos e.g. p22 line 53, p24 line 17,
Answer:

Typos have been corrected in the manuscript

Re: Manuscript submission cover letter February 19th, 2016

Dear Editor:

We are submitting a revised version of the manuscript entitled "**Modelling an aerobic biotrickling filter for biogas desulfurization through a multi-step oxidation mechanism**" authored by Luis R. López, Antonio D. Dorado, Mabel Mora, Xavier Gamisans, Javier Lafuente and David Gabriel.

The following author is responsible for correspondence:
David Gabriel
Department of Chemical, Biological and Environmental Engineering
School of Engineering, Building Q
Universitat Autònoma de Barcelona
08193, Bellaterra, Barcelona
Phone: +34 935811587
Fax+34 935812013
e-mail david.gabriel@uab.cat

The manuscript has been revised according to reviewer comments. A separated file with a point-by-point answer to all reviewer comments is attached. We think we have answered all questions properly. For sure, the quality of the manuscript has improved a lot.

I look forward to your response with respect to possible publication.

.

Yours sincerely,

David Gabriel
Associate Professor
Department of Chemical Engineering
Universitat Autonoma de Barcelona
Barcelona, Spain

LIST OF SUGGESTED REVIEWERS

First Name	Eveline
Last Name	Volcke
Department	Department of Biosystems Engineering
Institution	Ghent University
E-mail Address	Eveline.Volcke@UGent.be
Reason	Expert in modelling biological systems both in wastewater and wastegas treatment

First Name	German
Last Name	Aroca
Department	Escuela Ingeniería Bioquímica
Institution	Universidad Católica de Valparaíso
E-mail Address	garoca@ucv.cl
Reason	Several publications in bioreactor modelling, including H_2S removal in biotrickling filters

First Name	Zarook
Last Name	Sharefdeen
Department	Department of Chemical Engineering
Institution	American University of Sharjah
E-mail Address	zshareefdeen@aus.edu
Reason	Expert in biofiltration modelling

ANSWERS to Reviewer's comments to the Author:

We deeply thank the reviewer comments and observations since most of them helped to improve the quality and readability of the manuscript. We have addressed all comments point by point as detailed below. Changes in the manuscript are indicated with a P (page) and L (line) code.

Reviewer #1: Overall, I think this is a good paper. Some comments: Perhaps consider the mass transfer at the interfaces. Meaning, there will be some transfer at the gas to liquid and liquid to biomass interfaces. Also, I think it would be meaningful to consider wetted vs non wetted biofilms and how this would effect your model; having worked with biotrickling filters, there are differences in effluent concentrations when trickling rates are high enough to wet a decent fraction of the packing material.

Answer:

We thank the reviewer by his short but very interesting and useful comments. We agree with the reviewer that mass transfer at the interfaces must be considered in order to have a more realistic approach of the model. Regarding the first comment about gas-liquid mass transfer, a global mass transfer coefficient referred to the liquid phase (K_L) was considered in this work (equation 3). Thus, such global coefficient already included the mass transfer both in the gas boundary layer an in the liquid boundary layer (assuming the concept of the double-film theory). In any case, the schematic of the model in the former version (figure 3) was confusing since it was drawn as if no mass transfer resistance occurred in the gas phase.

Derived from the reviewer comment, we thought interesting to include some short sentences about the contribution of both resistances to the overall G-L transport resistance. The individual mass transfer coefficients for both gas species oxygen (O_2) and hydrogen sulfide (H_2S) were determined using the Billet and Schultes correlations for k_g and k_l. Result showed that the contribution of the gas phase was only a 0.18% for O_2 and a 9.7% for H_2S. To clarify, the following modifications and comments were added:

(P3L24) **"**However, biogas desulfurization requires of much longer gas contact times and, consequently, lower gas velocities that may increase mass transfer resistance in the gas phase."

"Gas-Liquid mass transport is described by a gas-liquid global mass transfer coefficient referred to the liquid phase (KL) that considers both the individual gas and liquid mass transfer resistances". This comment was added both in the description of model assumptions (assumption 6) in section SM2 of the Supplementary Material file and in section 2.2 of the main manuscript (P9L1)

The schematic of the model (now in figure 1) has been modified to show the concentration change in the gas boundary layer when approaching the G-L interface.

(P16L14) "The $K_{L,O_2}$was determined using the Billet and Schultes correlations [34] for the gas and liquid individual mass transfer coefficients *kg* and *kl*, respectively, which was in close agreement with K_{L,O_2} determined by Dorado et al. [9]. It is worth highlighting that only the liquid-side resistance was significant since based on Billet and Schultes correlations the contribution of

individual mass transfer resistances in the gas phase to the overall resistance for both gas species oxygen (O_2) and hydrogen sulfide (H_2S) were only 0.18% and 9.7% for O_2 and H_2S, respectively."

Regarding to the second comment about liquid-biofilm mass transfer, we included a diffusion term described by Fick's law in the liquid phase in the former version of the manuscript (equation 4). We agree with the reviewer about its significance since we really verified running simulations without this term that this term was completely necessary to properly fit our experimental data. We did not deeply show with simulations that importance in the manuscript but to clarify, the following comments were added:

"Mass transfer resistance in the liquid-biofilm interface was described by Fick's law considering that the whole thickness of the liquid phase acted as the liquid boundary layer for mass transport resistance" This comment was added both in the description of model assumptions (assumption 7) in section SM2 of the Supplementary Material file and in section 2.2 in the main manuscript (P9L12)

Regarding the modeling approach about the use of fully wetted or wetted/non-wetted biofilms we agree with the reviewer that this would have a clear impact due to the changing amount of water in the packed bed when the TLV is modified. This is not trivial and no clear consensus exists about the use of one or another modeling approach since lumping of certain parameters may result in similar modeling results. A careful analysis from a modeling perspective must be performed. However, this was not the scope of the manuscript since the TLV was kept constant throughout the study. The following sentence was added:

(P4L3) "Despite no clear consensus has been reached so far and a careful analysis from a modeling perspective must be performed, modeling of biotrickling filters using a wetted/non-wetted biofilm approach seems necessary when the TLV is modified due to the changing amount of water in the packed bed."

Reviewer #2: This contribution presents a model for an aerobic biotrickling filter (BTF) for biogas desulfurization. The model applied to describe the biological processes is the one from Mora et al. [27]. The BTF setup and experimental results regarding the influence of trickling liquid velocity and flow pattern were presented before, by [26]. So the main novelty of this contribution lies in modelling the BTF as such, and in the model calibration and validation based on experimental data. Part of the experimental data used for calibration were published in [26] (Figure 4A and 5A&B from this contribution overlap with Figure 2a from [26]).

Overall, I think the objectives and novelty of the paper should be stated more clearly. The introduction needs to be rewritten in this respect. The results and discussion need to be more to the point. The whole text could be written more compactly without loss of essential information - in fact it could make the message more clear. Figures can be made more clear; the number of figures can be reduced; a graphical representation from the information from Table 2 would allow easier interpretation. The generality of the presented results and the

general added value of this contribution needs to be elaborated on, given that the model is calibrated and validated for a specific model set-up.

Note: part of the results in this contribution were previously presented at the EMChIE2015 conference. In my view, they are definitely sufficiently interesting for a journal publication, but that conference paper was written more to-the-point and had a clearer structure than this contribution - so please reconsider it.

The present manuscript contains quite some typos and English language errors.
Answer:
We agree with the reviewer comments, thus, we have tried to focus the revised version on the BTF modeling. We want to stress that, in our opinion, the novelty of the paper was already clearly stated in the first version of the manuscript, however the introduction has been modified following the reviewer comments in order to stress the novelty of this work and the contribution on BTF desulfurization modelling. The numbers of figures has been reduced, considering the specific comments of the reviewer. Table 2 (sensitivity results for key BTF model parameters**)** was not represented graphically since different figures would be need in order to represent the sensitivity value for each output variable for all the model parameter studied, and therefore a table was considered more appropriate to show in a compact manner the sensitivity analysis results.

SPECIFIC COMMENTS

1-Abstract
line 44: 'respirometric techniques': this is not the focus of this paper but was addressed by Mora et al. [27]
Answer:
(P1 L20) The sentence was removed

2- Abstract: lines 46-51: no need to give a definition of sensitivity analysis in the abstract. Leave out or specify output parameters and process variables.
Answer:
The output process variables studied were included in the sentence as follows:
(P1, L21) "…showed the highest influence on the estimation of the H2S removal efficiency the accumulated mass of sulfur and the sulfate concentration in the liquid phase."

3-Introduction
The introduction should introduce the subject and identify knowledge gaps that will be addressed in this contribution. I expect the introduction of BTF for H_2S removal from biogas and the modelling of BTF in general.
Answer:
Knowledge gaps were already stated in the former version of the manuscript (now in P3,L6-24). According to the reviewer suggestions, the introduction was modified including a brief introduction about BTF for H_2S removal from biogas. The following paragraph was added in the introduction:

(P2, L15) “Obtaining energy from non-renewable sources is becoming too expensive or too environmentally damaging nowadays. A energy source with high potential for green energy production is biogas. However, in order to have a suitable biogas utilization, impurities such as H2S and reduced sulfur compounds (RSC) produced during the anaerobic fermentation of S-bearing organic molecules must be removed [1]. Removal of H2S is strictly necessary to avoid corrosion of internal combustion engines during co-generation processes as well as for proper performance of further biogas upgrading technologies [2]. Biological technologies such as biotrickling filters (BTF) have demostrated to be a suitable, competitive treatment technology for biogas conditioning when compared to physical-chemical technologies. However, main effort has been focus on experimental works, studying different pollutant loads [3], using different packing materials [4], different oxygen mass transfer devices [5], pH conditions [6] or gas-liquid flow pattern [7]. Tough process modeling has shown to be a crucial tool to evaluate the technical [1] and economical feasibility [2] of biological processes prior full-scale implementation, few efforts have been made in this direction on biogas desulfurization in BTFs.”

4-Introduction

References cited should either be applicable to this topic or be very general; this is not the case for [1]-[4]. Also [5]-[8] seem to be 'thrown in'. Specify what the individual references are about rather than listing references all together.

Answer:

General references or not directly applicable to the topic have been removed. Former paragraph starting from P3L4 until P3L8 has been removed. In general, references have been cited individually and an individual explanation has been provided instead of referencing all together at the end of the sentence. However some references have been kept grouped where the sentence points to a common fact.

5-Introduction

The introduction on biodegradation mechanism and kinetics (p3 line 41 till p4 line 37) is not relevant for the introduction since the biological model was not developed in this contribution. At most, it could be summarized in the model description

Answer:

The introduction on biodegradation mechanism and kinetics has been removed from the introduction section and was summarized in the kinetic model description. Paragraph starting on P4L20 until P5L9 has been removed from the introduction section and summarized on section 2.2.2 (P11L4 to P12L2).

6-Introduction

part. p5 lines29-37 do not belong in the introduction either.

Answer:

This paragraph has been also moved to kinetic model description on P11.

7-Materials and Methods

Before giving details on the reactor dimension and packing, specify the general layout and operating principle (p5, line 48).

Answer:

The operating principle of the reactor is now explained just at the beginning of the section and rewritten as follows:

P5L22: "A laboratory-scale BTF reactor, with an ancillary unit for air supply, was used in this study to remove high loads of H_2S from biogas mimics streams (Fig.1). The biogas mimics consisted in controlled mixtures of H2S and nitrogen (N_2) fed at the top of the BTF (1). An air flow (2) was firstly fed to an aeration column (3) for air supply to increase the dissolved oxygen (DO) concentration in the liquid phase. Exhaust air (4) from the aeration column was fed at the top of the BTF under a co-current flow pattern and mixed with the biogas inlet stream at an O2/H2S supplied ratio of 41.2 (v v^{-1}). After biological degradation on the BTF bed (5), the treated biogas stream (6) leaves the reactor. The liquid phase was continuously recycled from bottom-to-top of the BTF at a trickling liquid velocity (TLV) of 4.4 m h^{-1} (7). The liquid recirculation line (8) was previously oxygenated in an aeration column. The DO concentration in the recycle and purge lines was monitored in-situ in all the experiments. The reactor pH was also controlled at pHs of around 6.5 and 7 using an ON/OFF control system by automated addition of NaOH 1M or HCl 1 M. An empty bed residence time (EBRT) of 118 s and an average hydraulic retention time (HRT) of 30 ± 4 h were maintained throughout the study by regulating the purge pump (9) and the mineral medium pump (10). Regarding the packing bed characteristics, the reactor diameter was 7.14 cm with a packed bed volume of $2.80 \cdot 10^{-3}$ m^3 (Vbed). Polypropylene Pall rings of 15.9 mm diameter (MACH engineering products, USA) with a specific surface area of 354 m^2 m^{-3} were used."

8-Materials and Methods

Explicitly specify the experimental dataset and the periods 1-2-3. Are these periods consecutive?

Answer:

Experimental conditions presented on data provided on Table 1 (H_2S inlet concentration, H_2S Loading Rate, O_2/H_2S volumetric ratio) are commonly enough to describe the operating conditions to facilitate the comparison between different systems with different dimensions. Periods 1-2-3 were not consecutive, all experiments were performed in between a time span of 15 months. The following phrase was added to clarify:

(P7L10) "Periods of table 1 does not correspond to consecutive periods, all experiments were performed in between a time span of 15 months."

9-Materials and Methods

Specify gas flow rate (constant for all experiments?).

Answer:

Gas flow rate is not specified since the key parameter is the gas contact time (EBRT). The gas flow rate can be determined relating the EBRT and the volume of the packed bed. The following phrase was added in order to clarify this.

(P7L4) "…in the lab-scale BTF set up (Fig. 1) operating at constant EBRT and constant biogas flow."

10-Materials and Methods

Is O_2 concentration varying - O_2/H_2S variations only caused by varying H_2S?

Answer:

The O_2/H_2S volumetric ratio varied only due to H_2S inlet concentration increase since the air flow rate was kept constant in this work. The following phrase was added in order to clarify this: (P7L4) "…in the lab-scale BTF set up (Fig. 1) operating at constant EBRT and constant biogas flow."

11-Materials and Methods

Separate description of experimental setup and the model (lines 7, 12 and 42 do not fit here; also reconsider the paragraph starting on p6, line 48).

Answer:

Lines describing model variables on experimental setup description have been removed.

12-Materials and Methods

Figure 1 and Figure 3 could be left out and replaced by (and extended version of) Figure S2, detailing how the different layers in the BTF are described - the description on p7 referring to different indices is difficult to follow without a figure.

Answer:

Figure 1 and 3 and Figure S2 have been merged in order to have a complete description in a single figure (new Figure 1) to help the comprehension of the BTF set up, BTF discretization and biological mechanisms of H_2S biological oxidation

13-Materials and Methods

The model description could be written more concisely by describing the meaning of the different balances and by listing the parameters in a 'nomenclature' section.

Answer:

The parameters have been listed in a nomenclature section.

14-Materials and Methods

2.2.2. 'Kinetic model'. Not only kinetic, but also stoichiometry, right? Rather entitle this section 'modelling biological and chemical sulfur conversions'.

Answer:

Right, the name has been changed. To avoid confusion with elemental sulfur, S-compounds has been used instead of sulfur.

(P11L3) "2.2.2 Modeling of biological and chemical S-compounds conversions"

15-Materials and Methods

It would be a strong added value to summarize the biological reactions in Gujer matrix format, to have a clear overview of the state variables and the model stoichiometry and kinetics.

Answer:

The model proposed by Mora et al. 2016 to describe the multi-step sulfide oxidation bioprocess has been summarized in the Gujer Matrix format in Tables 2 and 3 in which the stoichiometry and the kinetic expressions, respectively, are described.

16-Materials and Methods

This whole section needs to be significantly shortened, given that the model was developed by Mora et al. [27].

Answer:

We agree with the reviewer. Since part of the introduction related to general considerations about biodegradation mechanism and kinetics has been moved to this section (see answer to comment #5) the description of the model by Mora et al has been moved to the supplementary material Section SM-4.

17-Materials and Methods

p11, line 28 'no previous works has intended to model such range of intermediate products of biological sulfide oxidation'. If this is a major novelty, it should already be stated in the introduction and. I would also expect a discussion later in the article on whether or not it is important to consider a multi-step oxidation mechanism.

Answer:

This sentence has been moved to the introduction section (P5L16). The discussion about this major novelty has been added as a final discussion on the result section as follows:

(P21 L2) "Especially, accurate model predictions under high H_2S-LR and O_2 limiting conditions (period 1) could be useful for predicting elemental sulfur accumulation in industrial BTF installations. Therefore, maintenance tasks can be strategically planned"

18-Materials and Methods

2.3 Model implementation.

p13 'set of PDE was discretized'. This information comes late - needed to interpret mass balances.

Answer:

Yes. This paragraph has been moved to (P8L8) in the model development section just before the mass balances.

19. Results and discussion

3.1 Give a definition of the sensitivity function. Did you consider relative or absolute sensitivity? This will of course impact the comparability of the numbers obtained.

Answer:

Sensitivity function definition was included as follows:

(P13L8) "Sensitivity was assessed by increasing and decreasing model parameters by 10% and comparing the relative change of the output variables to a relative change of the model parameter."

Also the word "relative" was added before "sensitivity analysis" throughout the manuscript (mostly in section 3.1, page 13) to indicate that the relative sensitivity was assessed.

20. Results and discussion

Also reconsider the structure of this section, emphasizing the main points. First describe most sensitive parameters, then the least sensitive, afterwards discuss.

Answer:

In the former version of the manuscript the most sensitive output variables were firstly described and, afterwards, the less sensitive. Also, the discussion was already based only on the most sensitive parameters (with higher relative sensitivity function value than 0.1). However, the first sentence in P13L24 was changed to follow the same structure from more to less sensitive variables throughout the discussion.

(P13L24) "The most sensitive output variables were the RE and $C_{L,SO42-}$ that exhibited comparable sensitivities between them at a 10% increase while m_{S0} was the less sensitive output variable due to its cumulative nature."

21. Results and discussion

p15 'O2 transport rather than H2S transport is the limiting step'. But O2 transport and H2S transport take place in separate reactors, right?

Answer:

The goal of using an external aeration column was to improve the O_2 gas-liquid mass transport before air enters the BTF column. The total amount of oxygen supplied to the BTF was the contribution of that supplied to the liquid phase in the aeration column plus the excess air from the aeration column that passed through the packed bed of the reactor. The contribution of the O_2 transferred in the aeration column was estimated to be between 10 and 30% of the total (aeration column + reactor) O_2 transferred. This discussion has already been made in previous works by Lopez et al. No changes were made to the manuscript.

22. Results and discussion

3.2 The first paragraph (starting on p16 line 49) rather belongs to 'Materials and methods'.

Answer:

The paragraph was moved to the Materials and Methods section (now in P12L10)

23 Results and discussion

p17 '157g of elemental sulfur'. How was this amount determined?

Answer:

Since Kmax is the relation between the maximum amount of elemental sulfur that could be accumulated inside SOB cells before this accumulation completely blocked the biological sulfide consumption such maximum amount of elemental sulfur was determined using the substrate switch constant (Kmax) and the biomass concentration estimated by the model (X) according to $K_{max} = \frac{m_{S^0 max}}{X}$. This comment was added to the manuscript as:

(P16L7) "Since Kmax is the relation between the maximum amount of elemental sulfur that could be accumulated inside SOB cells before this accumulation completely blocked the biological sulfide consumption, this maximum amount of elemental sulfur was determined using the substrate switch constant (Kmax) and the biomass concentration estimated by the model (X) according to $K_{max} = \frac{m_{S^0 max}}{X}$. Thus, under the calibration conditions, a maximum amount of 157 g of elemental

sulfur could be accumulated inside SOB cells, well above the amount of elemental sulfur produced."

24. Results and discussion

p17 Clarify that the results presented in Fig4 and Fig5 are the model calibration results (also in caption Fig 4).

Answer:

Caption in figure 4 was changed. The sentence in the manuscript was changed to:

(P17L4) "In Fig. 3 and Fig. 4 experimental results and model predictions of the effect of stepwise LR increases due to H_2S inlet concentration increases corresponding to the model calibration period are presented".

25. Results and discussion

p17 line 59 'Fig 4'. Where to look exactly?

Answer:

Truly, in Figure 4 (now Figure 3) there was no RE plotted but the H_2S concentration. The sentence was rewritten as follows:

(P21 L21) "Experimental data in both figures indicate that the system was able to remove almost 100% of H_2S inlet concentration at all H_2S-LR (Fig. 3A and 3B)."

26. Results and discussion

p20, line 26 'Sulfate concentration increases during steady state'. If the concentration changes, steady state has not yet been reached. What causes the change - do you expect it to keep going on?

Answer:

We agree with the reviewer. We meant "stationary feeding period" instead because the inlet conditions were constant. In fact, a BTF hardly reaches steady-state conditions since there is biomass growth, changes in the preferential paths inside the packed bed etc… Pseudo-steady state conditions were replaced by stationary feeding period throughout the manuscript.

27. Results and discussion

p21 'Overall, the model described processes occurring in the three phases'. Specify which figures correspond to which phase.

Answer:

The sentence was confusing. The sentence now reads as:

(P20L22) "Overall, the model showed to be valid to describe the main processes occurring in the three phases of a BTF, gas phase (Fig. 3A and 3B), liquid phase (Fig. 4A) and solid phase as elemental sulfur (Fig. 4B) in a co-current flow mode configuration"

28. Conclusions

The conclusions are too general. Specify conclusions related to the model set-up, calibration and validation separately.

Answer:

The conclusions have been modified, describing separately each part of the work from the sensitivity analysis until the constant feeding validation period and the dynamic validation period. Most of this section has been rewritten as follows:

(P21L21) "…… A preliminary assessment through a relative sensitivity analysis allowed determining the most sensitive parameters of the model. Parameters related to O_2 mass transport exhibited a larger influence to model output variables considered (RE, $C_{L,SO42-}$ and m^{S0}). The proposed model was calibrated using experimental data, which allowed describing accurately the outlet H_2S concentration profile along the BTF bed during H2S-LR increments. Besides describing properly sulfate production, elemental sulfur, the main intermediate product during H_2S oxidation, was correctly predicted. Mass transfer parameters (δ_B, δ_L, K_L,H_2S) and kinetic parameters (X, $\mu_{max,2}$) were estimated during BTF model calibration.

Moreover, the BTF model was validated under a stationary feeding period and a dynamic H_2S-LR period. Proper gas phase description during both periods was obtained. More importantly, elemental sulfur and sulfate were also in agreement with experimental data. Dynamic validation results demonstrated that the model is able to predict correctly the BTF operation when a variable H_2S-LR profile is applied. Hence the BTF model here presented is capable to predict the BTF performance under similar conditions as those found in real plants, making it a suitable tool in order to develop and design control strategies towards process optimization of desulfurizing BTFs."

29. Conclusions

The last part (p22 lines 19-29) belongs to the discussion rather than the conclusions section.

Answer:

This section was moved to the last part of the discussion on the results section

(P21L2) "Especially, accurate model predictions under high H_2S-LR and O_2 limiting conditions (period 1) could be useful for predicting elemental sulfur accumulation in industrial BTF installations. Therefore, maintenance tasks can be strategically planned. Moreover, the development of the BTF model can be used for the development and simulation of control strategies towards process optimization. Parameters related to O_2 transport are crucial in order to completely oxidaize H2S and avoid the formation of elemental sulfur in the BTF bed, since an excessive accumulation of elemental sulfur can significantly diminish the reactor performance. Therefore, control strategies must be based on the improvement of the oxygen transfer to the liquid phase towards process optimization."

OTHER REMARKS

Mind using uniform terminology throughout the manuscript:

- steady state (p6) or 'stationary'?

Answer:

See answer to comment #26

- ancillary column - oxygenation column - aeration column
Answer:
Aeration column has been used along the complete manuscript

'biogas mimics stream': just write 'biogas stream' and specify in the M&M section that it is a synthetic stream.
Answer:
Biogas stream has been used along the complete manuscript

p7 line34, sentence incomplete
Answer:
The sentence has been completed as follows

(P7L24) "…interface occurring in the aeration column."

p10 'sump' - you mean a buffer tank? Was not specified in the description of the installation.
Answer:
The sentence has been changed to:
P6L22
"Liquid present in the bottom section of the BTF (7) was recycled to the aeration column"

Figure 4A and Figure 5A&B should be grouped in one figure so it is clear to which LR the results correspond.
Answer:
We tried to group these figures in a single figure but it was too packed that was hardly understable. We kept them split in two as it was presented in the first version of the manuscript. However to clarify Figure 5 (now figure 4), we added the H2S inlet concentration profile to have a clearer reference.

replace 'in coherence with', 'in concordance with' by 'in agreement with' or 'correspond with'.
Answer:
They have been changed along the manuscript

References
- all authors should be listed for each publication, do not use 'et al.'
Answer:
All authors are now listed in the references

- give full and accurate reference, including volume and page numbers, e.g. for [26] and [27]
Answer:
Reference [26] now reference [7] does not have a volume and page numbers yet.
Reference [27] now reference [21] has been modified and the volume and page numbers have been added.

- avoid typos e.g. p22 line 53, p24 line 17,
Answer:
Typos have been corrected in the manuscript

Graphical Abstract (for review)

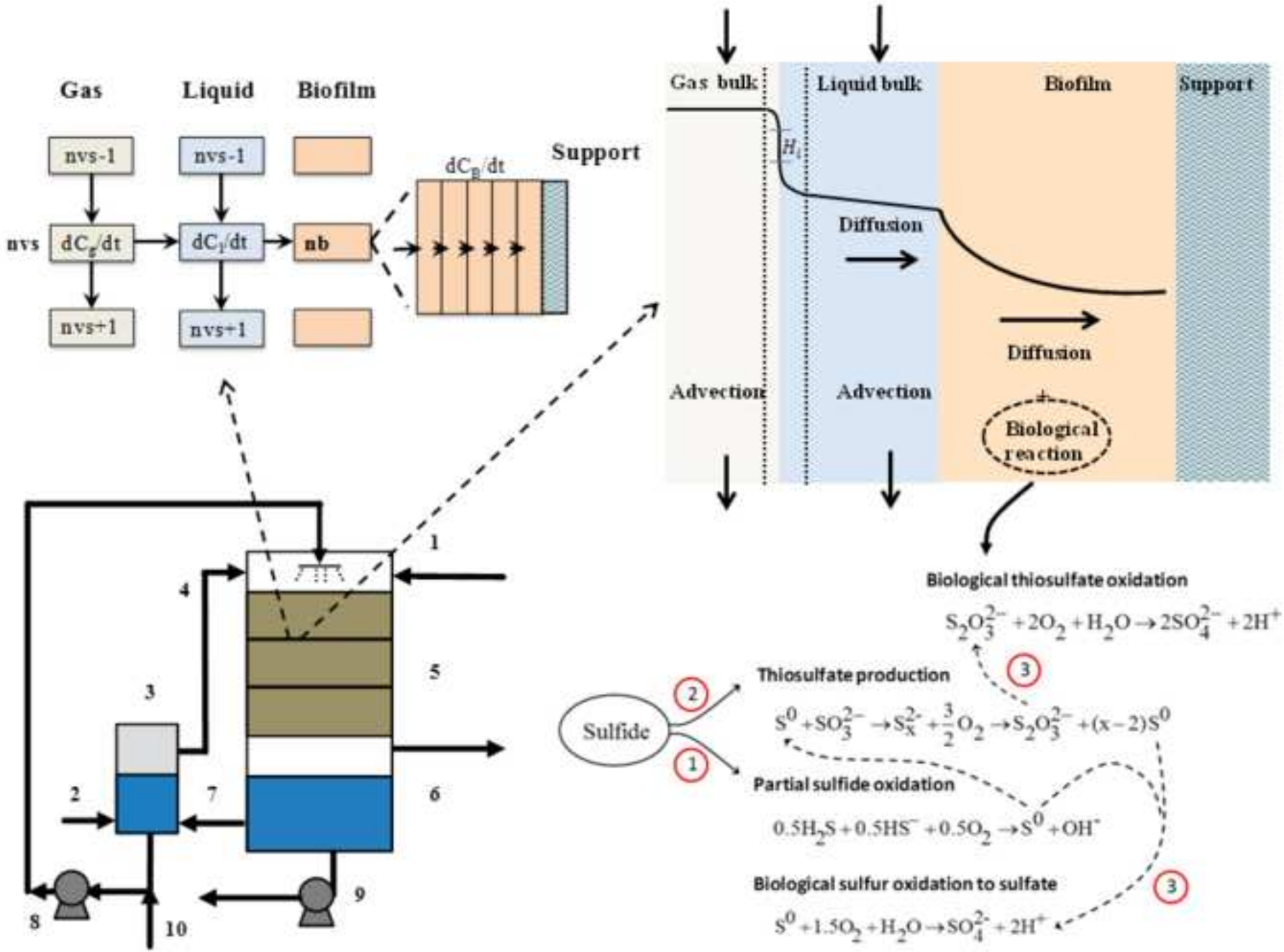

Highlights

- A model describing desulfurization of biogas in a biotrickling filter was developed
- Calibration at 5 H_2S loading rates allowed estimating 5 model parameters
- Model validation was performed with dynamic elemental sulfur and sulfate profiles.
- H_2S removal was influenced by G-L mass transfer and by biological degradation.
- G-L oxygen transfer is crucial to avoid sulfur accumulation in the packed bed.

Modeling an aerobic biotrickling filter for biogas desulfurization through a multi-step oxidation mechanism

L.R. López[a], A.D. Dorado[b], M. Mora[a], X. Gamisans[b], J. Lafuente[a], D. Gabriel[a*]

[a] GENOCOV Research Group, Department of Chemical, Biological and Environmental Engineering, Escola d'Enginyeria, Universitat Autònoma de Barcelona, 08193 Bellaterra, Spain.

~~[a] Universitat Autònoma de Barcelona, Department of Chemical Engineering, Escola d'Enginyeria, 08193 Bellaterra, Spain.~~

[b] Universitat Politècnica de Catalunya, Department of Mining Engineering and Natural Resources, Bases de Manresa 61-73, 08240 Manresa, Spain.

*Corresponding author e-mail: david.gabriel@uab.cat

Abstract

A dynamic model describing physical-chemical and biological processes for the removal of high loads of H_2S from biogas streams in biotrickling filters (BTFs) was developed, calibrated and validated for a wide range of experimental conditions in a lab-scale BTF. The model considers the main processes occurring in the three phases of a BTF (gas, liquid and biofilm) in a co-current flow mode configuration. Furthermore, this model attempts to describe accurately the intermediate (thiosulfate and elemental sulfur) and final products (sulfate) of H_2S oxidation~~. through a kinetic model developed using respirometric techniques~~. A sensitivity analysis was performed in order to focus parameters estimation efforts on those parameters that showed the highest influence on ~~modeling results over~~ the estimation of the H_2S removal efficiency, the accumulated mass of sulfur and the sulfate concentration in the

liquid phase ~~($C_{L,SO4}^{2-}$).~~ ~~main process variables.~~ Biofilm and liquid layer thicknesses, specific growth rate of biomass over elemental sulfur and the H_2S global mass transfer coefficient were the parameters that showed the highest influence on model outputs. Experimental data for model calibration corresponded to the operation of the BTF under stepwise increasing H_2S concentrations between 2000 and 10000 ppm_v. Once the model was calibrated, validation was performed by simulating a stationary feeding period~~pseudo- steady-state period~~ of 42 days of operation of the BTF at an average concentration of 2000 ppm_v and a dynamic operation period were the BTF was operated under variable inlet H_2S concentration between 1000 and 5000 ppm_v to simulate load fluctuations occurring in industrial facilities. The model described the reactor performance in terms of H_2S removal and predicted satisfactorily the main intermediate and final products produced during the biological oxidation process.

Keywords

Desulfurizing biotrickling filter; biogas; modeling; kinetics; sensitivity analysis; elemental sulfur

1. Introduction

Obtaining ~~E~~energy ~~related to~~from non-renewable sources ~~are~~is becoming too expensive or too environmentally damaging ~~to retrieve~~nowadays. ~~One~~A ~~stream~~energy source with high potential for green energy production is biogas. However, in order to have a suitable biogas utilization, impurities such as H_2S and reduced sulfur compounds (RSC) ~~coming from~~produced during the anaerobic fermentation of S-~~B~~bearing organic molecules must be removed [1]. Removal of H_2S is strictly necessary to avoid corrosion of internal combustion engines during co-generation processes as well as for proper performance of further biogas upgrading technologies [2]. Biological technologies such as biotrickling filters (BTF) ~~when~~

~~compared to physical-chemical technologies, such as biotrickling filters (BTF),~~ have demostrated to be a suitable, competitive treatment technology for biogas conditioning when compared to physical-chemical technologies. However, main effort has been focus on experimental works, studying different pollutant loads [3], using different packing materials [4], different oxygen mass transfer devices [5], pH conditions [6] or gas-liquid flow pattern [7]. Tough process modeling has shown to be a crucial tool to evaluate the technical [1] and economical feasibility [2] of biological processes prior full-scale implementation, few efforts have been made in this direction on biogas desulfurization in BTFs.

~~Process modeling has shown to be a crucial tool to evaluate the technical and economical feasibility of biological processes prior to full-scale implementation [1,2] and for the development of control strategies [3,4]. Mathematical modeling of liquid phase biological processes, such as those related to nutrients removal through different biological technologies, has been extensively studied and reported [5–8]. Also m~~Multiphase biological processes, such as biofiltration in biofilters and biotrickling filters (BTF) for the removal of different type of contaminants like volatile organic compounds (VOCs) [7–9] and ammonia [10,11], have been modeled describing both transient and steady-state conditions.

However, most BTF models have focused on VOCs removal [12], while literature available for H_2S BTFs modeling is scarce [13–15]. Therefore, a model describing properly the removal of high loads of H_2S in BTFs is still lacking in literature. Previous models for H_2S removal in BTFs have focused on removal of H_2S at odor level concentrations [13,14,16], while only few models in literature dealt with high loads of H_2S [17,18]. In most cases, the inherent complexity of such plug-flow, heterogeneous, multiphase bioreactors has been strongly simplified to avoid facing a large number of unidentifiable parameters. Often, G-L

mass transport, diffusion in the biofilm and biological degradation kinetics have been identified as the most relevant processes. The heterogeneity of the water-biofilm layers, as well as the kinetics and mechanisms considered to model H_2S removal in BTFs, are the two main aspects that have been addressed differently by several authors. Most models consider an homogeneous biofilm density, a biofilm completely wetted along the packed bed height [13,17,19] and H_2S and O_2 mass transfer from the gas to the liquid phase prior to their diffusion to the biofilm were degradation takes place. Usually, only mass transfer resistance in the liquid phase is considered for modeling G-L mass transport due to the high interstitial gas velocity in the packed bed. However, biogas desulfurization requires of much longer gas contact times and, consequently, lower gas velocities that may increase mass transfer resistance in the gas phase. Also, several alternatives have been proposed to model such bioreactors such as considering a partially or a fully wetted biofilm as well as considering or not adsorption of a fraction of the pollutant by the biofilm [14,20]. ~~However,~~Despite no clear consensus has been reached so far and a careful analysis from a modeling perspective must be performed, modeling of biotrickling filters using a wetted/non-wetted biofilm approach seems necessary when the TLV is modified due to the changing amount of water in the packed bed. ~~.~~

One of the most critical parts in the development of a model is how biodegradation mechanisms and kinetics are described, since depending on the operational conditions, the process might become biodegradation rate-controlled [15]. Different biodegradation kinetics models and degradation mechanisms have been used in order to describe the substrate consumption in BTFs models for H_2S removal. Eqs. 1 and 2 are usually lumped in a single equation describing the complete oxidation of sulfide to sulfate [14]. However, partial oxidation to elemental sulfur has been often observed in BTFs for biogas desulfurization [5]. For this reason, a two-step mechanism (Eqs. 1 and 2) is needed for proper system modeling.

$$H_2S + 0.5O_2 \rightarrow S^0 + H_2O \quad (1)$$

$$S^0 + 1.5O_2 \rightarrow SO_4^{2-} + H^+ \quad (2)$$

~~A Monod-type kinetic expression is often used to describe substrate consumption [13,14] in desulfurizing systems, being H_2S the only rate-limiting substrate. However, different authors have shown that the treatment of high-loads of H_2S, such as those found in biogas desulfurization processes, may lead to substrate inhibition or oxygen-limiting conditions. A multi-substrate type equation with a Haldane term for H_2S and a Monod term depending on the dissolved oxygen (DO) concentration inside the biofilm have been shown to describe well experimental oxygen uptake rate (OUR) and H_2S uptake rate profiles [20] during the characterization of H_2S-oxidizing biofilms in BTFs. Some authors have also proposed the use of a kinetic equation in which the ratio of elemental sulfur/sulfate produced is based on the DO concentration [21]. A product selectivity function for elemental sulfur or sulfate based on the sulfide oxidation activity and the OUR has been also considered [22,23]. It is well-known that elemental sulfur, the main intermediate product of H_2S biological oxidation, is formed due to O_2 transport limitations inside the BTF bed [24,7]. Thus, obtaining an accurate model that describes well the production and accumulation of intermediate products of H_2S biological oxidation is crucial to describe accurately biogas desulfurization in BTFs.~~ Obtaining an accurate model that describes well the production and accumulation of intermediate products of H_2S biological oxidation is crucial to describe accurately biogas desulfurization in BTFs. Recently, Mora et al. [21] have proposed a multi-step pathway for describing sulfide-oxidizing bacteria (SOB) as catalyst of H_2S oxidation to SO_4^{2-} considering the partial sulfide oxidation to elemental sulfur, as an intracellular product, and the sulfite and thiosulfate production as additional intermediates. Such mechanistic model was calibrated and

validated through homogeneous respirometric tests providing successful results in describing the main species of the H_2S oxidation process.

From a practical point of view, prediction of desulfurizing BTFs performance is essential. Low sulfate production rates can lead to an excessively elemental sulfur formation that accumulates into the packed bed. Consequently, a significant increase in pressure drop inside BTF bed occurs [22], with a considerable reduction of BTF operational life-span and process security. However, few works have addressed this topic so far. There is still the need for the development of tools that impulse the industrial application of this emerging biological-based technology. BTF models are essential in design steps, besides useful in the development of control strategies towards process optimization.

From the stated above, the aim of this work was to develop, calibrate and validate a dynamic model of an aerobic BTF for the removal of high-loads of H_2S from biogas streams. The BTF model attempts to describe intermediate and final products obtained from H_2S oxidation under stationary feeding periods~~pseudo steady state~~, transient and dynamic conditions. It has to be remarked that no previous works ha~~s~~ve intended to model such range of intermediate products of biological sulfide oxidation in BTFs for biogas desulfurization ~~To reduce the uncertainty due to general assumptions and parameters based on literature correlations, the model herein uses a multi-step kinetic model previously developed by Mora et al. [21] and calibrated using respirometric techniques with biomass samples obtained from the BTF set-up used herein.~~

2. Material and methods

2.1 Experimental setup and operating conditions

A laboratory-scale ~~biotrickling filter~~BTF reactor, with an ancillary unit for air supply, was used in this study to remove high loads of H_2S from biogas mimics streams (Fig.1). The biogas mimics ~~Operating principle of the BTF set-up is as follows accordingly to in Fig. 1: biogas~~ consisted in controlled mixtures of H_2S and nitrogen (N_2) ~~inlet stream is located at~~fed at the top of the BTF (1). A ~~which was an synthetic stream composed by H_2S and nitrogen (N2); n~~ a~~A~~ir flow- (2) was firstly fed to ~~the~~an ~~ancillary unit~~aeration column (3) for air supply to increase the dissolved oxygen (DO) concentration in the liquid phase. ~~;~~Exhaust air (4) from the aeration column was fed at the top of the BTF under a co-current flow pattern and mixed with the biogas inlet stream at an O_2/H_2S supplied ratio of 41.2 (v v^{-1}). After biological degradation on the BTF bed (5), ~~b~~the treated biogas stream (6) leaves the reactor. The ~~L~~liquid ~~present~~phase was continuously recycled from bottom-to-top ~~in the bottom section of the~~ of the BTF at a trickling liquid velocity (TLV) of 4.4 m h^{-1} (7) ~~was recycled to the aeration column~~. The liquid recirculation line (8) ~~stream~~was previously oxygenated in ~~the~~an aeration column ~~was directly fed from the top of the BTF at a trickling liquid velocity (TLV) of 4.4 m h^{-1}~~. The DO concentration in the recycle and purge lines w~~ere~~as monitored in-situ in ~~for~~ all the experiments. The reactor~~;~~ pH was also controlled at pHs of around 6.5 and 7 using an ON/OFF control system by automated addition of NaOH 1M or HCl 1 M.

An empty bed residence time (EBRT) of 118 s and an average hydraulic retention time (HRT) of 30 ± 4 h were maintained throughout the study by regulating the purge pump (9) and the mineral medium pump (10) ~~during reference conditions~~. Regarding the packing bed characteristics, the reactor diameter was 7.14 cm with a packed bed volume of $2.80 \cdot 10^{-3}$ m^3 (V_{ped}). Polypropylene Pall rings of 15.9 mm diameter (MACH engineering products, USA) with a specific surface area ~~per volume unit of packed bed (a)of~~ 354 m^2 m^{-3} were used.

~~The reactor diameter was 7.14 cm with a packed bed volume of 2.80 L. Polypropylene Pall rings of 15.9 mm diameter (MACH engineering products, USA) with a specific surface area~~

Formatted: Subscript

Formatted: Subscript

Formatted: Superscript

Formatted: Subscript

Formatted: English (United States)

~~of 354 m^2 m^{-3} were used. An empty bed residence time (EBRT) of 118 s and an average hydraulic retention time (HRT) of 30 ± 4 h were maintained during reference conditions. Air was supplied to the liquid phase by continuous aeration at an O_2/H_2S supplied ratio of 41.2 (v v^{-1}) using a digital mass flow controller (Bronkhorst, The Netherlands). Air flow was first fed to the ancillary unit for air supply to increase the dissolved oxygen (DO) concentration in the liquid phase. Inlet and outlet DO concentrations from the oxygenation column where also simulated. Exhaust air from the oxygenation column was fed at the top of the BTF under co-current flow pattern. Oxygen consumption along the BTF column is also described by model equations. The liquid recirculation stream previously oxygenated in the aeration column was directly fed from the top of the BTF at a trickling liquid velocity (TLV) of 4.4 m h^{-1}. The DO concentration in the recycle and purge line were monitored in situ for all the experiments; pH was also controlled around 6.5 and 7 using an ON/OFF control system by automated addition of NaOH 1M or HCl 1 M.~~

Furthermore, H_2S, O_2 and carbon dioxide (CO_2) in the gas phase were monitored on-line through three gas phase streams obtained from the gas outlet stream and from gas sampling ports were monitored on-line with an electrochemical H_2S(g) sensor (Sure-cell, Euro-Gas Management Services, UK), O_2 gas sensor (O_2 SL sensor, Euro-Gas Management Services, UK) an CO_2 gas sensor (CO_2 probe GMP343 Vaisala Carbocap, Vaisala, Finland). Sampling ports were located along the BTF height at 0.24 m, 0.51 m and 0.7 m in order to monitor the H_2S concentration profile along the BTF bed and therefore compare it with simulated data. Further information about gas concentration measurement can be founded on Supplementary Material, section SM.-1. –Also, detailed information of the BTF inoculation, analytical methods and related information can be found elsewhere [7].

The calibration of model parameters was performed using data obtained during stepwise H_2S Loading Rate (H_2S-LR) ~~LR~~ increments as a consequence of H_2S inlet concentration ($Cg_{,H2S,in}$) increase (Period 1-Table 1) in the lab-scale BTF set up (Fig. 1) operating at constant EBRT and constant bio~~air~~gas flow. For model validation under stationary H_2S feeding ~~pseudo steady state conditions~~, a period of 42 days was simulated at a constant $Cg_{,H2S,in}$ ~~H_2S inlet concentration~~ of 2000 ppm_v (Period 2-Table 1). In addition, model was also validated under dynamic conditions (Period 3-table 1) by simulating variable H_2S-LR conditions due to $Cg_{,H2S,in}$ increase (Fig. 2) emulating daily load fluctuations as those commonly found in real facilities. The averages of maximum and minimum H_2S-LR ~~loading rate~~ values are shown in Table 1. ~~-~~Periods ~~of~~in ~~t~~Table 1 do~~es~~ not correspond to consecutive periods. ~~, a~~All experiments were performed in between a time span of 15 months.

Formatted: Subscript

Formatted: Subscript

2.2 Model development

A three phase model (gas, liquid and biofilm) was considered to model reactor dynamics under a co-current flow pattern configuration. The model also considered the main processes occurring in the aeration column attached to the bioreactor (Supplementary Material, Fig. S1).

2.2.1 Biotrickling filter model

The BTF model incorporates mathematical expressions for the following mechanisms occurring in the packed bed: mass transport by advective flow in the gas and liquid phases, mass transfer at the gas-liquid interface, mass transfer by diffusion at the liquid-biofilm interface, internal diffusion in the ~~liquid and~~ biofilm phase~~s~~ and biological reaction in the biofilm as schematized in Fig. 1~~3~~. Also, the model considered oxygen mass transfer at the gas-liquid interface occurring in the aeration column.

Model equations were built based on the above mentioned mechanisms and assumptions often assumed in BTF models in literature [13,14,20], which can be found in Supplementary Material, section SM-2. Since transport of compounds in the axial direction is modeled as plug flow, the BTF bed was discretized in vertical layers in order to simulate a sequence of continuous stirred tank reactors (CSTR) [23]. Vertical layers (*nvs*) were numbered starting from the top of the BTF (*nvs*=1) to the biogas outlet (*nvso*). Similarly, the biofilm layers (*nb*) ~~was~~ were also divided in different subdivisions starting from the biofilm surface (*nb*=1) to the biofilm subdivision in contact with the packed material (*nbp*). The set of partial differential equations was discretized in space along the bed height and biofilm thickness. The conversion of the tubular reactor into a serial of stirred reactors was verified running simulations at different discretizations and optimizing results and time computing. As a result, an optimal discretization of the biofilter was found, resulting in eight nodes along the bed height (*nvs=8*) and ten nodes along the biofilm thickness (*nb=10*).

The following equations describe the mass balances in the gas, liquid and biofilm phases ~~mass balances~~ and their initial conditions in the BTF:

Mass balance for the gas phase in the BTF

$$\frac{dC_{g,i}^{nvs}}{dt} = \frac{F_T}{V_{g,nvs}} \cdot \left(C_{g,i}^{nvs-1} - C_{g,i}^{nvs}\right) - \frac{K_{L,i} \cdot a}{\varepsilon_g} \cdot \left(\frac{C_{g,i}^{nvs}}{H_i} - C_{L,i}^{nvs}\right) \qquad (3)$$

initial conditions: $t=0,\ C_{g,i}^{nvs}=0$

at the BTF inlet (*nvs*=1): $C_{g,i}^{nvs-1}=C_{g,i}^{in}$

~~subindex~~ Where ~~superscripts~~subscripts *i* refers to either gaseous H_2S or O_2, while $C_{g,i}^{nvs}$ and $C_{L,i}^{nvs}$ are the concentrations of component *i* in the bulk gas phase and bulk liquid phase for a certain layer, respectively (g m^{-3}); ~~F_T is the total (biogas + air) gas flow rate (m^3 h^{-1}); $V_{g,nvs}$ is~~

Formatted: CHISA

Formatted: Font: (Default) Times New Roman, 12 pt, Italic

Formatted: Font: (Default) Times New Roman, 12 pt

Formatted: Font: (Default) Times New Roman, 12 pt, Italic

Formatted: Font: (Default) Times New Roman, 12 pt

Formatted: Font: (Default) Times New Roman, 12 pt

Formatted: Font: (Default) Times New Roman, 12 pt

Formatted: Font: (Default) Times New Roman, 12 pt

Formatted: Font color: Black

~~the empty volume of the packed bed (m^{-3}) of layer *nvs*; H_i is the gas-liquid dimensionless Henry coefficient for component *i* (-); $K_{L,i}$ is the gas-liquid mass transfer coefficient of component *i* ($m\ h^{-1}$) and *a* is the specific surface area per volume unit of packed bed ($m^2\ m^{-3}$).~~

$V_{g,\,nvs}$ (m^3) is calculated as $V_{g,nvs}=\frac{V_b \cancel{V_{bed}} \varepsilon_g}{nvs}$ where $\mathcal{E}_g$ is the gas phase porosity, which represents the volume fraction occupied by the gas phase in the packed and V_{bed} is the empty volume of the packed bed. Notice that G-L mass transport is described by a gas-liquid global mass transfer coefficient referred to the liquid phase (K_L) that considers both the individual gas and liquid mass transfer resistances.

Mass balance for the liquid phase in the BTF

$$\frac{dC_{L,i}^{nvs}}{dt}=\frac{F_L}{V_{l,nvs}}\cdot\left(C_{L,i}^{nvs-1}-C_{L,i}^{nvs}\right)+\frac{K_{L,i}\cdot a}{\varphi}\cdot\left(\frac{C_{g,i}^{nvs}}{H_i}-C_{L,i}^{nvs}\right)-\frac{a\cdot D_i}{\varphi\cdot\delta_L}\cdot\left(C_{L,i}^{nvs}-C_{B,i}^{nvs,1}\right) \quad (4)$$

initial conditions: t=0, $C_{L,\,i}^{nvs}=0$

at the BTF inlet (*nvs*=1): $C_{L,\,i}^{nvs-1}=C_{L,\,i}^{RE}$

subscripts ~~subindex~~ *i* refers to S^{2-}, SO_4^{2-},$S_2O_3^{2-}$ and DO concentration, the compounds considered in the liquid phase of the BTF;~~, while $V_{l,nvs}$ is liquid volume (m^3) of layer *nvs*; $C_{B,i}^{nvs,1}$ is the concentration of component *i* at the biofilm surface ($g\ m^{-3}$); $C_{L,i}^{RE}$ is the concentration of compound *i* in the recirculation flow ($g\ m^{-3}$); F_L is the liquid flow rate ($m^3\ h^{-1}$); D_i is the diffusivity of component *i* in water ($m^2\ h^{-1}$) and δ_L is the thickness of the water layer (m).~~ $V_{l,\,nvs}$ (m^3) is calculated as $V_{l,nvs}=\frac{V_{bed}\cdot\varphi}{nvs}\frac{\cancel{V_{bed}\cdot\varphi}}{nvs}$ where φ is the volume fraction occupied by the liquid phase in the packed bed according to the dynamic hold-up measured (-). Notice that mass transfer resistance in the liquid-biofilm interface was described by Fick's law considering that the whole thickness of the liquid phase acted as the liquid boundary layer for mass transport resistance.

Formatted: Superscript

Mass balances for the biofilm ~~of~~ in the BTF

For the first layer of the biofilm (*nb*=1) and all BTF layers (*nvs*=1 to *nvso*)

$$\frac{dC_{B,i}^{nvs,1}}{dt}=\frac{D_i}{\delta_B\cdot\delta_L}\cdot\left(C_{L,i}^{nvs}-C_{B,i}^{nvs}\right)-\frac{D_i}{\delta_{B\text{-}nb}^{\ 2}}\cdot\left(C_{B,i}^{nvs,1}-C_{B,i}^{nvs,nb+1}\right)+\sum\nu_{ij}\cdot r_{B,j} \qquad (5)$$

~~where subindex *j* indicates the rate equation in which component *i* is participating.~~

For the inner layers of the biofilm (*nb*=2 to *nb=nbp-1*) and all BTF layers (*nvs*=1 to *nvso*)

$$\frac{dC_{B,i}^{nvs,nb}}{dt}=D_i\cdot\frac{\partial^2 C_{B,i}^{nvs,nb}}{\partial\delta_{B\text{-}nb}^{\ 2}}+\sum\nu_{ij}\cdot r_{B,j} \qquad (6)$$

For the closest layer to the packing material (*nbp*) and all BTF layers (*nvs*=1 to *nvso*)

$$\frac{dC_{B,i}^{nvs,nbp}}{dt}=\frac{D_i}{\delta_{B\text{-}nb}^{\ 2}}\cdot\left(C_{B,i}^{nvs,nb-1}-C_{B,i}^{nvs,nbp}\right)+\sum\nu_{ij}\cdot r_{B,j} \qquad (7)$$

initial conditions in Eqs. 5, 6 and 7: t=0, $C_{B,\,i}^{nvs,nb}=0$

boundary conditions in Eqs. 5, 6 and 7: x=0, $C_{B,i}=C_{l,i}$

x=δ_B, $\frac{\partial C_{B,i}^{nvs,nbp}}{\partial t}=0$

in Eqs. 5, 6 and 7, subscripts~~subindex~~ *i* refers to S^{2-}, SO_4^{2-}, $S_2O_3^{2-}$ and DO concentration, the compounds considered in the biofilm phase of the BTF, while subscripts *j* indicates the rate equation in which component *i* is participating. ~~$C_{B,i}^{nvs,nb}$ is the concentration of component *i* at the biofilm subdivision *nb* (g m^{-3}); $\delta_{B\text{-}nb}$ is the thickness of one biofilm subdivision (m) and δ_B is the biofilm thickness (m); υ_i is the stoichiometric coefficient for compound *i* in each process rate ( ); and r_{Bj} is the rate equation for each biological process considered (g m^{-3} h^{-1}).~~

According to the BTF configuration, mass balances in the sump of the reactor (Eq. 8) and in the aeration column (Eqs. 9-10) were included.

Mass balance for the liquid phase in the sump of the BTF

$$\frac{dC_{L,i}^{P}}{dt}=\frac{F_L\cdot C_{L,i}^{nvs}-F_{L,P}\cdot C_{L,i}^{P}+F_{L,In}\cdot C_{L,i}^{In}-F_L\cdot C_{L,i}^{RE}}{V_{L,D}} \qquad (8)$$

initial conditions: t=0, $C^{P}_{L,\,i}=0$

subscripts~~subindex~~ *i* refers to S^{2-}, SO_4^{2-}, $S_2O_3^{2-}$ and DO concentration, the compounds considered in the liquid phase of the BTF, ~~while F_L, $F_{L,In}$ and $F_{L,P}$ are the liquid flow rate, the liquid purge rate and the fresh liquid mineral medium flow rate, respectively ($m^3\ h^{-1}$); $V_{L,P}$ is the volume of liquid in the sump of the BTF (m^3); $C^{P}_{L,i}$ is the concentration of compound *i* in the purge flow ($g\ m^{-3}$) ,$C^{RE}_{L,i}$ is the concentration of compound *i* in the recirculation flow ($g\ m^{-3}$); and $C^{In}_{L,i}$ is the concentration of compound *i* in the mineral medium ($g\ m^{-3}$).~~ Notice that $C^{P}_{L,i}$ and $C^{RE}_{L,i}$ are equal except for dissolved oxygen because of the aeration column located in the recirculation line.

Mass balance for the gas phase in the aeration column

$$\frac{dC^{out}_{g,\,O_2}}{dt}=\frac{F_{O_2}}{V_{gG\_AC}}\cdot\left(C^{AC}_{g,\,O_2}-C^{out}_{g,\,O_2}\right)-K_{L,O_2,AC}a\left(\frac{C^{out}_{g,\,O_2}}{H_{O_2}}-C^{RE}_{L,O_2}\right) \qquad (9)$$

initial conditions : t=0, $C^{AC}_{g,\,O_2}=0$

~~F_{O_2} is the inlet air flow rate to the aeration column (m3 h − 1); V_{gG_AC} is the gas phase volumne of the aeration column (m^3); C^{AC}_{g,O_2} and C^{out}_{g,O_2} are the oxygen inlet and outlet concentration in the aeration column , respectively ($g\ m^{-3}$); $K_{L,O_2,AC}a$ is the gas-liquid mass transfer coefficient for oxygen in the aeration column (h^{-1}); H_i is the O_2 gas-liquid dimensionless Henry coefficient (-);~~

Mass balance for the liquid phase in the aeration column

$$\frac{dC^{RE}_{L,O_2}}{dt}=\frac{F_L}{V_{L\_AC}}\cdot\left(C^{P}_{L,O_2}-C^{RE}_{L,i}\right)+K_{L,O_2,AC}\cdot\left(\frac{C^{out}_{g,\,O_2}}{H_{O_2}}-C^{RE}_{L,i}\right) \qquad (10)$$

Formatted: Font: (Default) Times New Roman

initial conditions: t=0, $C^{P}_{L,O_2}=0$

~~V_{L_AC} is the liquid volume of the aeration column (m^3)~~

2.2.2 ~~Modelling~~Modeling of biological and chemical ~~sulfide~~sulfides-compounds conversions

A Monod-type kinetic expression is often used to describe substrate consumption [13,14] in desulfurizing systems, being H_2S the only rate-limiting substrate. However, different authors have shown that the treatment of high-loads of H_2S, such as those found in biogas desulfurization processes, may lead to substrate inhibition or oxygen-limiting conditions. A multi-substrate type equation with a Haldane term for H_2S and a Monod term depending on the dissolved oxygen (DO) concentration inside the biofilm have been shown to describe well experimental oxygen uptake rate (OUR) and H_2S uptake rate profiles [20] during the characterization of H_2S-oxidizing biofilms in BTFs. Some authors have also proposed the use of a kinetic equation in which the ratio of elemental sulfur/sulfate produced is based on the DO concentration [24]. A product selectivity function for elemental sulfur or sulfate based on the sulfide oxidation activity and the OUR has been also considered by other authors [25,26]. It is well-known that elemental sulfur, the main intermediate product of H_2S biological oxidation, is formed due to O_2 transport limitations inside the BTF bed [7,27].

Formatted: Line spacing: Double

According to the abovementioned findings in literature, the kinetic model proposed by Mora et al. [21] was used herein. The multi-step sulfide oxidation mechanism (Figure 1D) has been summarized in Tables 2 and 3, in which the stoichiometry and the kinetic expressions that describe each of the reactions occurring during the process have been specified. In short, the kinetic model considers that H_2S is partially oxidized to elemental sulfur, which is intracellularly stored, but also to sulfite, which in presence of sulfide reacts to subsequently

form thiosulfate. Then, once sulfide is completely depleted, elemental sulfur and thiosulfate are further oxidized to sulfate, the end product of the reaction. Further information about the biological and chemical sulfide conversions can be found on Supplementary Material, section SM-4 and elsewhere [21].

~~**Kinetic model: multi-step sulfide oxidation**~~

~~A Monod-type kinetic expression is often used to describe substrate consumption [13,14] in desulfurizing systems, being H_2S the only rate-limiting substrate. However, different authors have shown that the treatment of high loads of H_2S, such as those found in biogas desulfurization processes, may lead to substrate inhibition or oxygen limiting conditions. A multi-substrate type equation with a Haldane term for H_2S and a Monod term depending on the dissolved oxygen (DO) concentration inside the biofilm have been shown to describe well experimental oxygen uptake rate (OUR) and H_2S uptake rate profiles [20] during the characterization of H_2S-oxidizing biofilms in BTFs. Some authors have also proposed the use of a kinetic equation in which the ratio of elemental sulfur/sulfate produced is based on the DO concentration [24]. A product selectivity function for elemental sulfur or sulfate based on the sulfide oxidation activity and the OUR has been also considered [25,26]. It is well known that elemental sulfur, the main intermediate product of H_2S biological oxidation, is formed due to O_2 transport limitations inside the BTF bed [7,27]. Thus, obtaining an accurate model that describes well the production and accumulation of intermediate products of H_2S biological oxidation is crucial to describe accurately biogas desulfurization in BTFs. To reduce the uncertainty due to general assumptions and parameters based on literature correlations, the model herein uses a multi-step kinetic model (Fig. 1) previously developed by Mora et al. [21] and calibrated using respirometric techniques with biomass samples obtained from the BTF set up used herein.~~

Formatted: Font: (Default) Times New Roman, 12 pt

Formatted: Font: (Default) Times New Roman, 12 pt

Formatted: Font: (Default) Times New Roman, 12 pt

Formatted: Font: (Default) Times New Roman, 12 pt

Biological degradation of H_2S is described with a multi-step sulfide oxidation kinetic model (Fig. 3) based on Mora et al. [27]. The kinetic model considers that H_2S is partially oxidized to elemental sulfur, which is intracellularly stored, but also to sulfite, which in presence of sulfide reacts to subsequently form thiosulfate. Then, once sulfide is completely depleted, elemental sulfur and thiosulfate are further oxidized to sulfate, the end product of the reaction. It has to be remarked that no previous works has intended to model such range of intermediate products of biological sulfide oxidation in BTFs for biogas desulfurization. Eqs. 11 to 13 correspond to the biological oxidation rates of sulfide, elemental sulfur and thiosulfate. Eq. 14 describes thiosulfate chemical production rate.

$$r_{B,SS}=\left(\frac{1}{Y_{XSS}}\right)\cdot\mu_{max,1}\cdot\left(\frac{C_{B,SS}^{nvs,nb}}{k_{SS}+C_{B,SS}^{nvs,nb}+\frac{C_{B,SS}^{2}}{k_{iS}}}\right)\cdot\left(1-\left(\frac{\left(\frac{C_{B,S}^{nvs,nb}}{X}\right)}{K_{max}}\right)^{\alpha}\right)\left(1-\frac{\left(\frac{C_{B,S}^{nvs,nb}}{X}\right)}{K_{max}}\right)^{\alpha}\cdot\left(\frac{C_{B,OD}^{nvs,nb}}{C_{B,OD}^{nvs,nb}+k_{\sigma}}\right)\cdot X \quad (11)$$

$$r_{B,S}=\left(\frac{1}{Y_{XS}}\right)\cdot\mu_{max,2}\cdot\left(\frac{C_{B,S}^{nvs,nb}}{X}\right)^{2/3}\cdot\left(\frac{K}{C_{B,SS}^{nvs,nb}+K}\right)\cdot\left(\frac{C_{B,OD}^{nvs,nb}}{C_{B,OD}^{nvs,nb}+k_{\sigma}}\right)\cdot X \quad (12)$$

$$r_{B,TS}=\left(\frac{1}{Y_{XTS}}\right)\cdot\mu_{max,3}\cdot\left(\frac{C_{B,TS}^{nvs,nb}}{C_{B,TS}^{nvs,nb}+K_{TS}}\right)\cdot\left(\frac{K}{C_{B,SS}^{nvs,nb}+K}\right)\cdot\left(\frac{C_{B,OD}^{nvs,nb}}{C_{B,OD}^{nvs,nb}+k_{\sigma}}\right)\cdot X \quad (13)$$

$$r_{B,TS\_P}=k\cdot C_{B,SS}^{\beta} \quad (14)$$

subscriptssubindexes SS, S and TS refer to the reaction rate for S^{2-}, S^0 and $S_2O_3^{2-}$ consumption, respectively, while Y_{XSS}, Y_{XS} and Y_{XTS} are the biomass growth yield using S^{2-}, S^0 and $S_2O_3^{2-}$ as substrate respectively (g VSS g^{-1} S); $\mu_{max,1}$, $\mu_{max,2}$ and $\mu_{max,3}$ are the specific growth rates for SOB over S^{2-}, S^0 and $S_2O_3^{2-}$, respectively in h^{-1}, g X $^{1/3}$ $g^{-1/3}$ S h^{-1} and h^{-1}; k_{SS}, k_{σ} are the affinity constants for sulfide and for oxygen, respectively, in g S m^{-3} and g DO m^{-3}; k_{iS} is the sulfide inhibition constant in g S m^{-3}; K_{max} is the maximum intracellular elemental sulfur stored to biomass in g S $g^{-1/3}$ VSS; α is a constant (dimensionless); X is the biomass concentration in g X m^{-3}; K is the substrate switch constant g S m^{-3}; K_{TS} is the

affinity constant for $S_2O_3^{2-}$ consumption in g S m^{-3}; k is the kinetic constant for $S_2O_3^{2-}$ production under biotic conditions; and β is a constant (dimensionless). The model proposed by Mora et al. [21] to describe the multi step sulfide oxidation bioprocess has been summarized in Tables 2 and 3 in which the stoichiometry and the kinetic expressions, respectively, used to describe each of the reactions occurring during the process have been specified. Further information about the biological and chemical sulfide conversions can be founded on Supplementary Material, section SM-4 and elsewhere [21].

H_2S biodegradation kinetics (Eq.11) is described by a Haldane equation since substrate inhibition caused by sulfide over sulfide oxidation is considered. Furthermore, oxygen limitation was described by including a Monod type kinetic term in the rate equations. In addition, accumulation of intracellular elemental sulfur by SOB was considered in order to describe the experimental decrease of the sulfide oxidation rate observed due to accumulation of intracellular elemental sulfur. SOB in the BTF was *Thiotrix sp.* according to pyrosequencing analysis performed during the kinetic model development [21]. Such filamentous γ proteobacteria forms intracellular deposits of elemental sulfur as intermediary product during sulfide oxidation [28].

Elemental sulfur biodegradation kinetics (Eq. 12) was described using a shrinking particle model analogous to that used for biological consumption of other solid substrates such as Poly-hydroxy-butyrate (PHB). A non-competitive inhibition term was included in order to describe the substrate switch. Dissolved oxygen and thiosulfate limitation were described by a multi substrate Monod type kinetic expression. Similarly, thiosulfate oxidation to sulfate (Eq.

Formatted: Font: Times New Roman, Font color: Auto

Formatted: Font color: Auto

Formatted: Font: Times New Roman, Font color: Auto

Formatted: Font color: Auto

Formatted: Font: Times New Roman, Font color: Auto

Formatted: Font color: Auto

Formatted: Font: Times New Roman, Font color: Auto

Formatted: Font color: Auto

~~13) was described considering a Monod type kinetic for substrate consumption, while potential chemical oxidation of sulfide to form thiosulfate was also considered (Eq. 14).~~

2.3 Model implementation

~~The set of partial differential equations was discretized in space along the bed height and biofilm thickness. The conversion of the tubular reactor into a serial of stirred reactors was verified running simulations at different discretizations and optimizing results and time computing. As a result, an optimal discretization of the biofilter was found, resulting in eight nodes along the bed height (*nvs*) and ten nodes along the biofilm thickness (*nb*).~~

The resulting set of ordinary differential equations was solved using MATLAB in a home-made modeling environment. A variable order method was used for solving stiff differential equations based on the numerical differentiation formulas (NDFs), which are generally more efficient than the closely related family of backward differentiation formulas (BDFs), also known as Gear's methods. Since the inlet H_2S concentration was changed throughout the BTF operation, inlet concentration profiles were used as input variable of the model.

Model parameters were estimated during calibration by curve-fitting of experimental data to model predictions to describe the dynamics of a lab-scale BTF for biogas desulfurization. A minimization routine on MATLAB, based on a non-lineal multidimensional minimization (Nelder-Mead) was used. The objective function to minimize was based on RE and $C_{L,SO4}^{2-}$ according to the sensitivity analysis, and also to take into account both the gas-phase and the liquid-phase dynamics, respectively. Also, m_S^0 was not included in the objective function because experimental m_S^0 was not anatilically measured but determined through mass balances [7].

In order to evaluate the goodness of model predictions to experimental data, the efficiency criterion proposed by Nash and Sutcliffe [28] was used. Such efficiency criterion mathematically measures how well a model simulation fits the available experimental data. The efficiency coefficient (NSE) is defined as one minus the sum of the absolute squared differences between the predicted and observed data normalized by the variance of the observed data during the period under investigation according to Eq. ~~15~~11. Essentially, the closer the model efficiency to 1, the more accurate the model is.

$$NSE=1-\frac{\sum_{i=1}^{i=n}\left(y_e-y_m\right)^2}{\sum_{i=1}^{n}\left(y_e-\bar{y}_e\right)^2} \quad (~~15~~11)$$

3. Results and discussion

3.1 Sensitivity analysis

Before the model calibration, a sensitivity analysis was performed in order to determine the parameters that showed the highest influence on model outputs over the main process variables.

Sensitivity ~~analysis~~ was assessed by increasing and decreasing ~~by 10% the values of~~ model parameters by 10% and comparing the relative change of the output variables to a relative change of the ~~value of the~~ model parameter. As stated in Deshusses et al. [14], model parameters fall in the following categories: physical-chemical properties, system specifications (dimensions), biokinetics and mass transfer parameters. In the present work, parameters belonging to all parameter categories were included to perform the relative

Formatted: Indent: First line: 0 cm

Formatted: CHISA, Indent: First line: 0.5 cm

Formatted: English (United States)

Formatted: Font: (Default) Times New Roman, Font color: Auto, English (United States), Do not check spelling or grammar

Formatted: Font: (Default) Times New Roman, Font color: Auto, English (United States), Do not check spelling or grammar

Formatted: Font: (Default) Times New Roman, Font color: Auto, English (United States), Do not check spelling or grammar

Formatted: Font: (Default) Times New Roman, Font color: Auto, English (United States), Do not check spelling or grammar

Formatted: Font: (Default) Times New Roman, Font color: Auto, English (United States), Do not check spelling or grammar

sensitivity analysis of the main output variables on biofiltration such as the H_2S removal efficiency (RE), the accumulated mass of elemental sulfur (m_S^0) and the sulfate concentration in the liquid phase ($C_{L,SO4}^{2-}$). ~~To perform the sensitivity analysis~~In order to determine the relative sensitivity, model parameters were varied 0.9 and 1.1 times the reference value while simulating the stepwise load increase of period 1 (Table 1). Relative ~~Sensitivity~~ sensitivity analysis results were chosen as those corresponding to the H_2S inlet concentration of 10000 ppm_v (Table ~~2~~4) because of a larger relative sensitivity of the model at these inlet concentration. Only those parameters that showed a relative sensitivity higher than 0.10 in at least one of the output variables are shown in Table ~~2~~4. Similar results in terms of relative sensitivity were obtained for the 4000, 6000 and 8000 ppmv concentration steps simulated (results not shown).

The most sensitive output variables were the RE and $C_{L,SO4}^{2-}$, ~~which~~that exhibited comparable sensitivities between them at a 10% increase while m_S^0 was the less sensitive output variable due to its cumulative nature.

~~Because of its cumulative nature, m_S^0 was the less sensitive output variable compared to RE and $C_{L,SO4}^{2-}$, which exhibited comparable sensitivities between them at a 10% increase.~~ However, at a 10% decrease results indicated that RE was highly influenced by parameters of all categories abovementioned to a higher extent than $C_{L,SO4}^{2-}$. Thus, both RE and $C_{L,SO4}^{2-}$ were the sole output variables selected to be included in the objective function during the calibration stage. Despite the low relative sensitivity of m_S^0, the most sensitive parameters were those parameters related to its formation, *i.e.* O_2 and H_2S mass transfer coefficients $(K_{L,O_2}, K_{L,H_2S}, D_{O_2})$, physical-chemical properties (H_{O_2}, H_{H_2S}) and parameters related to its consumption ($\mu_{max,2}$). This result was somehow expected since elemental sulfur formation directly depends on the oxygen availability and the S/DO ratio in the liquid phase that result from their transfer efficiency and solubility.

Formatted: Font color: Auto, Do not check spelling or grammar

Formatted: Normal

Besides the system specific parameters and physical-chemical parameters, the relative sensitivity analysis showed that biokinetic and mass transfer parameters were the most sensitive, which are often the most difficult to determine experimentally [29,30] and usually obtained by curve fitting of model estimations to experimental data [31,32]. Both RE and $C_{L,SO4}^{2-}$ were mostly influenced by physical-chemical parameters such as O_2 and H_2S Henry coefficients (H_{O_2}, H_{H_2S}); system specific parameters such as the specific interfacial area (a); by mass transfer parameters such as the O_2 and H_2S mass transfer coefficients, liquid layer thickness and O_2 diffusivity $\left(K_{L,O_2}, K_{L,H_2S}, \delta_L, D_{O_2} \right)$; and by kinetic parameters such as the specific growth rate for sulfur and to the O_2 half-saturation constant $\left(\mu_{max,2}, k_O \right)$. Consequently, the relative sensitivity analysis indicated that H_2S removal was either influenced by gas-liquid mass transfer and by biological degradation. However, parameters related with O_2 mass transfer such as K_{L,O_2}, H_{O_2} and D_{O_2} exhibited a larger influence compared to the corresponding H_2S parameters. Such result is in consonance with previous works that reported that O_2 transport rather than H_2S transport is usually the limiting step in high-load H_2S biogas desulfurization [3,33]. López et al. [7] showed that the effectiveness of O_2 G-L mass transfer due the trickling liquid velocity (TLV) regulation was a key factor to improve H_2S oxidation in high-load H_2S biogas desulfurization.

Regarding the biokinetic parameters, $\mu_{max,2}$ was the most sensitive parameter, even if exhibited lower sensitivities compared with mass transport and physical-chemical parameters. This result indicates that elemental sulfur accumulation plays a major role as intermediate and that must be included and properly described by any kinetic model. Sulfide oxidation rate can be limited by excessive elemental sulfur accumulation, which is directly influenced by the rate at which elemental sulfur is consumed ($\mu_{max,2}$). In the kinetic model used in the present

work, intermediate reactions such as elemental sulfur production and biodegradation are considered, which means that both the inhibitory or the catalytic effect caused by each species over other bioreactions are reflected.

Excluding those parameters that can be determined using correlations ($K_{L,O2}$), or physical-chemical parameters that can be found in literature (D_{O2}, H_{H2S}, H_{O2}), or provided by the packing manufacturer (a), the most sensitive parameters were selected for model calibration. Five parameters were selected for curve-fitting estimation during model calibration: namely, biomass and liquid layer thickness (δ_B, δ_L), specific growth rate for sulfur ($\mu_{max,2}$), biomass concentration (X) and H_2S global mass transfer coefficient ($K_{L,H2S}$). The number of parameters was selected according to the number of variables assessed (H_2S gas concentrations along the bed height, sulfate concentration and mass of elemental sulfur accumulated).

3.2 Model parameters estimation

~~Model parameters were estimated during calibration by curve fitting of experimental data to model predictions to describe the dynamics of a lab-scale BTF for biogas desulfurization. A minimization routine on MATLAB, based on a non-lineal multidimensional minimization (Nelder-Mead) was used. The objective function to minimize was based on RE and $C_{L,SO4}^{2-}$ according to the sensitivity analysis, and also to take into account both the gas-phase and the liquid-phase dynamics, respectively. Also, m_s^0 was not included in the objective function because experimental m_s^0 was not anatilically measured but determined through mass balances [7].~~ A summary of the BTF model parameters is shown in Tables 5~~3~~ and 4~~6~~, while Fig. ~~4~~ 3 and Fig. ~~5~~ 4 show the comparison of model predictions using the parameters estimated and the experimental data corresponding to the calibration period (Table 1).

Biomass concentration (X) estimated by the model (Table 5~~3~~) was in ~~coherence~~ agreement with the amount of elemental sulfur produced (22.37 g) and the K_{max} determined by Mora et al. [21]~~[26]~~. Since K_{max} is the relation between the maximum amount of elemental sulfur that could be accumulated inside SOB cells before this accumulation completely blocked the biological sulfide consumption, this maximum amount of elemental sulfur was determined using the substrate switch constant (K_{max}) and the biomass concentration estimated by the model (X) according to $K_{max} = \frac{m_{s^0 max}}{X}$. Thus, ~~Under~~ under the calibration conditions, a maximum amount of 157 g of elemental sulfur ~~could~~ could be accumulated inside SOB cells, well above the amount of elemental sulfur produced ~~before this accumulation completely blocked the biological sulfide consumption~~. The K_{L,H_2S} was in ~~concordance~~ agreement with K_{L,O_2} since both K_L values were related by the square root of the diffusivity of each species [13]. The K_{L,O_2} was determined using the ~~Onda~~ Billet and Schultes correlations [34] for the gas and liquid individual mass transfer coefficients *kg* and *kl*, respectively ~~[34][38]~~, which was in close agreement with K_{L,O_2} determined by Dorado et al. [9]. It is worth highlighting that only the liquid-side resistance was significant since based on Billet and Schultes correlations the contribution of individual mass transfer resistances in the gas phase to the overall resistance for both gas species oxygen (O_2) and hydrogen sulfide (H_2S) were only 0.18% and 9.7% for O_2 and H_2S, respectively. In addition, $\mu_{max,2}$ lies close to the range of values determined by Mora et al. [21] ($5 \cdot 10^{-4}$ -$1.1 \cdot 10^{-2}$ h^{-1}). The δ_B denotes that the biofilm was thick enough to contain active and inactive biomass inside the biofilm and that δ_B is in the typical range for H_2S-degrading biofilms [13]. Kim and Deshusses [14] reported a δ_B of 23 µm concluding that, in order to perform the removal of high H_2S loads in biogas, higher δ_B must be achieved. The δ_L estimated during model calibration was in agreement with the value obtained by dividing D_{H_2S} by the K_{L,H_2S}. [13].

Formatted: Default Paragraph Font, Font: (Default) Times New Roman, 12 pt, Font color: Auto, English (United States), Pattern: Clear

Formatted: Font: 12 pt

Formatted: Default Paragraph Font, Font: (Default) Times New Roman, 12 pt, Font color: Auto, English (United States), Pattern: Clear

Formatted: Default Paragraph Font, Font: (Default) Times New Roman, 12 pt, Font color: Auto, English (United States), Pattern: Clear

Formatted: Font: Italic

Formatted: Font: Italic

Formatted: Font: 12 pt

Formatted: Font: 12 pt

In Fig. ~~4~~ 3 and Fig. ~~5~~ 4 experimental results and model predictions of the effect of stepwise LR increases due to H_2S inlet concentration increases ~~are presented~~corresponding to the model calibration period are presented. Experimental data in both figures indicate that the system was able to remove almost 100% of inlet H_2S ~~inlet concentration at RE close to 100%~~ at all H_2S-LR (Fig. ~~4~~3A and 3B). However, 100% sulfate production only occurred at the lowest H_2S-LR corresponding to an inlet concentration of 2000 ppmv. Further information related to sulfate production in this experiment ~~values~~ can be found~~ed~~ elsewhere [7]. Thereafter, elemental sulfur was accumulated in the packed bed (Fig. ~~5A~~4A). At the highest H_2S-LR tested the sulfate production was lower than the elemental sulfur produced, which lead to a decrease of the concentration of sulfate measured in the liquid phase (Fig. ~~5B~~4B). Such behavior was directly related to the oxygen availability and the S/DO ratio in the liquid phase. A linear decrease of the inlet O_2/H_2S volumetric ratio (from 42.2 up to 8.4 % *v* v^{-1}) along the experiment led to limiting oxygen conditions. Thus, elemental sulfur production over sulfate production was favored. No thiosulfate production was detected experimentally neither was predicted by the model.

Regarding the goodness of model predictions to experimental data, high NSE values were obtained for the fitting of H_2S concentration measured at different bed heights (Fig. ~~4A~~3A and 3B). In the range of 2000 to 10000 ppm_v, the model described well experimental H_2S concentrations measured in the first and second sections, with NSE coefficients of E=0.90 and E=0.93, respectively. At an inlet concentration of 10000 ppmv, a Nash-Sutcliffe efficiency coefficient of 0.43 was obtained for the H_2S concentration measured at the BTF outlet, mainly due to a missmatch between model predictions and experimental data. However, the Nash-Sutcliffe efficiency coefficient at the BTF outlet in the range of 2000 to 8000 ppm_v was E=0.90.

Mismatch between model prediction and experimental data of the BTF outlet concentration during the 10000 ppm_v step mighty be related with the H_2S measurement system. At 10000 ppm_v a higher airflow rate is needed to dilute the biogas flow rate in order to measure H_2S concentrations inside the sensor measurement range. Therefore, less exact and precise experimental data is obtained. Additional details of BTF gas measurement system can be found in Supplementary Material, section S1 (Fig. S1).

Regarding to the predictions on the elemental sulfur accumulation (m_S^0), a Nash-Sutcliffe efficiency coefficient of E=0.94 was obtained, indicating an accurate fit of the model to experimental data for the production of elemental sulfur. From Fig. ~~5B~~ 4B it can be observed how the predicted sulfate concentration values fits almost perfectly to all experimental points, although during the step concentration of 4000 ppmv the simulated $C_{L,SO4}^{2-}$ was a 15% higher than the experimental measure. Such difference was attributed to a biological delay time of microorganisms in the BTF to start to produce sulfate, since the first step-wise LR increment up to 4000 ppm_v was the first performed in the reactor after a long stationary feeding period~~pseudo steady state operation~~ at 2000 ppm_v of 42 days. The model reproduced well the sudden $C_{L,SO4}^{2-}$ concentration deacrease during the last concentration step of 10000 ppm_v as a consequence of both the unfavorable S/DO ratio and the amount of elemental sulfur accumulated in the BTF bed. A NSE coefficient of E=0.75 was calculated for sulfate concentration predicted considering the whole period of the 2000-10000 ppm_v stepwise increase experiment (Fig. ~~5B~~4B).

3.3 Model Validation

After calibration, the response of the model was evaluated in a different experimental period from that used for calibration. A stationary feeding period of 42 days ~~of pseudo steady state~~

~~conditions~~ ~~were~~ was used to validate the model, corresponding to period 2 in Table 1. Experimental data of cumulative mass of elemental sulfur and sulfate concentration and model predictions under the stationary feeding period~~pseudo-steady-state conditions~~ for model validation are presented in Fig. ~~6~~5. The BTF performance during period 2 was always close to the optimal, since H_2S RE was 100% and sulfate selectivity higher than 100% was calculated. Since the H_2S-LR during the experimental period corresponded to more than 100% sulfate production, elemental sulfur was progressively de-accumulated from the packed bed (Fig. ~~6A~~5A). The relatively small amount of sulfate produced from such elemental sulfur de-accumulation compared to that produced due to the H_2S fed led to a relatively constant sulfate profile along the monitored period.

The above mentioned elemental sulfur de-accumulation was verified in order to determine if it was a miscalculation in the mass balance or during sulfate concentration by ionic chromatography (IC). For this reason sulfate concentration, directly related to elemental sulfur de-accumulation, was determined when sulfate production was higher than 100% (see Supplementary Material, section SM-3 for further detail).

Results showed that the sulfate concentration produced from elemental sulfur de-accumulation was higher than the experimental error of IC (5%) (Fig. S3). Therefore the sulfate concentration increases during ~~pseudo-steady-sta~~a stationary feeding period~~te conditions~~ due to elemental sulfur de-accumulation. ~~Elemental sulfur de-accumulated during this period correspond to the elemental sulfur previously accumulated, especially during the star-up period where 36 g of elemental sulfur were accumulated.~~

Formatted: CHISA

The model was able to accurately reproduce the elemental sulfur de-accumulation along this period. Despite of experimental data variability, model predictions showed an excellent agreement with experimental data. NSE of E=0.87 and E= 0.92 were obtained along period 2 for the cumulative mass of sulfur and sulfate concentration, respectively, reflecting that there were no significant difference between experimental sulfate concentration and that predicted by the model.

Moreover, the model was used to simulate the performance of the reactor under dynamic conditions (Table 1), in order to simulate daily load fluctuations commonly found in real facilities. Dynamic model validation results are shown in Fig. ~~6~~5. To properly assess the dynamics, the plant was fed a constant H_2S-LR of 56 g m^{-3} h^{-1} during 190h. Thereafter, the inlet dynamic profile was activated at an average H_2S-LR of 79 g m^{-3} h^{-1} with maximum and minimum peak H_2S-LR of 141 and 28 g m^{-3} h^{-1}.

The BTF model response properly fits the experimental data during the change of dynamics represented in Fig. ~~7~~6. During the first stage of 190h ~~under~~ during the stationary feeding period~~pseudo-steady-state conditions~~, the model predicted correctly the $C_{L,SO4}^{2-}$ experimental data. When variable H_2S-LR conditions were applied, a transient period with an increased sulfate concentration was observed until t=240h. Thereafter, $C_{L,SO4}^{2-}$ concentration remained oscilating in a constant range. The model was able to reproduce properly both the transient period and the pseudo steady-state period under a variable inlet load. The goodness of the fitting was confirmed with a NSE coefficient of E=0.60.

Overall, the model showed to be valid to describe the main processes occurring in the three phases of a BTF ~~(gas, liquid and biofilm)~~, gas phase (Fig 3A and 3B), liquid phase (Fig. 4A)

and solid phase as elemental sulfur (Fig. 4B), ~~-~~in a co-current flow mode configuration. Thus, this model becomes a powerful tool to predict the main intermediate (elemental sulfur) and final product (sulfate) of H_2S oxidation along different operational conditions such as pseudo steady-state conditions and variable LR conditions. Especially, a~~A~~ccurate model predictions under high H_2S-LR and O_2 limiting conditions (period 1) could be useful for predicting elemental sulfur accumulation in industrial BTF installations. Therefore, maintenance tasks can~~ould~~ be strategically planned. Moreover, the development of the BTF model can be used for the development and simulation of control strategies towards process optimization. ~~Information obtained during the relative sensitivity analysis can be useful at the time of developing control strategies.~~ P~~p~~arameters related to O_2 transport are crucial in order to ~~obtain the~~ completely oxidaize~~tion of~~ H_2S and avoid the formation of elemental sulfur in the BTF bed, since an excessive accumulation of elemental sulfur can significantly diminish the reactor performance. Therefore, control strategies must be based on the improvement of the oxygen transfer to the liquid phase towards process optimization.

~~As an example, this model can help to develop control strategies in order to optimize process performance obtaining increasing RE while minimizing elemental sulfur accumulation~~.

4. Conclusions

A dynamic model for a BTF for high H_2S-LR biogas desulfurization in aerobic conditions ~~operating under high H_2S-LR conditions~~ was developed and successfully calibrated and validated, allowing a proper description of different operational scenarios such as LR increments due to H_2S concentration increases in the biogas stream. Furthermore the behavior of the different phases (gas, liquid and elemental sulfur) involved in the biogas desulfurization were correctly ~~simulated~~predicted. Also the application of a two-step sulfide oxidation

Formatted: Font: (Default) Times New Roman, 12 pt

Formatted: Font: (Default) Times New Roman, 12 pt

Formatted: Font: (Default) Times New Roman, 12 pt

Formatted: Not Superscript/ Subscrip

Formatted: Font color: Auto

kinetic model was successfully performed in order to describe intermediate oxidation products.

A preliminary assessment through a relative sensitivity analysis~~,~~ allowed ~~to~~ determine~~i~~ng the most sensitive parameters ~~to determine during model calibration~~of the model~~. The relative sensitivity analysis indicate that parameters~~. Parameters related to O_2 mass transport~~, exhibited a larger influence to model~~the~~ output variables ~~studied~~considered (RE ~~and~~, $C_{L,SO4}^{2-}$ and m_S^0~~), compared to the corresponding H_2S parameters~~.

The proposed model was calibrated using experimental data, which allow~~ing~~ed ~~to~~ describe~~ing~~ accurately the ~~H_2S~~ outlet H_2S concentration profile along the BTF bed during H_2S-LR increments. Besides describing properly sulfate production, ~~additionally~~ elemental sulfur, the main intermediate product during H_2S oxidation ~~product~~, was correctly ~~modeled~~predicted. Mass transfer parameters (δ_B, δ_L, $K_{L,H2S}$) and kinetic parameters (X, $\mu_{max,2}$) were estimated during BTF model calibration.

Moreover, the BTF model was ~~correctly~~ validated~~, describing two different periods, a pseudo-~~ under a stationary ~~H_2S-LR~~feeding period and a dynamic H_2S-LR period. Proper gas phase description during both periods was obtained~~, but more~~. More importantly, elemental sulfur and sulfate were also in agreement with experimental data. Dynamic validation~~s~~ results demonstrated that the model is able to predict correctly the BTF operation when a variable H_2S-LR profile is applied. Hence the BTF model here presented ~~expose that~~ is capable to ~~work on~~predict the BTF performance under similar conditions as those found~~ed~~ ~~o~~in real plants, making it a suitable tool in order to develop and design control strategies towards process optimization of desulfurizing BTF~~'~~s. ~~S~~

~~Accurate model predictions under high H_2S LR and O_2 limiting conditions (period 1) could be useful for predicting elemental sulfur accumulation in industrial BTF installations. Therefore, maintenance tasks could be strategically planned. Moreover, the development of the BTF model can be used for the development and simulation of control strategies towards process optimization. From the sensitivity analysis results, it can be concluded that parameters related to O_2 are crucial in order to obtain the complete oxidation of H_2S and avoid the formation of elemental sulfur in the BTF bed, since an excessive accumulation of elemental sulfur can significantly diminish the reactor performance. Therefore, control strategies must be based on the improvement of the oxygen transfer to the liquid phase towards process optimization.~~

Nomenclature Section

List of symbols

a	Specific surface area per volume unit of packed bed, $m^2\ m^{-3}$
$C_{B,i}^{nvs,1}$	Concentration of component *i* at the biofilm surface in layer *nvs*, $g\ m^{-3}$
$C_{B,i}^{nvs,nb}$	Concentration of component *i* at the biofilm subdivision *nb* in layer *nvs*, $g\ m^{-3}$
$C_{B,SS}$	Concentration of sulfide in the biofilm phase, $g\ m^{-3}$
$C_{B,S}$	Concentration of elemental sulfur in the biofilm phase, $g\ m^{-3}$
$C_{B,TS}$	Concentration of thiosulfate in the biofilm phase, $g\ m^{-3}$
$C_{B,DO}$	Concentration of dissolved oxygen in the biofilm phase, $g\ m^{-3}$
C_{g,O_2}^{AC}	Oxygen inlet concentration in the aeration column, $g\ m^{-3}$
C_{g,O_2}^{out}	Oxygen outlet concentration in the aeration column, $g\ m^{-3}$
$C_{g,i}^{nvs}$	Concentrations of component *i* in the bulk gas in layer *nvs*, $g\ m^{-3}$

Formatted: Indent: First line: 0 cm, Tab stops: Not at 12.17 cm

Formatted: Font: 12 pt, Bold, Font color: Black

Formatted: Underline

Formatted: Line spacing: Double

Formatted: Font: Italic

Formatted: Font: Italic

Formatted: Font: Italic

Formatted: Font: Italic

1	$C_{L,i}^{In}$	Concentration of compound *i* in the mineral medium, g m^{-3}
2	$C_{L,i}^{nvs}$	Concentrations of component *i* in the bulk liquid in layer *nvs*, g m^{-3}
3	$C_{L,i}^{P}$	Concentration of compound *i* in the purge flow, g m^{-3}
4	$C_{L,i}^{RE}$	Concentration of compound *i* in the recirculation flow, g m^{-3}
5	$C_{L,SO4}^{2-}$	Concentration of sulfate in the liquid phase, g m^{-3}
6	D_i	Diffusivity of component *i* in water, m^2 h^{-1}
7	*EBRT*	Empty Bed Residence Time ,s
8	$F_{L,In}^{1}$	Fresh liquid mineral medium flow rate, m^3 h^{-1}
9	$F_{L,P}$	Liquid purge flow rate, m^3 h^{-1}
10	F_L	Liquid flow rate, m^3 h^{-1}
11	F_T	Total (biogas + air) gas flow rate, m^3 h^{-1}
12	*HRT*	Hydraulic retention time, h
13	H_i	Gas-liquid dimensionless Henry coefficient for component *I*,-
14	$K_{L,O_2,AC}a$	Gas-liquid global mass transfer coefficient for O_2 in the aeration column, h^{-1}
15	$K_{L,i}$	Gas-liquid global mass transfer coefficient of component *i*, h^{-1}
16	K_{max}	Maximum intracellular S^0 stored to biomass, g S $g^{-1/3}$ VSS
17	K	Substrate switch constant, g S m^{-3}
18	K_{TS}	Affinity constant for $S_2O_3^{2-}$ consumption, g S m^{-3}
19	k_{SS}	Affinity constants for sulfide, g S m^{-3}
20	k_{is}	Sulfide inhibition constant, g S m^{-3}
21	k_o	Affinity constants for oxygen, g DO m^{-3}
22	k	Kinetic constant for $S_2O_3^{2-}$ production under biotic conditions, h^{-1}
23	m_S^0	Cumulative mass of elemental sulfur, g
24	$r_{Bj,}$	Rate equation for each biological process considered, g m^{-3} h^{-1}
25	*TLV*	Trickling Liquid Velocity,m h^{-1}

V_{bed}	Packed bed volume, m^3
$V_{g, nvs,}$	Empty volume of the packed bed of layer *nvs* m^3
$V_{l,nvs}$	Liquid volume of layer *nvs*, m^3
$V_{L,D}$	Volume of liquid in the sump of the BTF, m^3
V_{L_AC}	Liquid volume of the aeration column, m^3
V_{g_AC}	Gas phase volume of the aeration column, m^3
$Y_{X/S}$,	Biomass growth yield using S^0, g VSS g^{-1} S
$Y_{X/SS}$,	Biomass growth yield using S^{2-}, g VSS g^{-1} S
$Y_{X/TS}$,	Biomass growth yield using $S_2O_3^{2-}$, g VSS g^{-1} S
X	Biomass concentration, g X m^{-3}
υ_{ij}	Stoichiometric coefficient for compound *i* in process rate *j*,-
Greek letters	
α	Kinetic constant for elemental sulfur accumulation,-
$\mathcal{E}_g$	Gas phase porosity,-
ε	Packed bed porosity,-
δ_L	Thickness of the water layer, m
$\delta_{B\text{-}nb}$	Thickness of one biofilm subdivision, m
φ	Dynamic hold-up,-
β	Kinetic constant for thiosulfate ,-
$\mu_{max,1}$	Specific growth rates for SOB over S^{2-}, h^{-1}
$\mu_{max,2}$	Specific growth rates for SOB over S^0 , h^{-1} g $X^{1/3}$ g $S^{-1/3}$
$\mu_{max,3}$	Specific growth rates for SOB over $S_2O_3^{2}$, h^{-1}
Superscripts	

Formatted: Underline

Formatted: Underline

nvs Vertical layers

nb Biofilm subdivisions

RE Recycling line

Formatted: Indent: First line: 0 cm, Tab stops: Not at 12.17 cm

Aknowledgements

The Spanish government provided financial support through the CICYT project CTM2012-37927-C03. The Department of Chemical Engineering at UAB (Universitat Autònoma de Barcelona) is a unit of Biochemical Engineering of the Xarxa de Referència en Biotecnologia de Catalunya (XRB), Generalitat de Catalunya.

References

Formatted: Line spacing: Double

[1] N. Abatzoglou, S. Boivin, A review of biogas purification, Biofuels, Bioprod. Biorefining. 3 (2009) 42–71.

[2] P.S. Cartwright, P.E., Water Reuse. Water Encyclopedia, 1st ed., 2005.

[3] M. Fortuny, X. Gamisans, M.A. Deshusses, J. Lafuente, C. Casas, D. Gabriel, Operational aspects of the desulfurization process of energy gases mimics in biotrickling filters, Water Res. 45 (2011) 5665–5674.

[4] M. Fortuny, J.A. Baeza, X. Gamisans, C. Casas, J. Lafuente, M.A. Deshusses, D. Gabriel, Biological sweetening of energy gases mimics in biotrickling filters, Chemosphere. 71 (2008) 10–17.

[5] G. Rodriguez, A.D. Dorado, M. Fortuny, D. Gabriel, X. Gamisans, Biotrickling filters for biogas sweetening: Oxygen transfer improvement for a reliable operation, Process Saf. Environ. Prot. 92 (2014) 261–268.

[6] A.M. Montebello, T. Bezerra, R. Rovira, L. Rago, J. Lafuente, X. Gamisans, S. Campoy, M Baeza, D. Gabriel, Operational aspects, pH transition and microbial shifts of a H2S desulfurizing biotrickling filter with random packing material., Chemosphere. 93 (2013) 2675–82.

[7] L.R. López, T. Bezerra, M. Mora, J. Lafuente, D. Gabriel, Influence of trickling liquid velocity and flow pattern in the improvement of oxygen transport in aerobic biotrickling filters for biogas desulfurization, J. Chem. Technol. Biotechnol. (2015). doi:10.1002/jctb.4676.

[8] F.J. Álvarez-Hornos, C. Gabaldón, V. Martínez-Soria, P. Marzal, J.-M. Penya-roja, Mathematical modeling of the biofiltration of ethyl acetate and toluene and their mixture, Biochem. Eng. J. 43 (2009) 169–177.

[9] A.D. Dorado, G. Rodri-guez, G. Ribera, A. Bonsfills, D. Gabriel, J. Lafuente, X. Gamisans, Evaluation of Mass Transfer Coefficients in Biotrickling Filters: Experimental Determination and Comparison to Correlations, Chem. Eng. Technol. 32 (2009) 1941–1950.

[10] G. Baquerizo, J.P. Maestre, T. Sakuma, M.A.. Deshusses, X. Gamisans, D. Gabriel, J.

Lafuente, A detailed model of a biofilter for ammonia removal: Model parameters analysis and model validation, Chem. Eng. J. 113 (2005) 205–214.

[11] E.L. Cortus, S.P. Lemay, E.M. Barber, G.A. Hill, S. Godbout, A dynamic model of ammonia emission from urine puddles, 99 (2008) 390–402.

[12] W. Ahmed, Z.M. Shareefdeen, N.A. Jabbar, Dynamic modeling and analysis of biotrickling filters in continuous operation for H2S removal, Clean Technol. Environ. Policy. 16 (2013) 1757–1765.

[13] H. Li, J.C. Crittenden, J.R. Mihelcic, H. Hautakangas, Optimization of Biofiltration for Odor Control: Model Development and Parameter Sensitivity, 74 (2014) 5–16.

[14] S. Kim, M.A. Deshusses, Development and Experimental Validation of a Conceptual Model for Biotrickhg Ffltration of H2S, (2003) 119–128.

[15] J.S. Devinny, J. Ramesh, A phenomenological review of biofilter models, Chem. Eng. J. 113 (2005) 187–196.

[16] J. Silva, M. Morales, M. Cáceres, P. Morales, G. Aroca, Modelling of the biofiltration of reduced sulphur compounds through biotrickling filters connected in series: Effect of H2S, Electron. J. Biotechnol. 15 (2012).

[17] S. Sharvelle, M. Arabi, E. Mclamore, M.K. Banks, Model Development for

Biotrickling Filter Treatment of Graywater Simulant and Waste Gas . I, (2008) 813–825.

[18] G. Rodriguez, Eliminació de H2S mitjançant biofiltres percoladors: millora de la transferencia d'oxygen, Thesis 2013.

[19] Q. Liao, X. Tian, R. Chen, X. Zhu, Mathematical model for gas–liquid two-phase flow and biodegradation of a low concentration volatile organic compound (VOC) in a trickling biofilter, Int. J. Heat Mass Transf. 51 (2008) 1780–1792.

[20] W. Bonilla-Blancas, M. Mora, S. Revah, J.A. Baeza, J. Lafuente, X. Gamisans, D. Gabriel, A. Gonzalez-Sanchez, Application of a novel respirometric methodology to characterize mass transfer and activity of H2S-oxidizing biofilms in biotrickling filter beds, Biochem. Eng. J. 99 (2015) 24–34.

[21] M. Mora, L.R. López, J. Lafuente, J. Pérez, R. Kleerebezem, M. Van Loosdrecht, X. Gamisans, D. Gabriel, Respirometric characterization of aerobic sulfide, thiosulfate and elemental sulfur oxidation by S-oxidizing biomass, Water Res. 89 (2016) 282–292.

[22] R.R. Andreasen, R.E. Nicolai, T.G. Poulsen, Pressure drop in biofilters as related to dust and biomass accumulation, J. Chem. Technol. Biotechnol. 87 (2012) 806–816.

[23] M.A. Deshusses, G. Hamer, I.J. Dunn, Behavior of Biofilters for Waste Air Biotreatment. 1. Dynamic Model Development, 29 (1995) 1048–1058.

[24] A. Roosta, A. Jahanmiri, D. Mowla, A. Niazi, Mathematical modeling of biological sulfide removal in a fed batch bioreactor, Biochem. Eng. J. 58-59 (2011) 50–56.

[25] A. Mannucci, G. Munz, G. Mori, C. Lubello, Biomass accumulation modelling in a highly loaded biotrickling filter for hydrogen sulphide removal., Chemosphere. 88 (2012) 712–7.

[26] A. Gonzalez-Sanchez, M. Tomas, A.D. Dorado, X. Gamisans, A. Guisasola, J. Lafuente, D. Gabriel, Development of a kinetic model for elemental sulfur and sulfate formation from the autotrophic sulfide oxidation using respirometric techniques., Water Sci. Technol. 59 (2009) 1323–9.

[27] A.M. Montebello, M. Baeza, J. Lafuente, D. Gabriel, Monitoring and performance of a desulphurizing biotrickling filter with an integrated continuous gas/liquid flow analyser, Chem. Eng. J. 165 (2010) 500–507.

[28] J.E. Nash, J. V Sutcliffe, River flow forecasting through conceptual models part I: A discussion of principles, J. Hydrol. 10 (1970) 282–290.

[29] G. Munz, R. Gori, G. Mori, C. Lubello, Monitoring biological sulphide oxidation processes using combined respirometric and titrimetric techniques, Chemosphere. 76 (2009) 644–650.

[30] M. Mora, A. Guisasola, X. Gamisans, D. Gabriel, Examining thiosulfate-driven autotrophic denitrification through respirometry, Chemosphere. 113 (2014) 1–8.

[31] I. Iliuta, F. Larachi, Modeling simultaneous biological clogging and physical plugging in trickle-bed bioreactors for wastewater treatment, Chem. Eng. Sci. 60 (2005) 1477–1489.

[32] A.D. Dorado, E. Dumont, R. Muñoz, G. Quijano, A novel mathematical approach for the understanding and optimization of two-phase partitioning bioreactors devoted to air pollution control, Chem. Eng. J. 263 (2015) 239–248.

[33] A.M. Montebello, M. Fernández, F. Almenglo, M. Ramírez, D. Cantero, M. Baeza, et al., Simultaneous methylmercaptan and hydrogen sulfide removal in the desulfurization of biogas in aerobic and anoxic biotrickling filters, Chem. Eng. J. 200–202 (2012) 237–246.

[34] R. Billet, M. Schultes, Prediction of Mass Transfer columns with dumpled and Arranged packings. Updated Summary of the Calculation Method of Billet and Schultes, Chem. Eng. Res. Des. 77 (1999) 498–504.

[35] R. Perry, D. Green, J. Maloney, Perry's chemical engineers' handbook, 1997.

[36] R. Sander, Compilation of Henry's law constants, version 3.99, Atmos. Chem. Phys. Discuss. 14 (2014) 29615–30521.

[1] N. Abatzoglou, S. Boivin, A review of biogas purification, Biofuels, Bioprod. Biorefining. 3 (2009) 42–71. doi:10.1002/bbb.

[2] P.S. Cartwright, P.E., Water Reuse. Water Encyclopedia, 1st ed., 2005. doi:10.1002/047147844X.dw14.

[3] M. Fortuny, X. Gamisans, M.A. Deshusses, J. Lafuente, C. Casas, D. Gabriel, Operational aspects of the desulfurization process of energy gases mimics in biotrickling filters, Water Res. 45 (2011) 5665–5674. doi:10.1016/j.watres.2011.08.029.

[4] M. Fortuny, J.A. Baeza, X. Gamisans, C. Casas, J. Lafuente, M.A. Deshusses, et al., Biological sweetening of energy gases mimics in biotrickling filters, Chemosphere. 71 (2008) 10–17.

[5] G. Rodriguez, A.D. Dorado, M. Fortuny, D. Gabriel, X. Gamisans, Biotrickling filters for biogas sweetening: Oxygen transfer improvement for a reliable operation, Process Saf. Environ. Prot. 92 (2014) 261–268. doi:10.1016/j.psep.2013.02.002.

[6] A.M. Montebello, T. Bezerra, R. Rovira, L. Rago, J. Lafuente, X. Gamisans, et al., Operational aspects, pH transition and microbial shifts of a H2S desulfurizing biotrickling filter with random packing material., Chemosphere. 93 (2013) 2675–82. doi:10.1016/j.chemosphere.2013.08.052.

[7] L.R. López, T. Bezerra, M. Mora, J. Lafuente, D. Gabriel, Influence of trickling liquid velocity and flow pattern in the improvement of oxygen transport in aerobic biotrickling filters for biogas desulfurization, J. Chem. Technol. Biotechnol. (2015) n/a–n/a. doi:10.1002/jctb.4676.

[8] F.J. Álvarez-Hornos, C. Gabaldón, V. Martínez-Soria, P. Marzal, J. M. Penya-roja, Mathematical modeling of the biofiltration of ethyl acetate and toluene and their mixture, Biochem. Eng. J. 43 (2009) 169–177. doi:10.1016/j.bej.2008.09.014.

[9] A.D. Dorado, G. Rodri guez, G. Ribera, A. Bonsfills, D. Gabriel, J. Lafuente, et al., Evaluation of Mass Transfer Coefficients in Biotrickling Filters: Experimental Determination

Formatted: Indent: Left: 0 cm, First line: 0 cm, Space After: 7 pt, Line spacing: Multiple 1.2 li

and Comparison to Correlations, Chem. Eng. Technol. 32 (2009) 1941–1950. doi:10.1002/ceat.200900275.

[10] G. Baquerizo, J.P. Maestre, T. Sakuma, M.A. Deshusses, X. Gamisans, D. Gabriel, et al., A detailed model of a biofilter for ammonia removal: Model parameters analysis and model validation, Chem. Eng. J. 113 (2005) 205–214. doi:10.1016/j.cej.2005.03.003.

[11] E.L. Cortus, S.P. Lemay, E.M. Barber, G.A. Hill, S. Godbout, A dynamic model of ammonia emission from urine puddles, 99 (2008) 390–402. doi:10.1016/j.biosystemseng.2007.11.004.

[12] W. Ahmed, Z.M. Shareefdeen, N.A. Jabbar, Dynamic modeling and analysis of biotrickling filters in continuous operation for H2S removal, Clean Technol. Environ. Policy. 16 (2013) 1757–1765. doi:10.1007/s10098-013-0697-0.

[13] H. Li, J.C. Crittenden, J.R. Mihelcic, H. Hautakangas, Optimization of Biofiltration for Odor Control: Model Development and Parameter Sensi, 74 (2014) 5–16.

[14] S. Kim, M.A. Deshusses, Development and Experimental Validation of a Conceptual Model for Biotrickhg Ffltration of H2S, (2003) 119–128.

[15] J.S. Devinny, J. Ramesh, A phenomenological review of biofilter models, Chem. Eng. J. 113 (2005) 187–196. doi:10.1016/j.cej.2005.03.005.

[16] J. Silva, M. Morales, M. Cáceres, P. Morales, G. Aroca, Modelling of the biofiltration of reduced sulphur compounds through biotrickling filters connected in series: Effect of H2S, Electron. J. Biotechnol. 15 (2012). doi:10.2225/vol15-issue3-fulltext-7.

[17] S. Sharvelle, M. Arabi, E. Mclamore, M.K. Banks, Model Development for Biotrickling Filter Treatment of Graywater Simulant and Waste Gas . I, (2008) 813–825.

[18] G. Rodriguez, Eliminació de H2S mitjançant biofiltres percoladors: millora de la transferencia d'oxygen, Universitat Politecnica de Catalunya, 2013.

Formatted: Indent: Left: 0 cm, First line: 0 cm, Space After: 7 pt, Line spacing: Multiple 1.2 li

[19] Q. Liao, X. Tian, R. Chen, X. Zhu, Mathematical model for gas–liquid two-phase flow and biodegradation of a low concentration volatile organic compound (VOC) in a trickling biofilter, Int. J. Heat Mass Transf. 51 (2008) 1780–1792. doi:10.1016/j.ijheatmasstransfer.2007.07.007.

[20] W. Bonilla-Blancas, M. Mora, S. Revah, J.A. Baeza, J. Lafuente, X. Gamisans, et al., Application of a novel respirometric methodology to characterize mass transfer and activity of H2S-oxidizing biofilms in biotrickling filter beds, Biochem. Eng. J. 99 (2015) 24–34. doi:10.1016/j.bej.2015.02.030.

[21] M. Mora, L.R. López, J. Lafuente, J. Pérez, R. Kleerebezem, M. Van Loosdrecht, et al., Respirometric characterization of aerobic sulfide, thiosulfate and elemental sulfur oxidation by S-oxidizing biomass, Water Res. 89 (2016) 282–292. doi:10.1016/j.watres.2015.11.061.

[22] R.R. Andreasen, R.E. Nicolai, T.G. Poulsen, Pressure drop in biofilters as related to dust and biomass accumulation, J. Chem. Technol. Biotechnol. 87 (2012) 806–816. doi:10.1002/jctb.3757.

[23] M.A. Deshusses, G. Hamer, I.J. Dunn, Behavior of Biofilters for Waste Air Biotreatment. 1. Dynamic Model Development, 29 (1995) 1048–1058.

[24] A. Roosta, A. Jahanmiri, D. Mowla, A. Niazi, Mathematical modeling of biological sulfide removal in a fed batch bioreactor, Biochem. Eng. J. 58-59 (2011) 50–56. doi:10.1016/j.bej.2011.08.013.

[25] A. Mannucci, G. Munz, G. Mori, C. Lubello, Biomass accumulation modelling in a highly loaded biotrickling filter for hydrogen sulphide removal., Chemosphere. 88 (2012) 712–7. doi:10.1016/j.chemosphere.2012.04.026.

[26] A. Gonzalez-Sanchez, M. Tomas, A.D. Dorado, X. Gamisans, A. Guisasola, J. Lafuente, et al., Development of a kinetic model for elemental sulfur and sulfate formation from the autotrophic sulfide oxidation using respirometric techniques., Water Sci. Technol. 59 (2009) 1323–9. doi:10.2166/wst.2009.110.

Formatted: Indent: Left: 0 cm, First line: 0 cm, Space After: 7 pt, Line spacing: Multiple 1.2 li

[27] A.M. Montebello, M. Baeza, J. Lafuente, D. Gabriel, Monitoring and performance of a desulphurizing biotrickling filter with an integrated continuous gas/liquid flow analyser, Chem. Eng. J. 165 (2010) 500–507. doi:10.1016/j.cej.2010.09.053.

[28] J.E. Nash, J. V Sutcliffe, River flow forecasting through conceptual models part I: A discussion of principles, J. Hydrol. 10 (1970) 282–290. doi:10.1016/0022-1694(70)90255-6.

[29] G. Munz, R. Gori, G. Mori, C. Lubello, Monitoring biological sulphide oxidation processes using combined respirometric and titrimetric techniques, Chemosphere. 76 (2009) 644–650. doi:10.1016/j.chemosphere.2009.04.039.

[30] M. Mora, A. Guisasola, X. Gamisans, D. Gabriel, Examining thiosulfate-driven autotrophic denitrification through respirometry, Chemosphere. 113 (2014) 1–8. doi:10.1016/j.chemosphere.2014.03.083.

[31] I. Iliuta, F. Larachi, Modeling simultaneous biological clogging and physical plugging in trickle-bed bioreactors for wastewater treatment, Chem. Eng. Sci. 60 (2005) 1477–1489. doi:10.1016/j.ces.2004.10.016.

[32] A.D. Dorado, E. Dumont, R. Muñoz, G. Quijano, A novel mathematical approach for the understanding and optimization of two-phase partitioning bioreactors devoted to air pollution control, Chem. Eng. J. 263 (2015) 239–248. doi:10.1016/j.cej.2014.11.014.

[33] A.M. Montebello, M. Fernández, F. Almenglo, M. Ramírez, D. Cantero, M. Baeza, et al., Simultaneous methylmercaptan and hydrogen sulfide removal in the desulfurization of biogas in aerobic and anoxic biotrickling filters, Chem. Eng. J. 200–202 (2012) 237–246. doi:10.1016/j.cej.2012.06.043.

[34] R. Billet, M. Schultes, Prediction of mass transfer columns with dumpled and arranged packings Updated Summary of the Calculation Method of Billet and Schultes, Chem. Eng. Res. Des. 77 (1999) 498–504. doi:http://dx.doi.org/10.1205/026387699526520.

[35] R. Perry, D. Green, J. Maloney, Perry's chemical engineers' handbook, 1997.

Formatted: Indent: Left: 0 cm, First line: 0 cm, Space After: 7 pt, Line spacing: Multiple 1.2 li

~~[36] R. Sander, Compilation of Henry's law constants, version 3.99, Atmos. Chem. Phys. Discuss. 14 (2014) 29615–30521. doi:10.5194/acpd-14-29615-2014.~~

Formatted: Indent: Left: 0 cm, First line: 0 cm, Space After: 7 pt, Line spacing: Multiple 1.2 li

Formatted: Left, Space After: 7 pt, Line spacing: Multiple 1.2 li

TABLES

Table 1. Experimental conditions for the simulated periods

Period	[H_2S] (ppm_v)	LR (g S-H_2S m^{-3} h^{-1})	O_2/H_2S (% v v^{-1})	Period simulated (days)
1: Calibration and sensitivity analysis	2000	56.3	42.2	5
	4000	112.9	21.0	
	6000	169.6	14.0	
	8000	226.6	10.5	
	10000	283.8	8.4	
2: Stationary Validation	2000	56.3	42.2	42
3: Dynamic Validation	2758[a]	78.9	35.8	8
	5000[b]	141.1	84.4	
	1000[c]	28.1	16.8	

[a]Average concentration

[b]Maximum concentration

[c]Minimum concentration

Table 2. Process stoichiometry for the aerobic sulfide, thiosulfate and elemental sulfur oxidation by S-oxidizing biomass.

Process	Compounds				
	Sulfide	Thiosulfate	Sulfur	Sulfate	Oxygen
1. Growth on sulfide	$-\frac{1}{Y_{X/SS}}$		$\frac{1}{Y_{X/SS}}$		$-\frac{0.42^{*}}{Y_{X/SS}}$
2. Growth on elemental sulfur			$-\frac{1}{Y_{X/S}}$	$\frac{1}{Y_{X/S}}$	$-\frac{1.22^{*}}{Y_{X/S}}$
3. Growth on thiosulfate		$-\frac{1}{Y_{X/TS}}$		$\frac{2}{Y_{X/TS}}$	$-\frac{1.65^{*}}{Y_{X/TS}}$
4. Thiosulfate production		1	-2		-1.5

*Mora et al. [21]

Table 3. Process kinetics for the aerobic sulfide, thiosulfate and elemental sulfur oxidation by S-oxidizing biomass

Process	Process rate
1. Growth on sulfide	$\mu_{max,1}\cdot\left(\frac{C_{B,SS}C_{B,SS}^{nvs,nb}}{k_{SS}+C_{B,SS}C_{B,SS}^{nvs,nb}+\frac{C_{B,SS}^{2}}{k_{is}}}\right)\cdot\left(1-\left(\frac{\left(\frac{C_{B,S}C_{B,S}^{nvs,nb}}{X}\right)}{K_{max}}\right)^{\alpha}\right)\cdot\left(\frac{C_{B,DO}}{C_{B,DO}+k_o}\frac{C_{B,OD}^{nvs,nb}}{C_{B,OD}^{nvs,nb}+k_o}\right)\cdot X$
2. Growth on elemental sulfur	$\mu_{max,2}\cdot\left(\frac{C_{B,S}C_{B,S}^{nvs,nb}}{X}\right)^{2/3}\cdot\left(\frac{K}{C_{B,SS}C_{B,SS}^{nvs,nb}+K}\right)\cdot\left(\frac{C_{B,DO}}{C_{B,DO}+k_o}\frac{C_{B,OD}^{nvs,nb}}{C_{B,OD}^{nvs,nb}+k_o}\right)\cdot X$
3. Growth on thiosulfate	$\mu_{max,3}\cdot\left(\frac{C_{B,TS}C_{B,TS}^{nvs,nb}}{C_{B,TS}C_{B,TS}^{nvs,nb}+K_{TS}}\right)\cdot\left(\frac{K}{C_{B,SS}C_{B,SS}^{nvs,nb}+K}\right)\cdot\left(\frac{C_{B,OD}^{nvs,nb}C_{B,DO}}{C_{B,OD}^{nvs,nb}C_{B,DO}+k_o}\right)\cdot X$
4. Thiosulfate production	$k\cdot C_{B,SS}^{\beta}$

Formatted: Font: 10 pt
Formatted: Font: 10 pt, Font color: Auto
Formatted: Font: 10 pt
Formatted: Font: 10 pt, Font color: Auto
Formatted: Font: 10 pt
Formatted: Indent: First line: 1.25 cm
Formatted: Font: 9 pt
Formatted: Font: Times New Roman
Formatted: Font: Times New Roman, 12 pt

Table ~~2~~4. Sensitivity results for key BTF model parameters assessed at an inlet H_2S concentration of 10000 ppm_v

Parameter	Symbol	Units	Sensitivity, +Δ10 %			Sensitivity, -Δ10 %		
			RE (%)	m_S^0 (g-S)	$C_{L,SO4}^{2-}$ (g-S L^{-1})	RE (%)	m_S^0 (g-S)	$C_{L,SO4}^{2-}$ (g-S L^{-1})
Specific interfacial area	a	$m^2\ m^{-3}$	0,79	0,00	1,09	1,51	0,31	0,90
O_2 mass transfer coefficient	K_{L,O_2}	$m\ h^{-1}$	0,45	-0,30	0,68	1,20	-0,19	0,53
O_2 Diffusivity	D_{O_2}	$m^2\ h^{-1}$	0,40	-0,10	0,33	1,02	-0,05	0,25
Specific growth rate over sulfur	$\mu_{max,2}$	h^{-1}	-0,40	-0,22	0,27	-0,48	0,04	0,51
H_2S Henry's constant	H_{H_2S}	dimensionless	-0,30	-0,46	0,24	-0,08	-0,50	0,25
Biofilm layer thickness	δ_B	µm	-0,05	0,05	0,13	1,42	0,04	0,13
Biomass concentration	X	$g\ X\ m^{-3}$	0,06	0,12	0,11	1,31	0,12	0,11
Substrate switch	K_{max}	$g\ S\ g\ X^{-1}$	0,11	0,18	0,04	1,21	0,21	0,01
H_2S mass transfer coefficient	K_{L,H_2S}	$m\ h^{-1}$	-0,10	0,21	-0,04	-0,04	0,25	-0,07
O_2 half-saturation constant	k_o	$g\ DO\ m^{-3}$	0,14	0,08	-0,08	0,11	0,08	-0,09
Liquid layer thickness	δ_L	µm	-0,50	0,02	-0,25	-0,37	0,04	-0,31
O_2 Henry's constant	H_{O_2}	dimensionless	-1,41	0,22	-0,76	-0,72	0,55	-1,23

Table ~~3~~5. Summary of main parameters of the BTF model for biogas desulfurization

Parameter	Symbol	Value	Units	Reference
Biomass concentration	X	$139.7 \cdot 10^{3}$	g X m^{-3}	Calibrated
Biofilm layer thickness	δ_B	200	μm	Calibrated
Liquid layer thickness	δ_L	10	μm	Calibrated
Specific growth rate for sulfur	$\mu_{max,2}$	$2.17 \cdot 10^{-2}$	h^{-1}	Calibrated
H_2S Global mass transfer coefficient	K_{L,H_2S}	0.23	m h^{-1}	Calibrated
O_2 Global mass transfer coefficient in the BTF	K_{L,O_2}	0.38	m h^{-1}	[34]~~[34]~~
O_2 mass transfer coefficient in the Aeration column	$K_{L,O_2,AC}$	0.4	h^{-1}	Experimentally determined
Liquid hold-up	φ	$3.57 \cdot 10^{-2}$	dimensionless	Experimentally determined
Specific interfacial area	a	354.33	m^2 m^{-3}	Packing material manufacturer
Packing material porosity	ε	0.85	dimensionless	
H_2S diffusivity	D_{H_2S}	$5.80 \cdot 10^{-6}$	m^2 h^{-1}	[35]
O_2 diffusivity	D_{O_2}	$9.00 \cdot 10^{-6}$	m^2 h^{-1}	[35]
SO_4^{2-} diffusivity	$D_{SO_4^{2-}}$	$3.80 \cdot 10^{-3}$	m^2 h^{-1}	[35]
H_2S Henry's constant	H_{H_2S}	0.42	dimensionless	[36]
O_2 Henry's constant	H_{O_2}	32.80	dimensionless	[36]

Table 46. Summary of main biokinetic parameters of the BTF model for biogas desulfurization calibrated by Mora et al. [21]~~(2015)~~ through respirometry for the biotrickling filter modeled herein.

Parameter	Symbol	Value	Units
Specific growth rate for sulfide	$\mu_{max,1}$	0.41	h^{-1}
Specific growth rate for sulfide	$\mu_{max,3}$	0.012	h^{-1}
Sulfide affinity constant	k_{SS}	0.32	g S m^{-3}
Sulfide inhibition constant	k_{is}	42.4	g S m^{-3}
Oxygen affinity constant	k_o	0.11	g DO m^{-3}
maximum intracellular elemental sulfur stored in the biomass	K_{max}	0.252	g S $g^{-1/3}$ VSS
Thiosulfate affinity constant	K_{TS}	0.0023	g S m^{-3}
Kinetic constant for thiosulfate	k	6.35	h^{-1}
Substrate switch constant	K	0.014	g S m^{-3}
Kinetic constant for thiosulfate	β	0.530	dimensionless
Kinetic constant	α	1.71	dimensionless

Nomenclature Section

List of symbols

a	Specific surface area per volume unit of packed bed, $m^2 m^{-3}$
$C_{B,i}^{nvs,1}$	Concentration of component *i* at the biofilm surface, $g\ m^{-3}$
$C_{B,i}^{nvs,nb}$	Concentration of component *i* at the biofilm subdivision *nb*, $g\ m^{-3}$
C_{S,O_2}^{AC}	Oxygen inlet concentration in the aeration column, $g\ m^{-3}$
C_{S,O_2}^{out}	Oxygen outlet concentration in the aeration column, $g\ m^{-3}$
$C_{S,i}^{nvs}$	Concentrations of component *i* in the bulk gas phase for a certain layer, $g\ m^{-3}$
$C_{L,i}^{In}$	Concentration of compound *i* in the mineral medium, $g\ m^{-3}$
$C_{L,i}^{nvs}$	Concentrations of component *i* in the bulk liquid phase for a certain layer, $g\ m^{-3}$
$C_{L,i}^{P}$	Concentration of compound *i* in the purge flow, $g\ m^{-3}$
$C_{L,i}^{RE}$	Concentration of compound *i* in the recirculation flow, $g\ m^{-3}$
$C_{L,SO4}^{2}$	Concentration of sulfate in the liquid phase, $g\ m^{-3}$
D_i	Diffusivity of component *i* in water, $m^2 h^{-1}$
EBRT	Empty Bed Residence Time ,s
$F_{L,In}^{1}$	Fresh liquid mineral medium flow rate, $m^3 h^{-1}$
$F_{L,P}$	Liquid purge flow rate, $m^3 h^{-1}$
F_L	Liquid flow rate, $m^3 h^{-1}$
F_T	Total (biogas + air) gas flow rate, $m^3 h^{-1}$
HRT	Hydraulic retention time, h
H_i	Gas-liquid dimensionless Henry coefficient for component *I*,
$K_{L,O_2,AC}a$	Gas-liquid mass transfer coefficient for oxygen in the aeration column, h^{-1}
$K_{L,i}$	Gas-liquid global mass transfer coefficient of component *i*,
K_{max}	Maximum intracellular S^0 stored to biomass, $g\ S\ g^{-1/3}$ VSS
K_I	Substrate switch constant, $g\ S\ m^{-3}$
K_{IS}	affinity constant for $S_2O_3^{2-}$ consumption, $g\ S\ m^{-3}$
k_{SS}	Affinity constants for sulfide, $g\ S\ m^{-3}$
k_{IS}	Sulfide inhibition constant in $g\ S\ m^{-3}$
k_o	Affinity constants for oxygen, $g\ DO\ m^{-3}$
k	kinetic constant for $S_2O_3^{2-}$ production under biotic conditions, h^{-1}
r_{Bi}	Rate equation for each biological process considered, $g\ m^{-3} h^{-1}$
TLV	Trickling Liquid Velocity,m h^{-1}
V_{bed}	Packed bed volume, m^3
$V_{g,\ nvs,}$	Empty volume of the packed bed of layer *nvs* m^3
$V_{l,nvs}$	Liquid volume of layer *nvs*, m^3
$V_{L,D}$	Volume of liquid in the sump of the BTF, m^3
V_{L_AC}	Liquid volume of the aeration column, m^3
V_{g_AC}	Gas phase volume of the aeration column, m^3
$Y_{XS,}$	Biomass growth yield using S^0, g VSS g^{-1} S
$Y_{XSS,}$	Biomass growth yield using S^{2-}, g VSS g^{-1} S

Formatted: Line spacing: Multiple 1.15 li

Formatted: Indent: Left: 0 cm, First line: 0 cm, Line spacing: Multiple 1.15 li

Formatted: Line spacing: Multiple 1.15 li

Formatted: Indent: Left: 0 cm, First line: 0 cm, Line spacing: Multiple 1.15 li

Formatted: Line spacing: Multiple 1.15 li

Formatted: Indent: Left: 0 cm, First line: 0 cm, Line spacing: Multiple 1.15 li

Formatted: Superscript

Formatted: Line spacing: Multiple 1.15 li

$Y_{xTS,}$ Biomass growth yield using $S_2O_3^{2-}$, g VSS g^{-1} S

X Biomass concentration, g X m^{-3}

υ_{ij} Stoichiometric coefficient for compound *i* in each process rate,

Greek letters

$\mathcal{E}_{g,}$ Gas phase porosity,

ε Packed bed porosity,

δ_L Thickness of the water layer, m

$\delta_{B\text{-}nb}$ Thickness of one biofilm subdivision, m

φ Dynamic hold-up,

β Kinetic constant for thiosulfate ,

$\mu_{max,1}$ Specific growth rates for SOB over S^{2-}, h^{-1}, g $X^{1/3}$ $g^{-1/3}$

$\mu_{max,2}$ Specific growth rates for SOB over S^0 g $X^{1/3}$ $g^{-1/3}$

$\mu_{max,3}$ Specific growth rates for SOB over $S_2O_3^{2-}$ g $X^{1/3}$ $g^{-1/3}$

Superscripts

nvs Vertical layers

nb Biofilm subdivisions

RE Recycling line

Subscripts

i *Component i*

b

Modeling an aerobic biotrickling filter for biogas desulfurization through a multi-step oxidation mechanism

L.R. López[a], A.D. Dorado[b], M. Mora[a], X. Gamisans[b], J. Lafuente[a], D. Gabriel[a*]

[a] GENOCOV Research Group, Department of Chemical, Biological and Environmental Engineering, Escola d'Enginyeria, Universitat Autònoma de Barcelona, 08193 Bellaterra, Spain.

[b] Universitat Politècnica de Catalunya, Department of Mining Engineering and Natural Resources, Bases de Manresa 61-73, 08240 Manresa, Spain.

*Corresponding author e-mail: david.gabriel@uab.cat

Abstract

A dynamic model describing physical-chemical and biological processes for the removal of high loads of H_2S from biogas streams in biotrickling filters (BTFs) was developed, calibrated and validated for a wide range of experimental conditions in a lab-scale BTF. The model considers the main processes occurring in the three phases of a BTF (gas, liquid and biofilm) in a co-current flow mode configuration. Furthermore, this model attempts to describe accurately the intermediate (thiosulfate and elemental sulfur) and final products (sulfate) of H_2S oxidation.. A sensitivity analysis was performed in order to focus parameters estimation efforts on those parameters that showed the highest influence on the estimation of the H_2S removal efficiency, the accumulated mass of sulfur and the sulfate concentration in the liquid phase. Biofilm and liquid layer thicknesses, specific growth rate of biomass over elemental sulfur and the H_2S global mass transfer coefficient were the parameters that showed the highest influence on model outputs. Experimental data for model calibration corresponded to

the operation of the BTF under stepwise increasing H_2S concentrations between 2000 and 10000 ppm_v. Once the model was calibrated, validation was performed by simulating a stationary feeding period of 42 days of operation of the BTF at an average concentration of 2000 ppm_v and a dynamic operation period were the BTF was operated under variable inlet H_2S concentration between 1000 and 5000 ppm_v to simulate load fluctuations occurring in industrial facilities. The model described the reactor performance in terms of H_2S removal and predicted satisfactorily the main intermediate and final products produced during the biological oxidation process.

Keywords

Desulfurizing biotrickling filter; biogas; modeling; kinetics; sensitivity analysis; elemental sulfur

1. Introduction

Obtaining energy from non-renewable sources is becoming too expensive or too environmentally damaging nowadays. An energy source with high potential for green energy production is biogas. However, in order to have a suitable biogas utilization, impurities such as H_2S and reduced sulfur compounds (RSC) produced during the anaerobic fermentation of S-bearing organic molecules must be removed [1]. Removal of H_2S is strictly necessary to avoid corrosion of internal combustion engines during co-generation processes as well as for proper performance of further biogas upgrading technologies [2]. Biological technologies such as biotrickling filters (BTF) have demostrated to be a suitable, competitive treatment technology for biogas conditioning when compared to physical-chemical technologies. However, main efforts have focused on experimental works, studying different pollutant loads [3], using different packing materials [4], different oxygen mass transfer devices [5], pH

conditions [6] or the gas-liquid flow pattern [7]. Tough process modeling has shown to be a crucial tool to evaluate the technical [1] and economical feasibility [2] of biological processes prior to full-scale implementation, few efforts have been made in this direction on biogas desulfurization in BTFs.

Multiphase biological processes, such as biofiltration in biofilters and biotrickling filters (BTF) for the removal of different type of contaminants like volatile organic compounds (VOCs) [7–9] and ammonia [10,11], have been modeled describing both transient and steady-state conditions. However, most BTF models have focused on VOCs removal [12], while literature available for H_2S BTFs modeling is scarce [13–15]. Therefore, a model describing properly the removal of high loads of H_2S in BTFs is still lacking in literature. Previous models for H_2S removal in BTFs have focused on removal of H_2S at odor level concentrations [13,14,16], while only few models in literature dealt with high loads of H_2S [17,18]. In most cases, the inherent complexity of such plug-flow, heterogeneous, multiphase bioreactors has been strongly simplified to avoid facing a large number of unidentifiable parameters. Often, G-L mass transport, diffusion in the biofilm and biological degradation kinetics have been identified as the most relevant processes. The heterogeneity of the water-biofilm layers as well as the kinetics and mechanisms considered to model H_2S removal in BTFs are the two main aspects that have been addressed differently by several authors. Most models consider an homogeneous biofilm density, a biofilm completely wetted along the packed bed height [13,17,19] and H_2S and O_2 mass transfer from the gas to the liquid phase prior to their diffusion to the biofilm were degradation takes place. Usually, only mass transfer resistance in the liquid phase is considered for modeling G-L mass transport due to the high interstitial gas velocity in the packed bed. However, biogas desulfurization requires of much longer gas contact times and, consequently, lower gas velocities that may increase mass transfer

resistance in the gas phase. Also, several alternatives have been proposed to model such bioreactors such as considering a partially or a fully wetted biofilm as well as considering or not adsorption of a fraction of the pollutant by the biofilm [14,20]. Despite no clear consensus has been reached so far and a careful analysis from a modeling perspective must be performed, modeling of biotrickling filters using a wetted/non-wetted biofilm approach seems necessary when the TLV is modified due to the variable amount of water in the packed bed.

One of the most critical parts in the development of a model is how biodegradation mechanisms and kinetics are described, since depending on the operational conditions, the process might become biodegradation rate-controlled [15]. Different biodegradation kinetics models and degradation mechanisms have been reported in order to describe the substrate consumption in BTFs models for H_2S removal. Eqs. 1 and 2 are usually lumped in a single equation describing the complete oxidation of sulfide to sulfate [14]. However, partial oxidation to elemental sulfur has been often observed in BTFs for biogas desulfurization [5]. For this reason, a two-step mechanism (Eqs. 1 and 2) is needed for proper system modeling.

$$H_2S+0.5O_2 \rightarrow S^0+H_2O \qquad (1)$$

$$S^0+1.5O_2 \rightarrow SO_4^{2-}+H^+ \qquad (2)$$

Obtaining an accurate model that describes well the production and accumulation of intermediate products of H_2S biological oxidation is crucial to describe accurately biogas desulfurization in BTFs. Recently, Mora et al. [21] have proposed a multi-step pathway for describing sulfide-oxidizing bacteria (SOB) as catalyst of H_2S oxidation to SO_4^{2-} considering the partial sulfide oxidation to elemental sulfur as an intracellular product, and the sulfite and thiosulfate production as additional intermediates. Such mechanistic model was calibrated and

validated through homogeneous respirometric tests providing successful results in describing the main species of the H_2S oxidation process.

From a practical point of view, prediction of desulfurizing BTFs performance is essential. Low sulfate production rates can lead to an excessive elemental sulfur formation that accumulates into the packed bed. Consequently, a significant increase in pressure drop inside BTF bed occurs [22], with a considerable reduction of BTF operational life-span and process security. However, few works have addressed this topic so far. There is still the need for the development of tools that impulse the industrial application of this emerging biological-based technology. BTF models are essential in design steps, besides useful in the development of control strategies towards process optimization.

From the stated above, the aim of this work was to develop, calibrate and validate a dynamic model of an aerobic BTF for the removal of high-loads of H_2S from biogas streams. The BTF model attempts to describe intermediate and final products obtained from H_2S oxidation under stationary feeding periods, transient and dynamic conditions. It has to be remarked that no previous works have intended to model such range of intermediate products of biological sulfide oxidation in BTFs for biogas desulfurization

2. Material and methods

2.1 Experimental setup and operating conditions

A laboratory-scale BTF reactor, with an ancillary unit for air supply, was used in this study to remove high loads of H_2S from biogas streams (Fig.1). The synthetic biogas consisted in controlled mixtures of H_2S and nitrogen (N_2) fed at the top of the BTF (1). An air flow (2) was firstly fed to an aeration column (3) for air supply to increase the dissolved oxygen (DO)

concentration in the liquid phase. Exhaust air (4) from the aeration column was fed at the top of the BTF under a co-current flow pattern and mixed with the biogas inlet stream at an O_2/H_2S supplied ratio of 41.2 (v v^{-1}). After biological degradation on the BTF bed (5), the treated biogas stream (6) leaves the reactor. The liquid phase was continuously recycled from bottom-to-top of the BTF at a trickling liquid velocity (TLV) of 4.4 m h^{-1} (7). The liquid recirculation line (8) was previously oxygenated in an aeration column. The DO concentration in the recycle and purge lines was monitored in-situ in all the experiments. The reactor pH was also controlled at pHs of around 6.5 and 7 using an ON/OFF control system by automated addition of NaOH 1M or HCl 1 M. An empty bed residence time (EBRT) of 118 s and an average hydraulic retention time (HRT) of 30 ± 4 h were maintained throughout the study by regulating the purge pump (9) and the mineral medium pump (10). Regarding the packed bed characteristics, the reactor diameter was 7.14 cm with a packed bed volume of $2.80 \cdot 10^{-3}$ m^3 (V_{bed}). Polypropylene Pall rings of 15.9 mm diameter (MACH engineering products, USA) with a specific surface area of 354 m^2 m^{-3} were used.

.

Furthermore, H_2S, O_2 and carbon dioxide (CO_2) in the gas phase were measured by through three side streams obtained from the outlet gas stream and from gas sampling ports. On-line monitoring was performed with an electrochemical H_2S(g) sensor (Sure-cell, Euro-Gas Management Services, UK), O_2 gas sensor (O_2 SL sensor, Euro-Gas Management Services, UK) and a CO_2 gas sensor (CO_2 probe GMP343 Vaisala Carbocap, Vaisala, Finland). Sampling ports were located along the BTF height at 0.24 m, 0.51 m and 0.7 m in order to monitor the H_2S concentration profile along the BTF bed and therefore compare it with simulated data. Further information about gas concentration measurement can be found on Supplementary Material, section SM.-1. Also, detailed information of the BTF inoculation, analytical methods and related information can be found elsewhere [7].

The calibration of model parameters was performed using data obtained during stepwise H_2S Loading Rate (H_2S-LR) increments as a consequence of H_2S inlet concentration ($Cg_{in,H2S}$) increase (Period 1-Table 1) in the lab-scale BTF set up (Fig. 1) operating at constant EBRT and constant biogas flow. For model validation under stationary H_2S feeding, a period of 42 days was simulated at a constant $Cg_{in,H2S}$ of 2000 ppm_v (Period 2-Table 1). In addition, model was also validated under dynamic conditions (Period 3-table 1) by simulating variable H_2S-LR conditions due to $Cg_{in,H2S}$ increase (Fig. 2) emulating daily load fluctuations as those commonly found in real facilities. The averages of maximum and minimum H_2S-LR are shown in Table 1. Periods in Table 1 do not correspond to consecutive periods. All experiments were performed in between a time span of 15 months.

2.2 Model development

A three phase model (gas, liquid and biofilm) was considered to model reactor dynamics under a co-current flow pattern configuration. The model also considered the main processes occurring in the aeration column attached to the bioreactor (Supplementary Material, Fig. S1).

2.2.1 Biotrickling filter model

The BTF model incorporates mathematical expressions for the following mechanisms occurring in the packed bed: mass transport by advective flow in the gas and liquid phases, mass transfer at the gas-liquid interface, mass transfer by diffusion at the liquid-biofilm interface, internal diffusion in the biofilm phase and biological reaction in the biofilm as schematized in Fig. 1. Also, the model considered oxygen mass transfer at the gas-liquid interface occurring in the aeration column.

Model equations were built based on the above mentioned mechanisms and assumptions often assumed in BTF models in literature [13,14,20], which can be found in Supplementary Material, section SM-2. Since transport of compounds in the axial direction is modeled as plug flow, the BTF bed was discretized in vertical layers in order to simulate a sequence of continuous stirred tank reactors (CSTR) [23]. Vertical layers (*nvs*) were numbered starting from the top of the BTF (*nvs*=1) to the biogas outlet (*nvso*). Similarly, the biofilm layers (*nb*) were also divided in different subdivisions starting from the biofilm surface (*nb*=1) to the biofilm subdivision in contact with the packed material (*nbp*). The set of partial differential equations was discretized in space along the bed height and biofilm thickness. The conversion of the tubular reactor into a serial of stirred reactors was verified running simulations at different discretizations and optimizing results and time computing. As a result, an optimal discretization of the biofilter was found, resulting in eight nodes along the bed height (*nvs=8*) and ten nodes along the biofilm thickness (*nb=10*).

The following equations describe the mass balances in the gas, liquid and biofilm phases and their initial conditions in the BTF:

Mass balance for the gas phase in the BTF

$$\frac{dC_{g,i}^{nvs}}{dt} = \frac{F_T}{V_{g,\,nvs}} \cdot \left(C_{g,\,i}^{nvs-1} - C_{g,\,i}^{nvs}\right) - \frac{K_{L,i} \cdot a}{\varepsilon_g} \cdot \left(\frac{C_{g,\,i}^{nvs}}{H_i} - C_{L,i}^{nvs}\right) \qquad (3)$$

initial conditions: $t=0,\ C_{g,\,i}^{nvs}=0$

at the BTF inlet (*nvs*=1): $C_{g,\,i}^{nvs-1}=C_{g,\,i}^{in}$

Where subscripts *i* refers to either gaseous H_2S or O_2, while $C_{g,\,i}^{nvs}$ and $C_{L,i}^{nvs}$ are the concentrations of component *i* in the bulk gas phase and bulk liquid phase for a certain layer (g m^{-3}), respectively; $V_{g,\,nvs}$ (m^3) is calculated as $V_{g,nvs}=\frac{V_b \cdot \varepsilon_g}{nvs}$ where ε_g is the gas phase porosity,

which represents the volume fraction occupied by the gas phase in the packed and V_b is the empty volume of the packed bed. Notice that G-L mass transport is described by a gas-liquid global mass transfer coefficient referred to the liquid phase (K_L) that considers both the individual gas and liquid mass transfer resistances.

Mass balance for the liquid phase in the BTF

$$\frac{dC_{L,i}^{nvs}}{dt} = \frac{F_L}{V_{L,nvs}} \cdot \left(C_{L,i}^{nvs-1} - C_{L,i}^{nvs}\right) + \frac{K_{L,i} \cdot a}{\varphi} \cdot \left(\frac{C_{g,i}^{nvs}}{H_i} - C_{L,i}^{nvs}\right) - \frac{a \cdot D_i}{\varphi \cdot \delta_L} \cdot \left(C_{L,i}^{nvs} - C_{B,i}^{nvs,1}\right) \quad (4)$$

initial conditions: $t=0,\ C_{L,i}^{nvs}=0$

at the BTF inlet (*nvs*=1): $C_{L,i}^{nvs-1}=C_{L,i}^{RE}$

subscripts *i* refers to S^{2-}, SO_4^{2-}, $S_2O_3^{2-}$ and DO concentration, the compounds considered in the liquid phase of the BTF; $V_{L,\,nvs}$ (m^3) is calculated as $V_{L,nvs}=\frac{V_b \cdot \varphi}{nvs}$ where φ is the volume fraction occupied by the liquid phase in the packed bed according to the dynamic hold-up measured (-). Notice that mass transfer resistance in the liquid-biofilm interface was described by Fick's law considering that the whole thickness of the liquid phase acted as the liquid boundary layer for mass transport resistance.

Mass balances for the biofilm in the BTF

For the first layer of the biofilm (*nb*=1) and all BTF layers (*nvs*=1 to *nvso*)

$$\frac{dC_{B,i}^{nvs,1}}{dt} = \frac{D_i}{\delta_B \cdot \delta_L} \cdot \left(C_{L,i}^{nvs} - C_{B,i}^{nvs}\right) - \frac{D_i}{\delta_{B\text{-}nb}^{\,2}} \cdot \left(C_{B,i}^{nvs,1} - C_{B,i}^{nvs,nb+1}\right) + \sum \nu_{ij} \cdot r_{B,j} \quad (5)$$

For the inner layers of the biofilm (*nb*=2 to *nb*=*nbp-1*) and all BTF layers (*nvs*=1 to *nvso*)

$$\frac{dC_{B,i}^{nvs,nb}}{dt} = D_i \cdot \frac{\partial^2 C_{B,i}^{nvs,nb}}{\partial \delta_{B\text{-}nb}^{\,2}} + \sum \nu_{ij} \cdot r_{B,j} \quad (6)$$

For the closest layer to the packing material (*nbp*) and all BTF layers (*nvs*=1 to *nvso*)

$$\frac{dC_{B,i}^{nvs,nbp}}{dt} = \frac{D_i}{\delta_{B\text{-}nb}^{\,2}} \cdot \left(C_{B,i}^{nvs,nb-1} - C_{B,i}^{nvs,nbp} \right) + \sum \nu_{ij} \cdot r_{B,j} \qquad (7)$$

initial conditions in Eqs. 5, 6 and 7: t=0, $C_{B,\,i}^{nvs,nb} = 0$

boundary conditions in Eqs. 5, 6 and 7: x=0, $C_{B,i} = C_{l,i}$

x=δ_B, $\frac{\partial C_{B,i}^{nvs,nbp}}{\partial t} = 0$

in Eqs. 5, 6 and 7, subscripts *i* refers to S^{2-}, SO_4^{2-}, $S_2O_3^{2-}$ and DO concentration, the compounds considered in the biofilm phase of the BTF, while subscripts *j* indicates the rate equation in which component *i* is participating.

According to the BTF configuration, mass balances in the sump of the reactor (Eq. 8) and in the aeration column (Eqs. 9-10) were included.

Mass balance for the liquid phase in the sump of the BTF

$$\frac{dC_{L,i}^{P}}{dt} = \frac{F_L \cdot C_{L,i}^{nvs} - F_{L,P} \cdot C_{L,i}^{P} + F_{L,In} \cdot C_{L,i}^{In} - F_L \cdot C_{L,i}^{RE}}{V_{L,D}} \qquad (8)$$

initial conditions: t=0, $C_{L,\,i}^{P} = 0$

subscript *i* refers to S^{2-}, SO_4^{2-}, $S_2O_3^{2-}$ and DO concentration, the compounds considered in the liquid phase of the BTF. Notice that $C_{L,i}^{P}$ and $C_{L,i}^{RE}$ are equal except for dissolved oxygen because of the aeration column located in the recirculation line.

Mass balance for the gas phase in the aeration column

$$\frac{dC_{g,\,O_2}^{out}}{dt} = \frac{F_{O_2}}{V_{g,\,AC}} \cdot \left(C_{g,\,O_2}^{AC} - C_{g,\,O_2}^{out} \right) - K_{L,O_2,AC}a \left(\frac{C_{g,\,O_2}^{out}}{H_{O_2}} - C_{L,O_2}^{RE} \right) \qquad (9)$$

initial conditions : t=0, $C_{g,\,O_2}^{AC} = 0$

Mass balance for the liquid phase in the aeration column

$$\frac{dC_{L,O_2}^{RE}}{dt} = \frac{F_L}{V_{L,\,AC}} \cdot \left(C_{L,O_2}^{P} - C_{L,i}^{RE}\right) + K_{L,O_2,AC} \cdot \left(\frac{C_{g,\,O_2}^{out}}{H_{O_2}} - C_{L,i}^{RE}\right) \quad (10)$$

initial conditions: $t=0,\ C_{L,O_2}^{P}=0$

2.2.2 Modeling of biological and chemical sulfides-compounds conversions

A Monod-type kinetic expression is often used to describe substrate consumption [13,14] in desulfurizing systems with H_2S as the sole rate-limiting substrate. However, different authors have shown that the treatment of high-loads of H_2S, such as those found in biogas desulfurization processes, may lead to substrate inhibition or oxygen-limiting conditions. A multi-substrate type equation with a Haldane term for H_2S and a Monod term depending on the dissolved oxygen (DO) concentration inside the biofilm have been shown to describe well experimental oxygen uptake rate (OUR) and H_2S uptake rate profiles [20] during the characterization of H_2S-oxidizing biofilms in BTFs. Some authors have also proposed the use of a kinetic equation in which the ratio of elemental sulfur/sulfate produced is based on the DO concentration [24]. A product selectivity function for elemental sulfur or sulfate based on the sulfide oxidation activity and the OUR has been also considered by other authors [25,26]. It is well-known that elemental sulfur, the main intermediate product of H_2S biological oxidation, is formed due to O_2 transport limitations inside the BTF bed [7,27].

According to the abovementioned findings in literature, the kinetic model proposed by Mora et al. [21] was used herein. The multi-step sulfide oxidation mechanism (Figure 1D) has been summarized in Tables 2 and 3, in which the stoichiometry and the kinetic expressions that describe each of the reactions occurring during the process have been specified. In short, the kinetic model considers that H_2S is partially oxidized to elemental sulfur, which is intracellularly stored, but also to sulfite, which in presence of sulfide reacts to subsequently

form thiosulfate. Then, once sulfide is completely depleted, elemental sulfur and thiosulfate are further oxidized to sulfate, the end product of the reaction. Further information about the biological and chemical sulfide conversions can be found on Supplementary Material, section SM-4 and elsewhere [21].

2.3 Model implementation

The resulting set of ordinary differential equations was solved using MATLAB in a home-made modeling environment. A variable order method was used for solving stiff differential equations based on numerical differentiation formulas (NDFs), which are generally more efficient than the closely related family of backward differentiation formulas (BDFs), also known as Gear's methods. Since the inlet H_2S concentration was changed throughout the BTF operation, inlet concentration profiles were used as input variable of the model. Model parameters were estimated during calibration by curve-fitting of experimental data to model predictions to describe the dynamics of a lab-scale BTF for biogas desulfurization. A minimization routine on MATLAB, based on a non-lineal multidimensional minimization (Nelder-Mead) was used. The objective function to minimize was based on th e H_2S removal efficiency (RE) and the concentration of sulfate in the liquid phase ($C_{L,SO4}^{2-}$) according to the sensitivity analysis, and also to take into account both the gas-phase and the liquid-phase dynamics, respectively. Also, the cumulative mass of elemental sulfur (m_S^0) was not included in the objective function because experimental m_S^0 was not anatilically measured but determined through mass balances [7].

In order to evaluate the goodness of model predictions to experimental data, the efficiency criterion proposed by Nash and Sutcliffe [28] was used. Such efficiency criterion mathematically measures how well a model simulation fits the available experimental data. The efficiency coefficient (NSE) is defined as one minus the sum of the absolute squared

differences between the predicted and observed data normalized by the variance of the observed data during the period under investigation according to Eq. 11. Essentially, the closer the model efficiency to 1, the more accurate the model is.

$$NSE=1-\frac{\sum_{i=1}^{i=n}\left(y_e-y_m\right)^2}{\sum_{i=1}^{n}\left(y_e-\bar{y}_e\right)^2} \quad (11)$$

3. Results and discussion

3.1 Sensitivity analysis

Before model calibration, a sensitivity analysis was performed in order to determine the parameters that showed the highest influence on model outputs over the main process variables. Sensitivity was assessed by increasing and decreasing model parameters by 10% and comparing the relative change of the output variables to a relative change of the model parameter. As stated in Deshusses et al. [14], model parameters fall in the following categories: physical-chemical properties, system specifications (dimensions), biokinetics and mass transfer parameters. In the present work, parameters belonging to all parameter categories were included to perform the relative sensitivity analysis of the main output variables on biofiltration such as RE, m_S^0 and $C_{L,SO4}^{2-}$. In order to determine the relative sensitivity, model parameters were varied 0.9 and 1.1 times the reference value while simulating the stepwise load increase of period 1 (Table 1). Relative sensitivity analysis results were chosen as those corresponding to the H_2S inlet concentration of 10000 ppm_v (Table 4) because of a larger relative sensitivity of the model at these inlet concentration. Only those parameters that showed a relative sensitivity higher than 0.10 in at least one of the output variables are shown in Table 4. Similar results in terms of relative sensitivity were obtained for the 4000, 6000 and 8000 ppmv concentration steps simulated (results not shown).

The most sensitive output variables were the RE and $C_{L,SO4}^{2-}$ that exhibited comparable sensitivities between them at a 10% increase while m_S^0 was the less sensitive output variable due to its cumulative nature. However, at a 10% decrease results indicated that RE was highly influenced by parameters of all categories abovementioned to a higher extent than $C_{L,SO4}^{2-}$. Thus, both RE and $C_{L,SO4}^{2-}$ were the sole output variables selected to be included in the objective function during the calibration stage. Despite the low relative sensitivity of m_S^0, the most sensitive parameters were those parameters related to its formation, *i.e.* O_2 and H_2S mass transfer coefficients $\left(K_{L,O_2}, K_{L,H_2S}, D_{O_2}\right)$, physical-chemical properties $\left(H_{O_2}, H_{H_2S}\right)$ and parameters related to its consumption ($\mu_{max,2}$). This result was somehow expected since elemental sulfur formation directly depends on the oxygen availability and the S/DO ratio in the liquid phase that result from their transfer efficiency and solubility.

Besides the system specific parameters and physical-chemical parameters, the relative sensitivity analysis showed that biokinetic and mass transfer parameters were the most sensitive, which are often the most difficult to determine experimentally [29,30] and usually obtained by curve fitting of model estimations to experimental data [31,32]. Both RE and $C_{L,SO4}^{2-}$ were mostly influenced by physical-chemical parameters such as O_2 and H_2S Henry coefficients (H_{O_2}, H_{H_2S}); system specific parameters such as the specific surface area (a); by mass transfer parameters such as the O_2 and H_2S mass transfer coefficients, liquid layer thickness and O_2 diffusivity $\left(K_{L,O_2}, K_{L,H_2S}, \delta_L, D_{O_2}\right)$; and by kinetic parameters such as the specific growth rate for sulfur and the O_2 half-saturation constant ($\mu_{max,2}$, k_o). Consequently, the relative sensitivity analysis indicated that H_2S removal was either influenced by gas-liquid mass transfer and by biological degradation. However, parameters related with O_2 mass transfer such as K_{L,O_2}, H_{O_2} and D_{O_2} exhibited a larger influence compared to the

corresponding H_2S parameters. Such result is in consonance with previous works that reported that O_2 transport rather than H_2S transport is usually the limiting step in high-load H_2S biogas desulfurization [3,33]. López et al. [7] showed that the effectiveness of O_2 G-L mass transfer due the trickling liquid velocity (TLV) regulation was a key factor to improve H_2S oxidation in high-load H_2S biogas desulfurization.

Regarding the biokinetic parameters, $\mu_{max,2}$ was the most sensitive parameter, even if exhibited lower sensitivities compared with mass transport and physical-chemical parameters. This result indicates that elemental sulfur accumulation plays a major role as intermediate and that must be included and properly described by any kinetic model. Sulfide oxidation rate can be limited by excessive elemental sulfur accumulation, which is directly influenced by the rate at which elemental sulfur is consumed ($\mu_{max,2}$). In the kinetic model used in the present work, intermediate reactions such as elemental sulfur production and biodegradation are considered, which means that both the inhibitory or the catalytic effect caused by each species over other bioreactions are reflected.

Excluding those parameters that can be determined using correlations ($K_{L,O2}$), or physical-chemical parameters that can be found in literature (D_{O2}, H_{H2S}, H_{O2}), or provided by the packing manufacturer (a), the most sensitive parameters were selected for model calibration. Five parameters were selected for curve-fitting estimation during model calibration: namely, biomass and liquid layer thickness (δ_B, δ_L), specific growth rate for sulfur ($\mu_{max,2}$), biomass concentration (X) and H_2S global mass transfer coefficient ($K_{L,H2S}$). The number of parameters was selected according to the number of variables assessed (H_2S gas concentrations along the bed height, sulfate concentration and mass of elemental sulfur accumulated).

3.2 Model parameters estimation

A summary of the BTF model parameters is shown in Tables 5 and 6, while Fig. 3 and Fig. 4 show the comparison of model predictions using the parameters estimated and the experimental data corresponding to the calibration period (Table 1).

Biomass concentration (X) estimated by the model (Table 5) was in agreement with the amount of elemental sulfur produced (22.37 g) and the K_{max} determined by Mora et al. [21]. Since K_{max} is the relation between the maximum amount of elemental sulfur that could be accumulated inside SOB cells before this accumulation completely blocked the biological sulfide consumption, this maximum amount of elemental sulfur was determined using the substrate switch constant (K_{max}) and the biomass concentration estimated by the model (X) according to $K_{max} = \frac{m_{S^0 max}}{X}$. Thus, under the calibration conditions, a maximum amount of 157 g of elemental sulfur could be accumulated inside SOB cells, well above the amount of elemental sulfur produced. The K_{L,H_2S} was in agreement with K_{L,O_2} since both $K_L$values were related by the square root of the diffusivity of each species [13]. The $K_{L,O_2}$was determined using the Billet and Schultes correlations [34] for the gas and liquid individual mass transfer coefficients *kg* and *kl*, respectively, which was in close agreement with K_{L,O_2} determined by Dorado et al. [9]. It is worth highlighting that only the liquid-side resistance was significant since based on Billet and Schultes correlations the contribution of individual mass transfer resistances in the gas phase to the overall resistance for both gas species oxygen (O_2) and hydrogen sulfide (H_2S) were only 0.18% and 9.7% for O_2 and H_2S, respectively. In addition, $\mu_{max,2}$ lies close to the range of values determined by Mora et al. [21] ($5 \cdot 10^{-4}$ -$1.1 \cdot 10^{-2}$ h^{-1}). The δ_B denotes that the biofilm was thick enough to contain active and inactive biomass inside the biofilm and that δ_B is in the typical range of H_2S-degrading biofilms [13]. Kim and Deshusses [14] reported a δ_B of 23 μm concluding that, in order to perform the removal of

high H_2S loads in biogas, higher δ_B must be achieved. The δ_L estimated during model calibration was in agreement with the value obtained by dividing D_{H_2S} by the $K_{L,H_2S.}$ [13].

In Fig. 3 and Fig. 4 experimental results and model predictions of the effect of stepwise LR increases due to H_2S inlet concentration increases corresponding to the model calibration period are presented. Experimental data in both figures indicate that the system was able to remove almost 100% of inlet H_2S at all H_2S-LR (Fig. 3A and 3B). However, 100% sulfate production only occurred at the lowest H_2S-LR corresponding to an inlet concentration of 2000 ppmv. Further information related to sulfate production in this experiment can be found elsewhere [7]. Thereafter, elemental sulfur was accumulated in the packed bed (Fig. 4A). At the highest H_2S-LR tested the sulfate production was lower than the elemental sulfur produced, which lead to a decrease of the concentration of sulfate measured in the liquid phase (Fig. 4B). Such behavior was directly related to the oxygen availability and the S/DO ratio in the liquid phase. A linear decrease of the inlet O_2/H_2S volumetric ratio (from 42.2 down to 8.4 *% v* v^{-1}) along the experiment led to limiting oxygen conditions. Thus, elemental sulfur production over sulfate production was favored. No thiosulfate production was detected experimentally neither was predicted by the model.

Regarding the goodness of model predictions to experimental data, high NSE values were obtained for the fitting of H_2S concentration measured at different bed heights (Fig. 3A and 3B). In the range of 2000 to 10000 ppm_v, the model described well experimental H_2S concentrations measured in the first and second sections, with NSE coefficients of E=0.90 and E=0.93, respectively. At an inlet concentration of 10000 ppmv, a Nash-Sutcliffe efficiency coefficient of 0.43 was obtained for the H_2S concentration measured at the BTF outlet, mainly due to a missmatch between model predictions and experimental data. However, the Nash-

Sutcliffe efficiency coefficient at the BTF outlet in the range of 2000 to 8000 ppm_v was E=0.90.

Mismatch between model prediction and experimental data of the BTF outlet concentration during the 10000 ppm_v step mighty be related with the H_2S measurement system. At 10000 ppm_v a higher airflow rate is needed to dilute the biogas flow rate in order to measure H_2S concentrations inside the sensor measurement range. Therefore, less exact and precise experimental data is obtained. Additional details of BTF gas measurement system can be found in Supplementary Material, section S1 (Fig. S1).

Regarding to the predictions on the elemental sulfur accumulation (m_S^0), a Nash-Sutcliffe efficiency coefficient of E=0.94 was obtained, indicating an accurate fit of the model to experimental data for the production of elemental sulfur. From Fig. 4B it can be observed how the predicted sulfate concentration values fits almost perfectly to all experimental points, although during the step concentration of 4000 ppmv the simulated $C_{L,SO4}^{2-}$ was a 15% higher than the experimental measure. Such difference was attributed to a biological delay time of microorganisms in the BTF to start to produce sulfate, since the first step-wise LR increment up to 4000 ppm_v was the first performed in the reactor after a long stationary feeding period at 2000 ppm_v of 42 days. The model reproduced well the sudden $C_{L,SO4}^{2-}$ concentration deacrease during the last concentration step of 10000 ppm_v as a consequence of both the unfavorable S/DO ratio and the amount of elemental sulfur accumulated in the BTF bed. A NSE coefficient of E=0.75 was calculated for sulfate concentration predicted considering the whole period of the 2000-10000 ppm_v stepwise increase experiment (Fig. 4B).

3.3 Model Validation

After calibration, the response of the model was evaluated in a different experimental period from that used for calibration. A stationary feeding period of 42 days was used to validate the model, corresponding to period 2 in Table 1. Experimental data of cumulative mass of elemental sulfur and sulfate concentration and model predictions under the stationary feeding period for model validation are presented in Fig. 5. The BTF performance during period 2 was always close to the optimal, since H_2S RE was 100% and sulfate selectivity higher than 100% was calculated. Since the H_2S-LR during the experimental period corresponded to more than 100% sulfate production, elemental sulfur was progressively de-accumulated from the packed bed (Fig. 5A). The relatively small amount of sulfate produced from such elemental sulfur de-accumulation compared to that produced due to the H_2S fed led to a relatively constant sulfate profile along the monitored period.

The abovementioned elemental sulfur de-accumulation was verified in order to determine if it was a miscalculation in the mass balance or during sulfate concentration by ionic chromatography (IC). For this reason sulfate concentration, directly related to elemental sulfur de-accumulation, was determined when sulfate production was higher than 100% (see Supplementary Material, section SM-3 for further detail). Results showed that the sulfate concentration produced from elemental sulfur de-accumulation was higher than the experimental error of IC (5%) (Fig. S3). Therefore the sulfate concentration increases during a stationary feeding period due to elemental sulfur de-accumulation.

The model was able to accurately reproduce the elemental sulfur de-accumulation along this period. Despite of experimental data variability, model predictions showed an excellent agreement with experimental data. NSE of E=0.87 and E= 0.92 were obtained along period 2 for the cumulative mass of sulfur and sulfate concentration, respectively, reflecting that there

were no significant difference between experimental sulfate concentration and that predicted by the model.

Moreover, the model was used to simulate the performance of the reactor under dynamic conditions (Table 1), in order to simulate daily load fluctuations commonly found in real facilities. Dynamic model validation results are shown in Fig. 5. To properly assess the dynamics, the plant was fed a constant H_2S-LR of 56 g m^{-3} h^{-1} during 190h. Thereafter, the inlet dynamic profile was activated at an average H_2S-LR of 79 g m^{-3} h^{-1} with maximum and minimum peak H_2S-LR of 141 and 28 g m^{-3} h^{-1}.

The BTF model response properly fits the experimental data during the change of dynamics represented in Fig. 6. During the first stage of 190h during the stationary feeding period, the model predicted correctly the $C_{L,SO4}^{2-}$ experimental data. When variable H_2S-LR conditions were applied, a transient period with an increased sulfate concentration was observed until t=240h. Thereafter, $C_{L,SO4}^{2-}$ concentration remained oscilating in a constant range. The model was able to reproduce properly both the transient period and the pseudo steady-state period under a variable inlet load. The goodness of the fitting was confirmed with a NSE coefficient of E=0.60.

Overall, the model showed to be valid to describe the main processes occurring in the three phases of a BTF , gas phase (Fig 3A and 3B), liquid phase (Fig. 4A) and solid phase as elemental sulfur (Fig. 4B), in a co-current flow mode configuration. Thus, this model becomes a powerful tool to predict the main intermediate (elemental sulfur) and final product (sulfate) of H_2S oxidation along different operational conditions such as pseudo steady-state conditions and variable LR conditions. Especially, accurate model predictions under high

H_2S-LR and O_2 limiting conditions (period 1) could be useful for predicting elemental sulfur accumulation in industrial BTF installations. Therefore, maintenance tasks can be strategically planned. Moreover, the development of the BTF model can be used for the development and simulation of control strategies towards process optimization. Parameters related to O_2 transport are crucial in order to completely oxidize H_2S and avoid the formation of elemental sulfur in the BTF bed, since an excessive accumulation of elemental sulfur can significantly diminish the reactor performance. Therefore, control strategies must be based on the improvement of the oxygen transfer to the liquid phase towards process optimization.

.4. Conclusions

A dynamic model for a BTF for high H_2S-LR biogas desulfurization in aerobic conditions was developed and successfully calibrated and validated, allowing a proper description of different operational scenarios such as LR increments due to H_2S concentration increases in the biogas stream. Furthermore the behavior of the different phases (gas, liquid and elemental sulfur) involved in the biogas desulfurization were correctly predicted. Also the application of a two-step sulfide oxidation kinetic model was successfully performed in order to describe intermediate oxidation products.

A preliminary assessment through a relative sensitivity analysis allowed determining the most sensitive parameters of the model. Parameters related to O_2 mass transport exhibited a larger influence to model output variables considered (RE, $C_{L,SO4}^{2-}$ and m_S^0). The proposed model was calibrated using experimental data, which allowed describing accurately the outlet H_2S concentration profile along the BTF bed during H_2S-LR increments. Besides describing properly sulfate production, elemental sulfur, the main intermediate product during H_2S

oxidation, was correctly predicted. Mass transfer parameters (δ_B, δ_L, $K_{L,H2S}$) and kinetic parameters (X, $\mu_{max,2}$) were estimated during BTF model calibration.

Moreover, the BTF model was validated under a stationary feeding period and a dynamic H_2S-LR period. Proper gas phase description during both periods was obtained. More importantly, elemental sulfur and sulfate were also in agreement with experimental data. Dynamic validation results demonstrated that the model is able to predict correctly the BTF operation when a variable H_2S-LR profile is applied. Hence the BTF model here presented is capable to predict the BTF performance under similar conditions as those found in real plants, making it a suitable tool in order to develop and design control strategies towards process optimization of desulfurizing BTFs.

Nomenclature Section

List of symbols

a	Specific surface area per volume unit of packed bed, $m^2\ m^{-3}$
$C_{B,i}^{nvs,1}$	Concentration of component *i* at the biofilm surface in layer *nvs*, $g\ m^{-3}$
$C_{B,i}^{nvs,nb}$	Concentration of component *i* at the biofilm subdivision *nb* in layer *nvs*, $g\ m^{-3}$
$C_{B,SS}$	Concentration of sulfide in the biofilm phase, $g\ m^{-3}$
$C_{B,S}$	Concentration of elemental sulfur in the biofilm phase, $g\ m^{-3}$
$C_{B,TS}$	Concentration of thiosulfate in the biofilm phase, $g\ m^{-3}$
$C_{B,DO}$	Concentration of dissolved oxygen in the biofilm phase, $g\ m^{-3}$
C_{g,O_2}^{AC}	Oxygen inlet concentration in the aeration column, $g\ m^{-3}$
C_{g,O_2}^{out}	Oxygen outlet concentration in the aeration column, $g\ m^{-3}$
$C_{g,i}^{nvs}$	Concentrations of component *i* in the bulk gas in layer *nvs*, $g\ m^{-3}$
$C_{L,i}^{In}$	Concentration of compound *i* in the mineral medium, $g\ m^{-3}$

1	$C_{L,i}^{nvs}$	Concentrations of component *i* in the bulk liquid in layer *nvs*, g m^{-3}
2	$C_{L,i}^{P}$	Concentration of compound *i* in the purge flow, g m^{-3}
3	$C_{L,i}^{RE}$	Concentration of compound *i* in the recirculation flow, g m^{-3}
4	$C_{L,SO4}^{2-}$	Concentration of sulfate in the liquid phase, g m^{-3}
5	D_i	Diffusivity of component *i* in water, m^2 h^{-1}
6	*EBRT*	Empty Bed Residence Time ,s
7	$F_{L,In}^{1}$	Fresh liquid mineral medium flow rate, m^3 h^{-1}
8	$F_{L,P}$	Liquid purge flow rate, m^3 h^{-1}
9	F_L	Liquid flow rate, m^3 h^{-1}
10	F_T	Total (biogas + air) gas flow rate, m^3 h^{-1}
11	*HRT*	Hydraulic retention time, h
12	H_i	Gas-liquid dimensionless Henry coefficient for component *I*,-
13	$K_{L,O_2,AC}a$	Gas-liquid global mass transfer coefficient for O_2 in the aeration column, h^{-1}
14	$K_{L,i}$	Gas-liquid global mass transfer coefficient of component *i*, h^{-1}
15	K_{max}	Maximum intracellular S^0 stored to biomass, g S $g^{-1/3}$ VSS
16	K	Substrate switch constant, g S m^{-3}
17	K_{TS}	Affinity constant for $S_2O_3^{2-}$ consumption, g S m^{-3}
18	k_{SS}	Affinity constants for sulfide, g S m^{-3}
19	k_{is}	Sulfide inhibition constant, g S m^{-3}
20	k_o	Affinity constants for oxygen, g DO m^{-3}
21	k	Kinetic constant for $S_2O_3^{2-}$ production under biotic conditions, h^{-1}
22	m_S^0	Cumulative mass of elemental sulfur, g
23	r_{Bj}	Rate equation for each biological process considered, g m^{-3} h^{-1}
24	*TLV*	Trickling Liquid Velocity,m h^{-1}
25	V_{bed}	Packed bed volume, m^3

1	$V_{g,\,nvs}$	Empty volume of the packed bed of layer *nvs* m^3
2	$V_{L,nvs}$	Liquid volume of layer *nvs*, m^3
3	$V_{L,D}$	Volume of liquid in the sump of the BTF, m^3
4	$V_{L,\,AC}$	Liquid volume of the aeration column, m^3
5	$V_{g,\,AC}$	Gas phase volume of the aeration column, m^3
6	$Y_{X/S}$,	Biomass growth yield using S^0, g VSS g^{-1} S
7	$Y_{X/SS}$,	Biomass growth yield using S^{2-} , g VSS g^{-1} S
8	$Y_{X/TS}$,	Biomass growth yield using $S_2O_3^{2-}$, g VSS g^{-1} S
9	X	Biomass concentration, g X m^{-3}
10	υ_{ij}	Stoichiometric coefficient for compound *i* in process rate *j*,-
11		
12	Greek letters	
13	α	Kinetic constant for elemental sulfur accumulation,-
14	$\mathcal{E}_g$	Gas phase porosity,-
15	ε	Packed bed porosity,-
16	δ_L	Thickness of the water layer, m
17	$\delta_{B\text{-}nb}$	Thickness of one biofilm subdivision, m
18	φ	Dynamic hold-up,-
19	β	Kinetic constant for thiosulfate ,-
20	$\mu_{max,1}$	Specific growth rates for SOB over S^{2-}, h^{-1}
21	$\mu_{max,2}$	Specific growth rates for SOB over S^0 , h^{-1} g X $^{1/3}$ g $S^{-1/3}$
22	$\mu_{max,3}$	Specific growth rates for SOB over $S_2O_3^2$, h^{-1}
23		
24		
25	Superscripts	

nvs	Vertical layers
nb	Biofilm subdivisions
RE	Recycling line

Aknowledgements

The Spanish government provided financial support through the CICYT project CTM2012-37927-C03. The Department of Chemical Engineering at UAB (Universitat Autònoma de Barcelona) is a unit of Biochemical Engineering of the Xarxa de Referència en Biotecnologia de Catalunya (XRB), Generalitat de Catalunya.

References

[1] N. Abatzoglou, S. Boivin, A review of biogas purification, Biofuels, Bioprod. Biorefining. 3 (2009) 42–71.

[2] P.S. Cartwright, P.E., Water Reuse. Water Encyclopedia, 1st ed., 2005.

[3] M. Fortuny, X. Gamisans, M.A. Deshusses, J. Lafuente, C. Casas, D. Gabriel, Operational aspects of the desulfurization process of energy gases mimics in biotrickling filters, Water Res. 45 (2011) 5665–5674.

[4] M. Fortuny, J.A. Baeza, X. Gamisans, C. Casas, J. Lafuente, M.A. Deshusses, D. Gabriel, Biological sweetening of energy gases mimics in biotrickling filters, Chemosphere. 71 (2008) 10–17.

[5] G. Rodriguez, A.D. Dorado, M. Fortuny, D. Gabriel, X. Gamisans, Biotrickling filters for biogas sweetening: Oxygen transfer improvement for a reliable operation, Process Saf. Environ. Prot. 92 (2014) 261–268.

[6] A.M. Montebello, T. Bezerra, R. Rovira, L. Rago, J. Lafuente, X. Gamisans, S. Campoy, M Baeza, D. Gabriel, Operational aspects, pH transition and microbial shifts

of a H2S desulfurizing biotrickling filter with random packing material., Chemosphere. 93 (2013) 2675–82.

[7] L.R. López, T. Bezerra, M. Mora, J. Lafuente, D. Gabriel, Influence of trickling liquid velocity and flow pattern in the improvement of oxygen transport in aerobic biotrickling filters for biogas desulfurization, J. Chem. Technol. Biotechnol. (2015). doi:10.1002/jctb.4676.

[8] F.J. Álvarez-Hornos, C. Gabaldón, V. Martínez-Soria, P. Marzal, J.-M. Penya-roja, Mathematical modeling of the biofiltration of ethyl acetate and toluene and their mixture, Biochem. Eng. J. 43 (2009) 169–177.

[9] A.D. Dorado, G. Rodri-guez, G. Ribera, A. Bonsfills, D. Gabriel, J. Lafuente, X. Gamisans, Evaluation of Mass Transfer Coefficients in Biotrickling Filters: Experimental Determination and Comparison to Correlations, Chem. Eng. Technol. 32 (2009) 1941–1950.

[10] G. Baquerizo, J.P. Maestre, T. Sakuma, M.A.. Deshusses, X. Gamisans, D. Gabriel, J. Lafuente, A detailed model of a biofilter for ammonia removal: Model parameters analysis and model validation, Chem. Eng. J. 113 (2005) 205–214.

[11] E.L. Cortus, S.P. Lemay, E.M. Barber, G.A. Hill, S. Godbout, A dynamic model of ammonia emission from urine puddles, 99 (2008) 390–402.

[12] W. Ahmed, Z.M. Shareefdeen, N.A. Jabbar, Dynamic modeling and analysis of biotrickling filters in continuous operation for H_2S removal, Clean Technol. Environ. Policy. 16 (2013) 1757–1765.

[13] H. Li, J.C. Crittenden, J.R. Mihelcic, H. Hautakangas, Optimization of Biofiltration for Odor Control: Model Development and Parameter Sensitivity, 74 (2014) 5–16.

[14] S. Kim, M.A. Deshusses, Development and Experimental Validation of a Conceptual Model for Biotrickhg Ffltration of H_2S, (2003) 119–128.

[15] J.S. Devinny, J. Ramesh, A phenomenological review of biofilter models, Chem. Eng. J. 113 (2005) 187–196.

[16] J. Silva, M. Morales, M. Cáceres, P. Morales, G. Aroca, Modelling of the biofiltration of reduced sulphur compounds through biotrickling filters connected in series: Effect of H2S, Electron. J. Biotechnol. 15 (2012).

[17] S. Sharvelle, M. Arabi, E. Mclamore, M.K. Banks, Model Development for Biotrickling Filter Treatment of Graywater Simulant and Waste Gas . I, (2008) 813–825.

[18] G. Rodriguez, Eliminació de H2S mitjançant biofiltres percoladors: millora de la transferencia d'oxygen, Thesis 2013.

[19] Q. Liao, X. Tian, R. Chen, X. Zhu, Mathematical model for gas–liquid two-phase flow and biodegradation of a low concentration volatile organic compound (VOC) in a trickling biofilter, Int. J. Heat Mass Transf. 51 (2008) 1780–1792.

[20] W. Bonilla-Blancas, M. Mora, S. Revah, J.A. Baeza, J. Lafuente, X. Gamisans, D. Gabriel, A. Gonzalez-Sanchez, Application of a novel respirometric methodology to characterize mass transfer and activity of H_2S-oxidizing biofilms in biotrickling filter beds, Biochem. Eng. J. 99 (2015) 24–34.

[21] M. Mora, L.R. López, J. Lafuente, J. Pérez, R. Kleerebezem, M. Van Loosdrecht, X. Gamisans, D. Gabriel, Respirometric characterization of aerobic sulfide, thiosulfate and elemental sulfur oxidation by S-oxidizing biomass, Water Res. 89 (2016) 282–292.

[22] R.R. Andreasen, R.E. Nicolai, T.G. Poulsen, Pressure drop in biofilters as related to dust and biomass accumulation, J. Chem. Technol. Biotechnol. 87 (2012) 806–816.

[23] M.A. Deshusses, G. Hamer, I.J. Dunn, Behavior of Biofilters for Waste Air Biotreatment. 1. Dynamic Model Development, 29 (1995) 1048–1058.

[24] A. Roosta, A. Jahanmiri, D. Mowla, A. Niazi, Mathematical modeling of biological

sulfide removal in a fed batch bioreactor, Biochem. Eng. J. 58-59 (2011) 50–56.

[25] A. Mannucci, G. Munz, G. Mori, C. Lubello, Biomass accumulation modelling in a highly loaded biotrickling filter for hydrogen sulphide removal., Chemosphere. 88 (2012) 712–7.

[26] A. Gonzalez-Sanchez, M. Tomas, A.D. Dorado, X. Gamisans, A. Guisasola, J. Lafuente, D. Gabriel, Development of a kinetic model for elemental sulfur and sulfate formation from the autotrophic sulfide oxidation using respirometric techniques., Water Sci. Technol. 59 (2009) 1323–9.

[27] A.M. Montebello, M. Baeza, J. Lafuente, D. Gabriel, Monitoring and performance of a desulphurizing biotrickling filter with an integrated continuous gas/liquid flow analyser, Chem. Eng. J. 165 (2010) 500–507.

[28] J.E. Nash, J. V Sutcliffe, River flow forecasting through conceptual models part I: A discussion of principles, J. Hydrol. 10 (1970) 282–290.

[29] G. Munz, R. Gori, G. Mori, C. Lubello, Monitoring biological sulphide oxidation processes using combined respirometric and titrimetric techniques, Chemosphere. 76 (2009) 644–650.

[30] M. Mora, A. Guisasola, X. Gamisans, D. Gabriel, Examining thiosulfate-driven autotrophic denitrification through respirometry, Chemosphere. 113 (2014) 1–8.

[31] I. Iliuta, F. Larachi, Modeling simultaneous biological clogging and physical plugging in trickle-bed bioreactors for wastewater treatment, Chem. Eng. Sci. 60 (2005) 1477–1489.

[32] A.D. Dorado, E. Dumont, R. Muñoz, G. Quijano, A novel mathematical approach for the understanding and optimization of two-phase partitioning bioreactors devoted to air pollution control, Chem. Eng. J. 263 (2015) 239–248.

[33] A.M. Montebello, M. Fernández, F. Almenglo, M. Ramírez, D. Cantero, M. Baeza, D.

Gabriel, Simultaneous methylmercaptan and hydrogen sulfide removal in the desulfurization of biogas in aerobic and anoxic biotrickling filters, Chem. Eng. J. 200–202 (2012) 237–246.

[34] R. Billet, M. Schultes, Prediction of Mass Transfer columns with dumpled and Arranged packings. Updated Summary of the Calculation Method of Billet and Schultes, Chem. Eng. Res. Des. 77 (1999) 498–504.

[35] R. Perry, D. Green, J. Maloney, Perry's chemical engineers' handbook, 1997.

[36] R. Sander, Compilation of Henry's law constants, version 3.99, Atmos. Chem. Phys. Discuss. 14 (2014) 29615–30521.

Table 1

Table 1. Experimental conditions for the simulated periods

Period	$[H_2S]$ (ppm_v)	LR (g S-H_2S m^{-3} h^{-1})	O_2/H_2S (% v v^{-1})	Period simulated (days)
1: Calibration and sensitivity analysis	2000	56.3	42.2	5
	4000	112.9	21.0	
	6000	169.6	14.0	
	8000	226.6	10.5	
	10000	283.8	8.4	
2: Stationary Validation	2000	56.3	42.2	42
3: Dynamic Validation	2758[a]	78.9	35.8	8
	5000[b]	141.1	84.4	
	1000[c]	28.1	16.8	

[a]Average concentration

[b]Maximum concentration

[c]Minimum concentration

Table 2

Table 2. Process stoichiometry for the aerobic sulfide, thiosulfate and elemental sulfur oxidation by S-oxidizing biomass.

Process	Compounds				
	Sulfide	Thiosulfate	Sulfur	Sulfate	Oxygen
1. Growth on sulfide	$-\frac{1}{Y_{X/SS}}$		$\frac{1}{Y_{X/SS}}$		$-\frac{0.42^{*}}{Y_{X/SS}}$
2. Growth on elemental sulfur			$-\frac{1}{Y_{X/S}}$	$\frac{1}{Y_{X/S}}$	$-\frac{1.22^{*}}{Y_{X/S}}$
3. Growth on thiosulfate		$-\frac{1}{Y_{X/TS}}$		$\frac{2}{Y_{X/TS}}$	$-\frac{1.65^{*}}{Y_{X/TS}}$
4. Thiosulfate production		1	-2		-1.5

*Mora et al. [21]

Table 3

Table 3. Process kinetics for the aerobic sulfide, thiosulfate and elemental sulfur oxidation by S-oxidizing biomass

Process	Process rate
1. Growth on sulfide	$\mu_{max,1}\cdot\left(\frac{C_{B,SS}}{k_{SS}+C_{B,SS}+\frac{C_{B,SS}^{2}}{k_{is}}}\right)\cdot\left(1-\left(\frac{\left(\frac{C_{B,S}}{X}\right)}{K_{max}}\right)^{\alpha}\right)\cdot\left(\frac{C_{B,DO}}{C_{B,DO}+k_{o}}\right)\cdot X$
2. Growth on elemental sulfur	$\mu_{max,2}\cdot\left(\frac{C_{B,S}}{X}\right)^{2/3}\cdot\left(\frac{K}{C_{B,SS}+K}\right)\cdot\left(\frac{C_{B,DO}}{C_{B,DO}+k_{o}}\right)\cdot X$
3. Growth on thiosulfate	$\mu_{max,3}\cdot\left(\frac{C_{B,TS}}{C_{B,TS}+K_{TS}}\right)\cdot\left(\frac{K}{C_{B,SS}+K}\right)\cdot\left(\frac{C_{B,DO}}{C_{B,DO}+k_{o}}\right)\cdot X$
4. Thiosulfate production	$k\cdot C_{B,SS}^{\beta}$

Table 4

1 Table 4. Sensitivity results for key BTF model parameters assessed at an inlet H_2S

2 concentration of 10000 ppm_v

3

			Sensitivity, +Δ10 %			Sensitivity, -Δ10 %		
Parameter	Symbol	Units	RE (%)	m_S^0 (g-S)	$C_{L,SO4}^{2-}$ (g-S L^{-1})	RE (%)	m_S^0 (g-S)	$C_{L,SO4}^{2-}$ (g-S L^{-1})
Specific interfacial area	a	$m^2\ m^{-3}$	0,79	0,00	1,09	1,51	0,31	0,90
O_2 mass transfer coefficient	K_{L,O_2}	$m\ h^{-1}$	0,45	-0,30	0,68	1,20	-0,19	0,53
O_2 Diffusivity	D_{O_2}	$m^2\ h^{-1}$	0,40	-0,10	0,33	1,02	-0,05	0,25
Specific growth rate over sulfur	$\mu_{max,2}$	h^{-1}	-0,40	-0,22	0,27	-0,48	0,04	0,51
H_2S Henry's constant	H_{H_2S}	dimensionless	-0,30	-0,46	0,24	-0,08	-0,50	0,25
Biofilm layer thickness	δ_B	μm	-0,05	0,05	0,13	1,42	0,04	0,13
Biomass concentration	X	$g\ X\ m^{-3}$	0,06	0,12	0,11	1,31	0,12	0,11
Substrate switch	K_{max}	$g\ S\ g\ X^{-1}$	0,11	0,18	0,04	1,21	0,21	0,01
H_2S mass transfer coefficient	K_{L,H_2S}	$m\ h^{-1}$	-0,10	0,21	-0,04	-0,04	0,25	-0,07
O_2 half-saturation constant	k_o	$g\ DO\ m^{-3}$	0,14	0,08	-0,08	0,11	0,08	-0,09
Liquid layer thickness	δ_L	μm	-0,50	0,02	-0,25	-0,37	0,04	-0,31
O_2 Henry's constant	H_{O_2}	dimensionless	-1,41	0,22	-0,76	-0,72	0,55	-1,23

4

Table 5

1 Table 5. Summary of main parameters of the BTF model for biogas desulfurization

Parameter	Symbol	Value	Units	Reference
Biomass concentration	X	$139.7 \cdot 10^{3}$	g X m^{-3}	Calibrated
Biofilm layer thickness	δ_B	200	μm	Calibrated
Liquid layer thickness	δ_L	10	μm	Calibrated
Specific growth rate for sulfur	$\mu_{max,2}$	$2.17 \cdot 10^{-2}$	h^{-1}	Calibrated
H_2S Global mass transfer coefficient	K_{L,H_2S}	0.23	m h^{-1}	Calibrated
O_2 Global mass transfer coefficient in the BTF	K_{L,O_2}	0.38	m h^{-1}	[34]
O_2 mass transfer coefficient in the Aeration column	$K_{L,O_2,AC}$	0.4	h^{-1}	Experimentally determined
Liquid hold-up	φ	$3.57 \cdot 10^{-2}$	dimensionless	Experimentally determined
Specific interfacial area	a	354.33	m^2 m^{-3}	Packing material
Packing material porosity	ε	0.85	dimensionless	manufacturer
H_2S diffusivity	D_{H_2S}	$5.80 \cdot 10^{-6}$	m^2 h^{-1}	[35]
O_2 diffusivity	D_{O_2}	$9.00 \cdot 10^{-6}$	m^2 h^{-1}	[35]
SO_4^{2-} diffusivity	$D_{SO_4^{2-}}$	$3.80 \cdot 10^{-3}$	m^2 h^{-1}	[35]
H_2S Henry's constant	H_{H_2S}	0.42	dimensionless	[36]
O_2 Henry's constant	H_{O_2}	32.80	dimensionless	[36]

2

Table 6

Table 6. Summary of main biokinetic parameters of the BTF model for biogas desulfurization calibrated by Mora et al. [21] through respirometry for the biotrickling filter modeled herein.

Parameter	Symbol	Value	Units
Specific growth rate for sulfide	$\mu_{max,1}$	0.41	h^{-1}
Specific growth rate for sulfide	$\mu_{max,3}$	0.012	h^{-1}
Sulfide affinity constant	k_{SS}	0.32	g S m^{-3}
Sulfide inhibition constant	k_{is}	42.4	g S m^{-3}
Oxygen affinity constant	k_o	0.11	g DO m^{-3}
maximum intracellular elemental sulfur stored in the biomass	K_{max}	0.252	g S $g^{-1/3}$ VSS
Thiosulfate affinity constant	K_{TS}	0.0023	g S m^{-3}
Kinetic constant for thiosulfate	k	6.35	h^{-1}
Substrate switch constant	K	0.014	g S m^{-3}
Kinetic constant for thiosulfate	β	0.530	dimensionless
Kinetic constant	α	1.71	dimensionless

Figure 1

Click here to download high resolution image

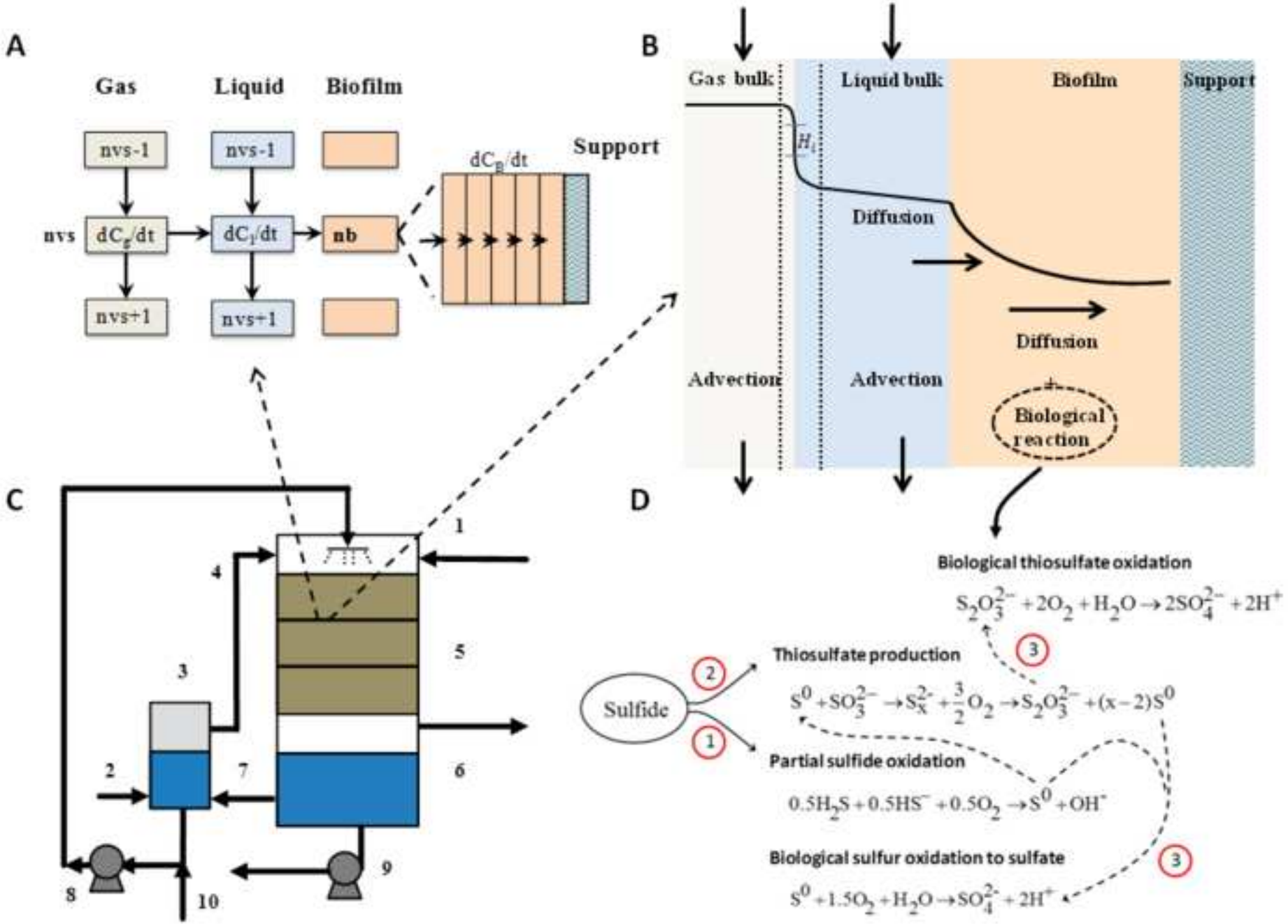

Figure 2

Click here to download high resolution image

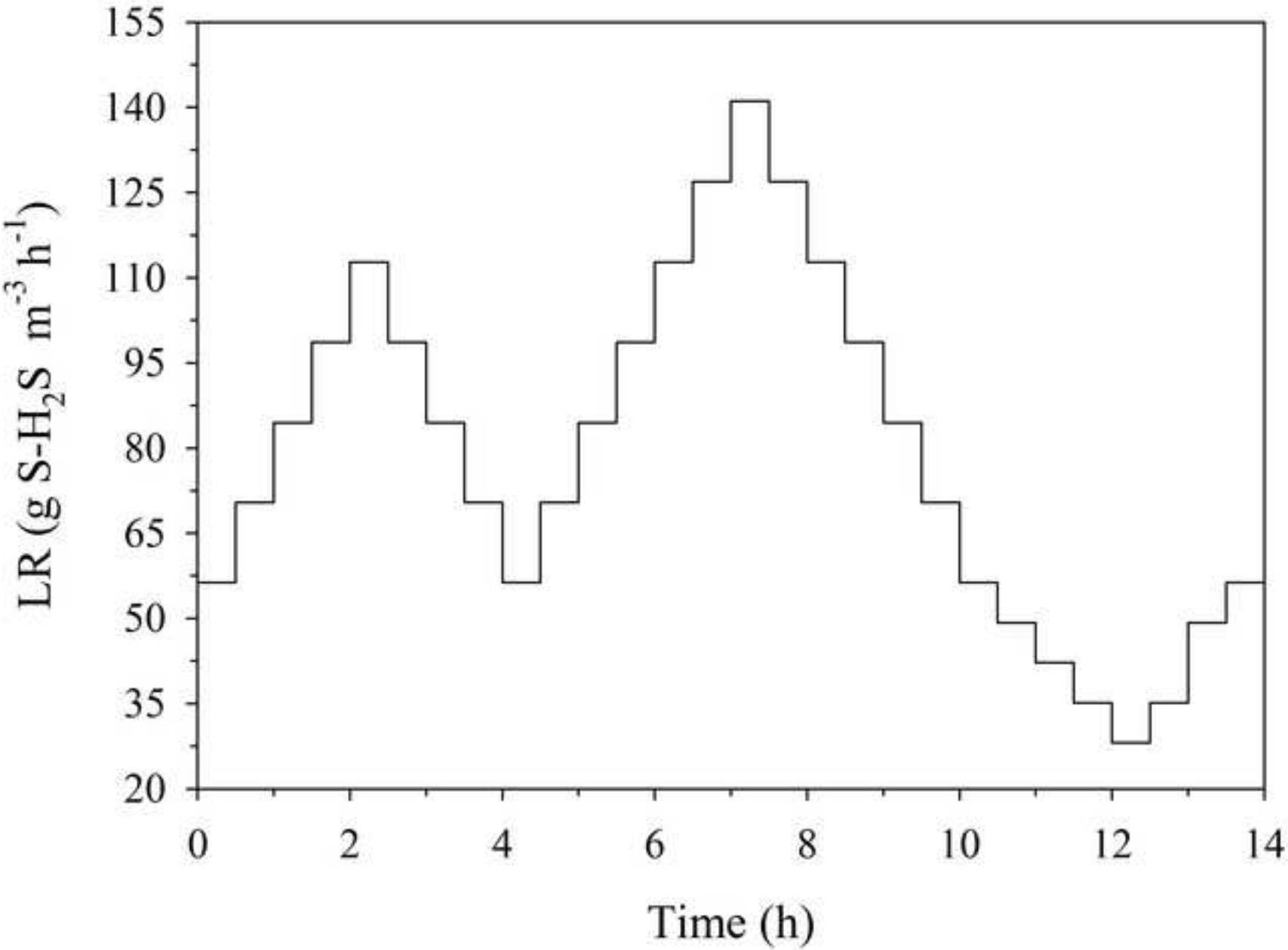

Figure 3

Click here to download high resolution image

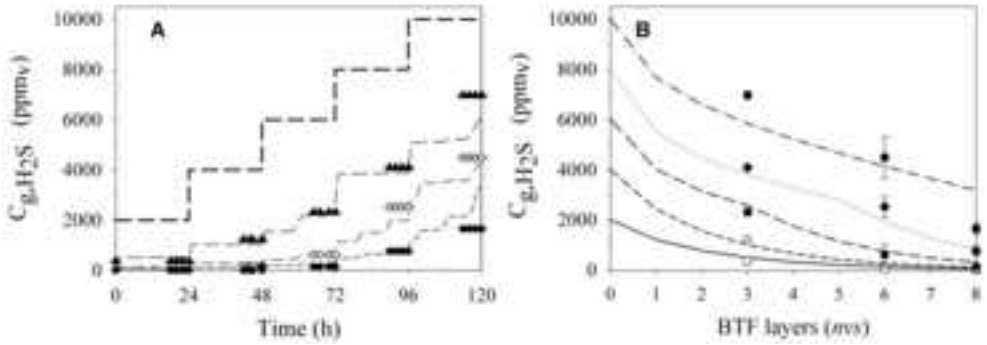

Figure 4

Click here to download high resolution image

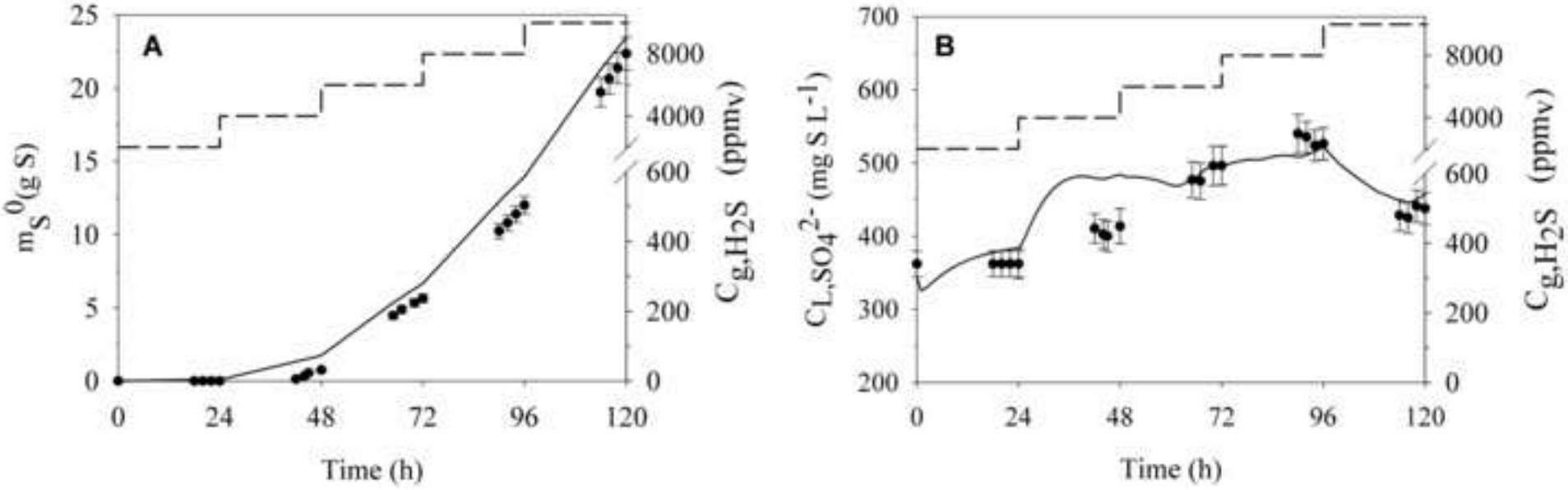

Figure 5

Click here to download high resolution image

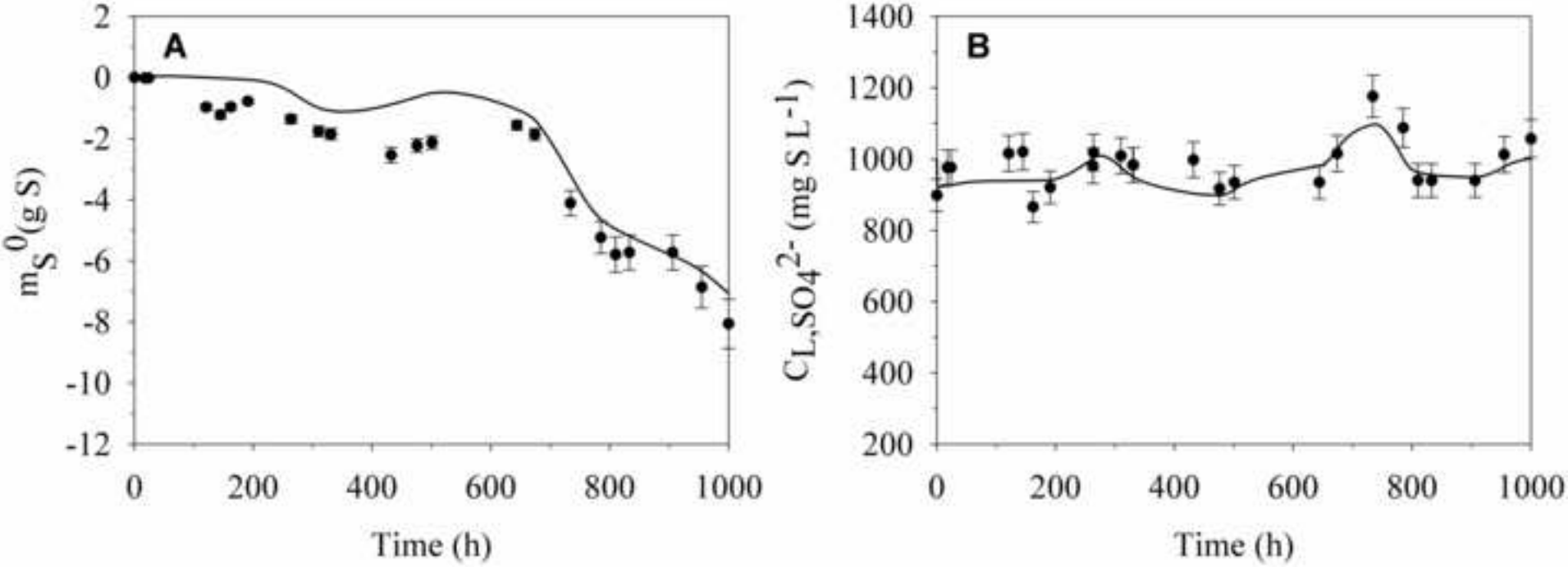

Figure 6

Click here to download high resolution image

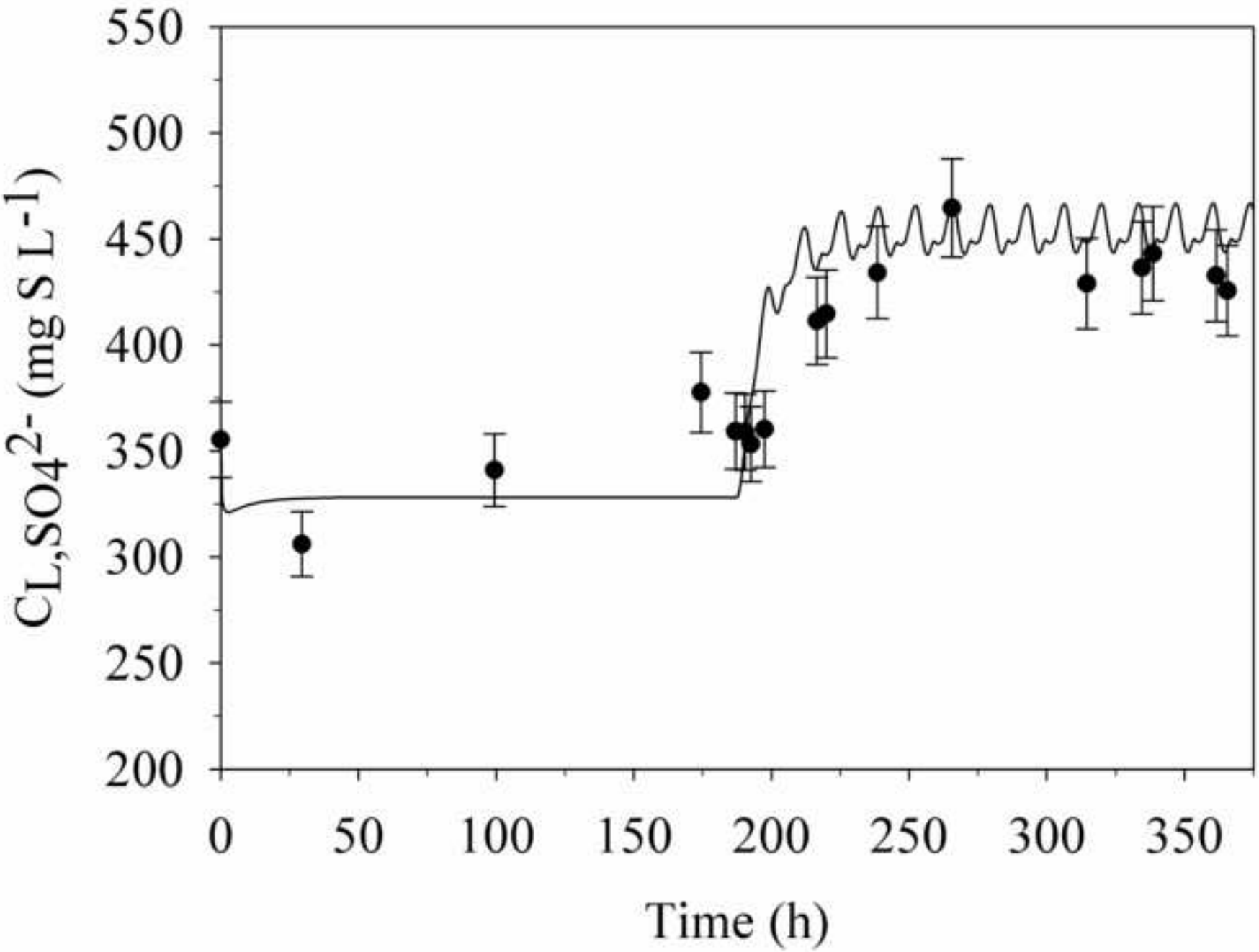

FIGURE CAPTIONS

Fig. 1. Schematic of the A) BTF discretization in *nvs* vertical layers and in *nb* subdivisions of the biofilm, B) schematic of the main phenomena considered in the model, C) co-current biotrickling filter setup, and D) biological mechanisms for H_2S oxidation. In Figure 1C numbers correspond to (1) the biogas inlet, (2) air inlet, (3) aeration column, (4) exhaust air from the oxygenation column, (5) main reactor, (6) biogas outlet from the BTF, (7) BTF liquid outlet , (8) liquid recycling pump, (9) liquid purge, (10) mineral medium and bicarbonate inlet. In Figure 1D numbers correspond to (1) partial sulfide oxidation to elemental sulfur (2) thiosulfate production from polysulfide pathway (3) biological oxidation of thiosulfate and intracellular elemental sulfur.

Fig. 2 . Variable H_2S-LR profile used for dynamic validation of the BTF model.

Fig. 3. Experimental and predicted H_2S concentration during period 1 after model calibration. A) experimental and simulated H_2S concentration profiles at different BTF bed heights. B) experimental and simulated H_2S concentration along the BTF height. Fig. 3A: Inlet H_2S concentration (solid line), experimental and simulated data from the 1st bed (▲ and medium dashed line), the 2nd bed (◊ and dashed-dot line), and the 3rd bed (● and short dashed line). Fig. 3B: Experimental and simulated data at a LR of 56.3 g S-H_2S m^{-3} h^{-1} (○ and solid line), 112.9 g S-H_2S m^{-3} h^{-1} (△ and short dashed line), 169.6 g S-H_2S m^{-3} h^{-1} (■ and medium dashed line), 226.6 g S-H_2S m^{-3} h^{-1} (◆ and dot line), and 283.8 g S-H_2S m^{-3} h^{-1} (⬣ and dashed dot line).

Fig. 4. H_2S inlet concentration (dashed line) and experimental (simbols) and predicted profiles (solid lines) of cumulative mass of (A) elemental sulfur and (B) sulfate during model calibration.

Fig. 5. Experimental (symbols) and model predictions (solid lines) during the stationary feeding period: (A) cumulative mass of sulfur and (B) sulfate concentration.

Fig. 6. Sulfate concentration comparison betweeen experimental data (symbol) and model predictions (solid line) during dynamic validation.

Supplementary Material

Click here to download Supplementary Material: Supplementary Material.docx